MEDNARODNA
PODIPLOMSKA ŠOLA
JOŽEFA STEFANA

6. ŠTUDENTSKA KONFERENCA MEDNARODNE PODIPLOMSKE ŠOLE JOŽEFA STEFANA

Zbornik – 2. del

6th JOŽEF STEFAN INTERNATIONAL POSTGRADUATE SCHOOL STUDENTS' CONFERENCE

Proceedings – Part 2

20. – 22. 05. 2014, LJUBLJANA

Zbornik 6. Študentske konference Mednarodne podiplomske šole Jožefa Stefana
(Proceedings of the 6th Jožef Stefan International Postgraduate School Students Conference)

Uredniki / Editors:
Nejc Trdin
Jernej Pavlič
Božidara Cvetković
Nemanja Aničić
Majda Pavlin
Andraž Rešetič

Fotografije / Photos:
Nikola Simidjievski

Založnik / Publisher:
Mednarodna podiplomska šola Jožefa Stefana, Ljubljana

Tisk / Print:
TISKARNA PLEŠKO d.o.o., Ljubljana

Naklada / Copies:
100 izvodov

Ljubljana, maj 2014

Konferenco organizira Študentski Svet Mednarodne podiplomske šole Jožefa Štefana
(The Conference is organized by Jožef Stefan International Postgraduate School - IPS Student Council)

CIP - Kataložni zapis o publikaciji
Narodna in univerzitetna knjižnica, Ljubljana

5/6(082)
378.046-021.68:001.891(497.4)(082)

MEDNARODNA podiplomska šola Jožefa Stefana. Študentska konferenca (6 ; 2014 ; Ljubljana)
Zbornik : 2. del = Proceedings : part 2 / 6. študentska konferenca Mednarodne podiplomske šole Jožefa Stefana = 6th Jožef Stefan International Postgraduate School Students' Conference, 20.-22. 05. 2014, Ljubljana ; [organizira študentski svet Mednarodne podiplomske šole Jožefa Štefana = organized by Jožef Stefan International Postgraduate School - IPS Student Council] ; uredili, edited by Nejc Trdin ... [et al.]. - Ljubljana : Mednarodna podiplomska šola Jožefa Stefana, 2014

ISBN 978-961-92871-7-0
1. Trdin, Nejc 2. Mednarodna podiplomska šola Jožefa Stefana (Ljubljana)
273797632

6. ŠTUDENTSKA KONFERENCA MEDNARODNE PODIPLOMSKE ŠOLE JOŽEFA STEFANA

ZBORNIK - 2. DEL

6th JOŽEF STEFAN INTERNATIONAL POSTGRADUATE SCHOOL STUDENTS' CONFERENCE

PROCEEDINGS - Part 2

Uredili / Edited by

Nejc Trdin, Jernej Pavlič, Božidara Cvetković, Nemanja Aničić, Majda Pavlin in
Andraž Rešetič

20. - 22. 5. 2014, Ljubljana

Organizacijski odbor / Organising Committee

Redakcijski odbor / Technical Review Committee

Kazalo (Table of Contents)

Ekotehnologija (Ecotechnology) 1

Ekotehnologija (Ecotechnology)

Automated method for dissolved gaseous mercury (DGM) measurements

Ermira Begu[1, 2], **Jože Kotnik**[1], **Milena Horvat**[1, 2]
[1] Jožef Stefan Institute, Department of environmental Sciences, Jamova 39,
Ljubljana 1000, Slovenia
[2] Jožef Stefan International Postgraduate School, Ljubljana, Slovenia
ermira.begu@ijs.si

Dissolved gaseous mercury (DGM) in natural water includes elemental mercury (Hg^0) and dimethyl mercury (DMeHg). Hg^0 is the main component (>95%), while DMeHg is unstable and present only deep waters. Due to low water solubility (about 60 µ g/L at 25 °C) and high volatility, Hg^0 evaporates from water surfaces and enters into global atmospheric mercury pool. Therefore, accurate measurements of dissolved Hg^0 of high importance in global mercury biogeochemical cycle. Dissolved Hg^0 is not stable in aqueous solutions, therefore the timing of analysis is of crucial importance. Ideally, continuous measurements with sufficient sensitivity, precision and accuracy would best fit the purpose. In this study, a comparison of manual and automated methods has been performed. The agreement between the methods is relatively good, although the manual method tends to produce slightly higher results (10 to 30%) in the concentration range of 20 to 1500 pg/L. Further improvements of the automated methods is under investigation. Except natural environments, very important application of automated DGM measurements is in the coal burning power plant sector equipped with the wet flue gas desulphurisation equipment (WFGD). Measurements of DGM can be used as a diagnostic tool to control the reduction of Hg^{2+} to elemental Hg which may consequently lead to the emissions of Hg^0 through the stack gases to the atmosphere.

Jožef Stefan“ Institute, Ljubljana, Slovenia

JOŽEF STEFAN
INTERNATIONAL
POSTGRADUATE SCHOOL

Automated method for dissolved gaseous mercury measurements

E. Begu[1, 2], J. Kotnik[1], M. Horvat[1, 2]

[1]Jožef Stefan Institute, Department of Environmental Sciences, Jamova 39, Ljubljana, Slovenia

[2] International Postgraduate School 'Jožef Stefan', Jamova 39, Ljubljana, Slovenia

Introduction

- Dissolved gaseous mercury (DGM) represent all gaseous mercury compounds in water environments (95 % of DGM is elemental mercury (Hg (0)) and <5% is dimethylmercury (DMeHg))
- The evasion of Hg (0) from oceanic waters to the global atmosphere plays an important role in the global mercury cycle
- The production of Hg(0) is a function of abiotic and biotic processes
- The levels of DGM in non contaminated surface waters represent between 1 to 30% of THg.
- Very sensitive methods are needed to accurately measure DGM.
- Manual methods have proved so far to be robust and to provide data which can be safety used in modelling of mercury biogeochemical and in the traceability.
- Automated methods are available for DGM measurements and showed good agreement with the manual ones.

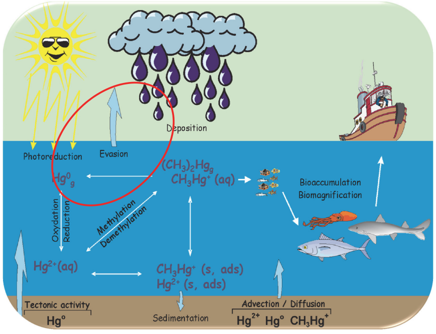

Manual method:

Cold vapor atomic fluorescence spectrophotometry (CV AFS) with gold pre-amalgamation.

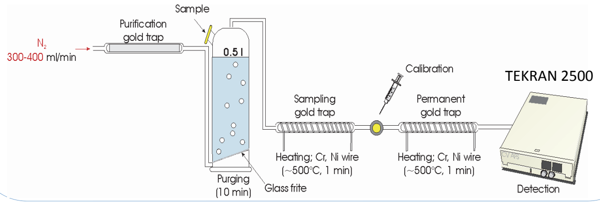

Automated bubbling system

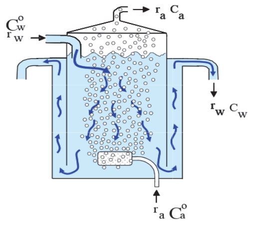

LUMEX

UT 3000

Results:

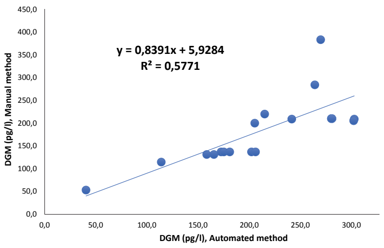

Lumex detector, air: water ratio 2,1/2,7

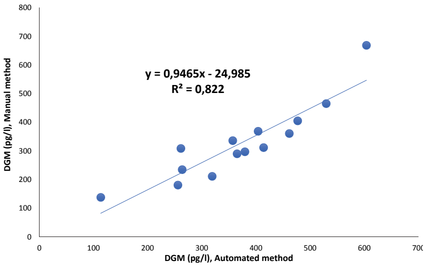

UT 3000 detector, air: water ratio is 2.8/2.8

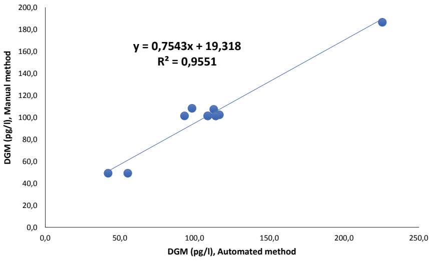

UT 3000 detector, air: water ratio is 2,7/1,8

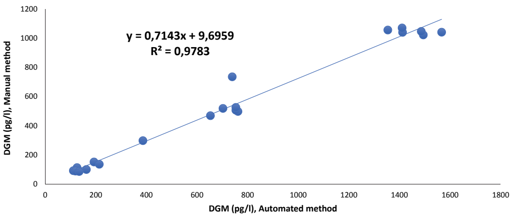

UT 3000 detector, air: water ratio is 3.9/2.9

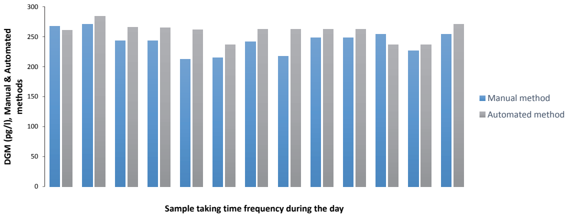

Lumex detector, air: water ratio is 2,3/2,7

Conclusions:

1. The main parameter affecting the automated method performance is the ***air: water flow ratio***
2. A air: water flow ratio close to 1 for the automated method, assures comparable results between methods
3. Good agreement and correlation was achieved between methods
4. The results obtained from the manual system for the same sample, are systematically higher for 10 to 30 %, which might be due to unaccounted factors in the formula used for calculations (automated method).

References:

1. Horvat M., Kotnik J., Logar M., Fajon V., Zvonarić T., Pirrone N.: Speciation of mercury in surface and deep-sea waters in the Mediterranean Sea, *Atmospheric Environment 37 Supplement No. 1 (2003) S93–S108*
2. *Andersson M. E., Gardfeldt K., Wangberg I.: A description of an automatic continuous equilibrium system for the measurement of dissolved gaseous mercury, Anal Bioanal Chem, 2008*
3. *Gardfeldt K., Horvat M., Sommar J., Kotnik J., Fajon V., Wangberg I., Lindqvist O.: Comparison of procedures for measurements of dissolved gaseous mercury in seawater performed on a Mediterranean cruise, Anal Bioanal Chem., 2002*
4. *Wangberg I., Gardfeldt K.: Measurement technique allowing continuous automatic determination of DGM in oceanic surface water, International Workshop on Mercury in the marine environment: A global metrology challenge, 2011*

First worldwide interlaboratory study on cytostatic compounds in aqueous samples

Marjeta Česen[1,2]**, Tina Kosjek**[1,2]**, Ester Heath**[1,2]
[1] Department of Environmental Sciences, Jožef Stefan Institute, Jamova 39, 1000 Ljubljana, Slovenia
[2] Jožef Stefan International Postgraduate School, Jamova 39, 1000 Ljubljana, Slovenia
marjeta.cesen@ijs.si

Increasing consumption and toxicity of cytostatic drugs raises concerns about their presence in the environment. In the absence of certified reference materials, interlaboratory comparisons are necessary if laboratories are to have confidence in their analytical abilities. The objective of this study was to perform an interlaboratory comparison to determine cyclophosphamide, ifosfamide, methotrexate and etoposide in surface water, wastewater and hospital wastewater. Laboratory performances were evaluated using z-score values, mean and median values, standard deviations (σ), repeatability and reproducibility. Overall, sample preparation was satisfactory. The smallest absolute differences between spiked values and participant's results were observed in surface waters. Repeatability was highest for methotrexate in all matrices and for three laboratories using LC-MS/MS (CV $\leq$ 12 %). Overall reproducibility was poor (CV: 27 % - 143 %) with the exception of MTX in sample C (CV: 8 %). This may be justified by the low number of participating laboratories.

MEDNARODNA
PODIPLOMSKA ŠOLA
JOŽEFA STEFANA

JOŽEF STEFAN
INTERNATIONAL
POSTGRADUATE SCHOOL

First worldwide interlaboratory study on cytostatic compounds in aqueous samples

Marjeta Česen, Tina Kosjek, Ester Heath

Jožef Stefan International Postgraduate School
(programme Ecotechnology)
Supervisor: Assoc. Prof. Dr. Ester Heath, co-supervisor: Dr. Tina Kosjek
Jožef Stefan Institute, Department of Environmental Sciences, Ljubljana, Slovenia

INTRODUCTION

Cytostatics as highly hazardous compounds have the potential to exhibit adverse effects on non-target organisms including cytotoxicity, genotoxicity, mutagenicity and teratogenicity in aqueous environment. This means that accurate and precise analysis of these compounds in environmental samples is necessary if they are to be monitored and controlled.The aim of this study was to perform an interlaboratory exercise for determining four commonly prescribed cytostatic drugs: cyclophosphamide (CP), ifosfamide (IF), etoposide (ETO) and methotrexate (MTX) in natural and wastewaters

CP

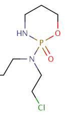

IF

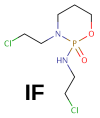

ETO

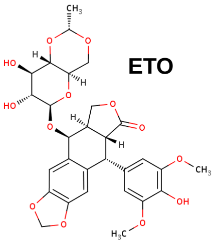

MTX

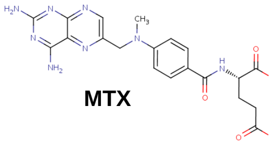

MATERIALS AND METHODS

Since no CRMs avaliable –> INTERLABORATORY COMPARISON

PURPOSE: information of participant measurement capabilities with respect to other laboratories and improving the quality of analytical results

participating laboratories from
Czech Republic,
The Netherlands,
Singapore, **Slovenia**,
Spain (2 laboratories), **UK**

LAB CODE	1	2	3	4	6	8	9
TECHNIQUE	LC/ MS-MS	LC/ MS-MS	LC/ MS-MS	UPLC/ MS-MS	LC/ MS-MS	LC/ MS-MS	GC/ MS
COMPOUNDS	CP, IF, ETO MTX	CP	CP, IF, ETO	CP, IF, MTX, ETO	CP, IF, MTX, ETO	CP, IF	CP, IF

Each participant received 4 samples:
- •spiked surface water (**A**)
- •non-spiked hospital wastewater (**B**)
- •spiked hospital wastewater (**C**)
- •spiked wastewater effluent (**D**)

	Spiked conc. (ng L^{-1})			
Sample/Compound	**CP**	**IF**	**ETO**	**MTX**
A	53	33	52	31
B	0	0	0	0
C	5239	394	3420	1141
D	23	55	127	432

Statistical evaluation of received data: z-score values (outliers), mean and median values, standard deviations (σ), repeatability (r) and reproducibility (R)

RESULTS AND DISCUSSION

- ❑ 219 data received -> 210 used in statistical evaluation (**3 outliers**, 6 <LOD)

  sample A: smallest absolute differences for **all compounds** (spiked values and mean/median values)

- ❑ **REPEATABILITY:**
  - highest for **MTX** in **all samples** (CVs ≤12 %)
- ❑ **REPRODUCIBILITY**:
  - **CVs high** (27 % ≤ CV ≤ 143 %), except for MTX in sample C,
  - large differences amongst samples,
  - low number of participating laboratories (ETO: 3 and MTX: 4).

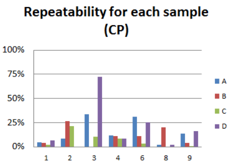

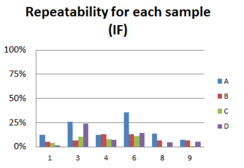

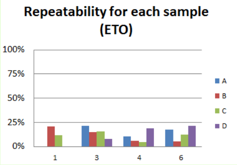

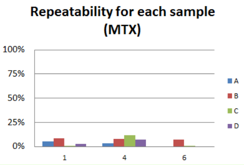

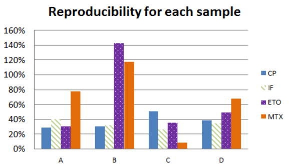

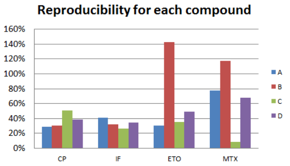

Acknowledgements
This work was financially supported by the EU through the EU FP7 project CytoThreat (Fate and effects of cytostatic pharmaceuticals in the environment and the identification of biomarkers for and improved risk assessment on environmental exposure (grant agreement No.: 265264) and by the Slovenian Research Agency ((program groups P1-0143 and L1-5457 and young researcher grant to M. Č.).

Occurrence and fate of benzophenone-type UV filters in the aqueous environment

Kristina Kotnik[1,2,3], **Tina Kosjek**[1], **Uroš Kranjc**[3], **Ester Heath**[1,2]
[1] Department of Environmental Sciences, Jožef Stefan Institute, Ljubljana, Slovenia
[2] Jožef Stefan International Postgraduate School, Ljubljana, Slovenia
[3] Ecological Engineering Institute Ltd, Maribor, Slovenia
kristina.pestotnik@ijs.si

This study evaluates the occurrence of five benzophenone-type UV filters in the aqueous environment and their behaviour under the influence of artificial and natural light. Analysis of fourteen water and sediment samples from lakes, rivers and sea revealed the presence of UV filters in the majority of the surface waters ≤ 820 ng L^{-1} (2-hydroxy-4-methoxybenzophenone) and up to 650 ng g^{-1} of benzophenone in sediment samples. The results of photodegradation studies were consistent with previous studies, indicating a high photostability of UV filters during 7 h of irradiation using either a monochromatic low pressure or medium pressure mercury lamp. Solar irradiation experiments also showed UV filters are photostable compounds, since no significant degradation was observed after 2 weeks of exposure to natural sunlight. However, 4 weeks of irradiation did result in elimination of ≤ 80 % of studied compounds.

MEDNARODNA
PODIPLOMSKA ŠOLA
JOŽEFA STEFANA

JOŽEF STEFAN
INTERNATIONAL
POSTGRADUATE SCHOOL

Occurrence and Fate of Benzophenone-type UV Filters in the Aqueous Environment

Kristina Kotnik, mag. farm.

Supervisor: Assoc. Prof. Dr. Ester Heath
Co-supervisor: Dr. Tina Kosjek

Jožef Stefan International Postgraduate School (Ecotechnology)
Jožef Stefan Institute, Department of Environmental Sciences, Ljubljana, Slovenia

INTRODUCTION

UV filters are a broad class of compounds used in cosmetic products, sunscreens and as additives in products such as textiles, plastics and coatings. Their increasing use leads to a widespread occurrence of UV filters in the environment, where they are recognised as emerging organic pollutants. The focus of this study was to evaluate the occurrence of five benzophenone-type UV filters in the aqueous environment and to investigate their behaviour and fate under the influence of artificial UV light and natural sunlight.

METHODS and MATERIALS

SAMPLE COLLECTION:

14 water & sediment samples, collected from rivers, lakes, sea sites and rivers near wastewater treatment plants (WWTPs)

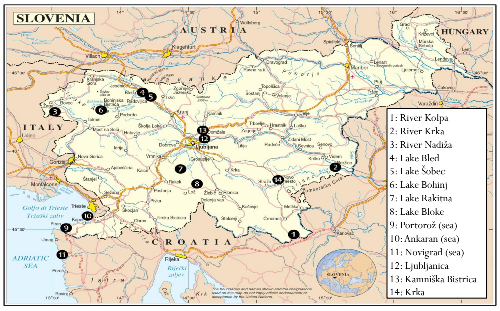

CHEMICAL ANALYSIS:

water samples → Solid Phase Extraction (SPE) ⟶ derivatization → GC-MSD

sediment samples → Microwave Assisted Extraction (MAE) → SPE clean-up ↗

CHEMICAL STRUCTURES OF THE STUDIED UV FILTERS

IUPAC name, INCI name	Abbreviation	Chemical structure	Mw	Log K_{ow}
Benzophenone	BP	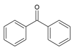	182	3.2
4-hydroxybenzophenone	H-BP	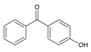	198	2.9
2,4-dihydroxybenzophenone Benzophenone-1	DH-BP	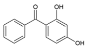	214	3.2
2-hydroxy-4-methoxybenzophenone Benzophenone-3	HM-BP	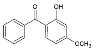	228	3.6
2,2'-dihydroxy-4-methoxybenzophenone Benzophenone-8	DHM-BP	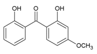	244	3.9

UV IRRADIATION

UV lamp
- MP (medium pressure)
- LP (low pressure)

SOLAR IRRADIATION

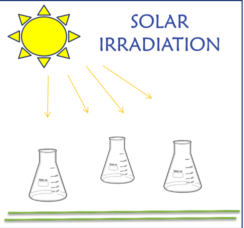

RESULTS

UV filter	Concentration range									
	Water (ng L^{-1})					Sediment (ng g^{-1})				
	Freq.	**Lake**	**River**	**Sea**	**River (WWTP)**	Freq.	**Lake**	**River**	**Sea**	**River (WWTP)**
BP	14/14	33-120	30-88	51-56	54-190	14/14	220-360	610-650	270-280	38-190
H-BP	5/14	7.2-8.4	<LOD	4.1-5.1	<LOD	0/14	<LOD	<LOD	<LOD	<LOD
HM-BP	14/14	38-820	9.4-120	96-380	5.9-24	14/14	10-17	23-32	10-13	2.5-7.4
DH-BP	10/14	2.9-130	1.9-11	5.6-11	2.9-3.2	7/14	2.5-3.7	2.6-3.5	2.0	3.1
DHM-BP	6/14	2.6-6.5	<LOD	2.4-5.3	<LOD	0/14	<LOD	<LOD	<LOD	<LOD

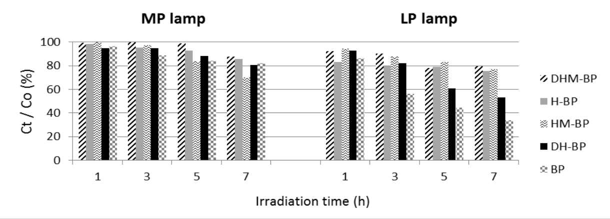

SOLAR IRRADIATION

- H-BP, HM-BP and DHM-BP:
  removal of approx. 40 % after 4 weeks of irradiation
- BP, DH-BP:
  removal of approx. 80 % after 4 weeks of irradiation
  pseudo-first-order elimination kinetics
  BP: $t_{1/2}$ = 13.3 days
  DH-BP: $t_{1/2}$ = 12.4 days

CONCLUSION

Results show that benzophenone-type UV filters are present in the aquatic environment, both in water and sediments. Photodegradation studies show that they exhibit high photostability indicating the potential of being persistent in the environment. Due to increasing consumption and possible toxic effects of UV filters on aquatic ecosystems, it is crucial to further investigate their presence in different environmental compartments and to better understand their environmental behaviour, cycling and fate.

Acknowledgements

The work was financially supported by the European Union (European Social Fund), by the Slovenian Research Agency (program group P1-0143) and Project L1 5457.

Investing in your future
Operation Part Financed By The European Union
European Social Fund

Dynamics of cave air ventilation in a dead-end passage of Postojna Cave (Pisani rov-Colourful gallery)

Bor Krajnc[1], Sonja Lojen[2], Janja Vaupotič[2], David Dominguez-Villar[3], Nives Ogrinc[2]
[1] Jožef Stefan International Postgraduate School, Ljubljana, Slovenia
[2] Department of Environmental Sciences, Jožef Stefan Institute, Ljubljana, Slovenia
[3] Centro Nacional de Investigación sobre la Evolución Humana, Burgos, Spain
bor.krajnc@ijs.si

The dynamics of cave ventilation is interesting for different fields of science e.g. speleology, paleoclimatology, ecosystem carbon dynamics research etc. This work is a preliminary research of a bigger project where the influences of subterranean CO_2 storage to the adjacent soil CO_2 effluxes will be studied. We studied the patterns and possible causes of cave ventilation in Pisani rov, a dead-end passage of the Postojna Cave. We used CO_2 concentrations and ^{222}Rn activity concentrations in cave air as indirect indicators of cave ventilation. To gain more information on the origin of cave air CO_2, stable carbon isotope analyses of cave air were performed. First results show that CO_2 and ^{222}Rn concentrations correspond to the temperature differences between cave and outside air. Further, the increase in cave CO_2 concentrations is related to the CO_2 derived from remineralized organic carbon.

MEDNARODNA
PODIPLOMSKA ŠOLA
JOŽEFA STEFANA

JOŽEF STEFAN
INTERNATIONAL
POSTGRADUATE SCHOOL

Dynamics of cave air ventilation in a dead-end passage of Postojna Cave (Pisani rov-Colourful gallery)

Bor Krajnc[1], Sonja Lojen[2], Janja Vaupotič[2], David Domínguez-Villar[3], Nives Ogrinc[2]
[1]Jožef Stefan International Postgraduate School, Ljubljana, Slovenia
[2]Department of Environmental Sciences, Jožef Stefan Institute, Ljubljana, Slovenia
[3]Centro Nacional de Investigación sobre la Evolución Humana, Burgos, Spain
bor.krajnc@ijs.si

Investing in your future
Operation part financed by the European Union
European Social Fund

Introduction

Cave ventilation can be an interesting process for studies of soil ecosystem CO_2 effluxes on calcareous areas. It has been shown that beside biological fluxes, also other processes such as carbonate weathering and ventilation of subterranean caves and cavities can contribute to those fluxes on such areas[1]-[7]. The presented work is a result of preliminary studies of a bigger project, where influences of abiotic CO_2 sources to the karstic forest soil CO_2 fluxes will be studied. Herein the aim of this work is to find patterns and possible causes of cave ventilation in Pisani rov, a dead-end passage from the Postojna Cave. CO_2 concentrations and ^{222}Rn activity concentrations were measured in cave air as indirect indicators of cave ventilation, while stable isotope composition of CO_2 was used to determine its possible sources.

Study area

Pisani rov (Colourful Gallery), a dead-end passage is a 920 m long horizontal passage which deviates from the main Postojna Cave passage to the north (Fig. 1) and terminates below the slopes of the Velika Jeršanova doline where the thickness of the cave celling is estimated to be around 30m [8]. At the end of Pisani rov we have five sampling locations (Fig. 2).

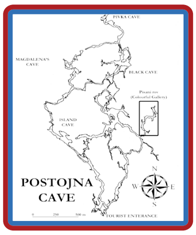

Figure 1: Location of Pisani rov in Postojna Cave (adopted from [9])

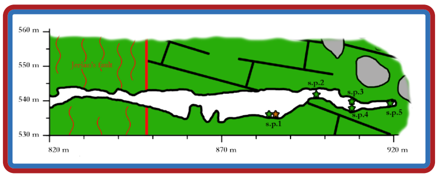

Figure 2: Cross section of the end of Pisani rov with marked sampling points (s.p.) (adopted from [10])

Methods

- Sampling performed twice a month in 2009, 2010, 2013 and 2014.
- Air for stable isotope analysis sampled from the five sampling points (Fig. 2).
- Stable isotope composition of cave air CO_2 determined with CF-IRMS (EUROPA 20-20) connected to ANCA-TG preparation module
- CO_2 concentration measured with TESTO 435, multi-functional measurement instrument.
- ^{222}Rn activity concentrations determined with alpha-scintillation cells (only first sampling point).
- Outside temperatures data gathered from the nearby meteorological station in Postojna.

Results and discussion

- Increase in outside temperature corresponds to the CO_2 concentration increase in the cave atmosphere and the decrease of the outside temperature causes a ventilation effect in the cave, which was also reflected in the decrease of CO_2 concentrations (Fig. 3).
- Stable isotope analysis of cave air CO_2 reveal that higher C_{CO2} corresponds to more negative $\delta^{13}C_{CO2}$ values (Fig. 3). This indicates more pronounced influence of remineralized organic carbon to CO_2.
- When low CO_2 concentrations in the cave air were observed, the $\delta^{13}C_{CO2}$ values were more positive (marked with blue arrows) suggesting the mixing of cave air with fresh outside air ($\delta^{13}C_{CO2} \approx -8‰$) and forced degassing of CO_2 from the drip waters.

*Operation part financed by The European Union, European Social Fund.

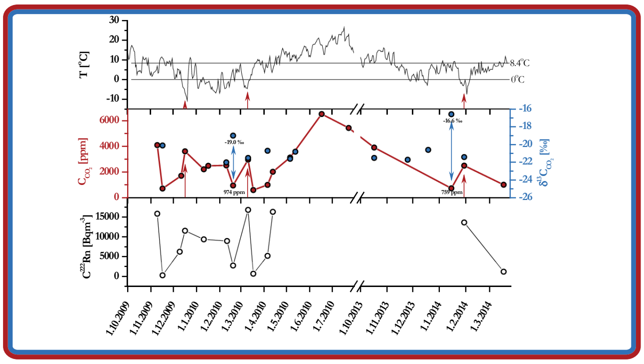

Figure 3: Average daily temperatures, cave air CO_2 concentrations (C_{CO2}), stable carbon isotope composition of cave CO_2 ($\delta^{13}C_{CO2}$) and radon activity concentrations ($C^{222}Rn$)

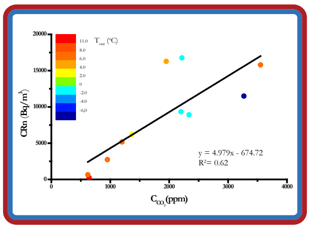

Figure 4: Correlation between ^{222}Rn and C_{CO2} with outside temperature colour scale

A positive correlation ($R^2 = 0.62$) between C_{CO2} and radon activity concentration ($C^{222}Rn$) was observed during the sampling periods in 2010 (Fig. 4). Concentrations of both gases increase during "stocking" period and decrease towards atmospheric values (≈380 ppm for C_{CO2} and ≈10-30 Bq m-3 for $C^{222}Rn$) during ventilation periods.

Conclusions

- Ventilation pattern with winter ventilation and summer stagnation periods.
- Main factor controlling the ventilation in Pisani rov is the difference in inside and outside air densities causing convective flow of the cave air.
- During ventilation periods the warm cave air could be pressed to the outside atmosphere through unknown fissures and cracks.
- During high CO_2 concentrations there is a pronounced influence of remineralized organic carbon to cave CO_2.
- Long-term studies related to cave ventilation and their influence on soil CO_2 fluxes will help us to understand the mechanisms in the ecosystem C budget and its relation to global environmental changes.

References

[1] M. Ferlan, G. Alberti, K. Eler, F. Batič, A. Peressotti, F. Miglietta, A. Zaldei, P. Simončič, D. Vodnik. Comparing carbon fluxes between different stages of secondary succession of a karst grassland. *Agriculture, Ecosystems & Environment*, 140 (1-2): 199–207, 2011.
[2] G. Plestenjak, K. Eler, D. Vodnik, M. Ferlan, M. Čater, T. Kanduč, P. Simončič, N. Ogrinc. Sources of soil CO2 in calcareous grassland with woody plant encroachment. *Journal of Soils and Sediments*, 12 (9): 1327–1338, 2012.
[3] M. Čater and N. Ogrinc. Soil respiration rates and δ13C(CO2) in natural beech forest (Fagus sylvatica L.) in relation to stand structure. *Isotopes in environmental and health studies*, 47 (2): 221–237, 2011.
[4] A.S. Kowalski, P. Serrano-Ortiz, I.A. Janssens, S. Sánchez-Moral, S. Cuezva, F. Domingo, A. Were, L. Alados-Arboledas. Can flux tower research neglect geochemical CO2 exchange? *Agricultural and Forest Meteorology*, 148 (6–7): 1045–1054, 2008.
[5] S. Cuezva, A. Fernandez-Cortes, D. Benavente, P. Serrano-Ortiz, A.S. Kowalski, S. Sanchez-Moral. Short-term CO2(g) exchange between a shallow karstic cavity and the external atmosphere during summer: Role of the surface soil layer. *Atmospheric Environment*, 45 (7): 1418–1427, 2011.
[6] P. Serrano Ortiz, S. Cuezva Robleño, A.S. Kowalski, S. Sánchez Moral. Cuantificación y procedencia de los intercambios de CO2 en un ecosistema carbonatado mediante la técnica de eddy covariance y el análisis de los isótopos estables de carbono. *Ecosistemas*, 19 (3): 41–46, 2010.
[7] O. Pérez-Priego, P. Serrano-Ortiz, E.P. Sánchez-Cañete, F. Domingo, A.S. Kowalski. Isolating the effect of subterranean ventilation on CO2 emissions from drylands to the atmosphere. *Agricultural and Forest Meteorology*, 180 (0): 194–202, 2013.
[8] S. Šebela. Accesses from the surface to the Postojna Cave system. *Annales. Series historia naturalis*, 20 (1): 55–64, 2010.
[9] T.R. Shaw. *Names from the past in Postojnska jama (Postojna cave)*. ZRC Publishing, 2006.
[10] S. Šebela and J. Čar. Velika Jeršanova doline - a former collapse doline = Velika Jeršanova dolina - nekdanja udornica. *Acta carsologica*, 29 (2): 201–212, 2000.

Determination of elements in river sediments at some selected Slovenian streams

Ana Kroflič[1,2], **Mateja Germ**[3], **Vekoslava Stibilj**[1]

[1] Department of Environmental Sciences, Jožef Stefan Institute, Ljubljana, Slovenia

[2] Jožef Stefan International Postgraduate School, Ljubljana, Slovenia

[3] Biotechnical Faculty, University of Ljubljana, Ljubljana, Slovenia

ana.kroflic@ijs.si

Industry, traffic and agriculture are main sources of environmental pollution. Pollutants are released into river and are eventually accumulated into sediments. Investigation of elements Cr, Cu, Zn, As, Se, Cd and Pb in sediments was the main goal of our study.

Before the determination, the samples need to be digested, which in not an easy task. Optimization of acid digestion in microwave oven, using HF, HCl and HNO_3 was made. For the determination of elements in sediments from selected streams in Notranjska and Central regions of Slovenia, optimized method has been used. Recorded concentration ranges were: 25 - 77 mg Cr kg^{-1}, 6 - 48 mg Cu kg^{-1}, <LOD - 1102 mg Zn kg^{-1}, 2 - 13 mg As kg^{-1}, <LOD - 0.4 mg Se kg^{-1}, <LOD - 1.2 mg Cd kg^{-1} and 14 - 23 mg Pb kg^{-1}. Investigated areas are mainly agricultural. Compared to rivers flowing through agricultural areas higher concentrations of some elements (Cr, Zn and Pb) were noticed in rivers that flow through industrial area.

Institut
”Jožef Stefan”
Ljubljana, Slovenija

MEDNARODNA
PODIPLOMSKA ŠOLA
JOŽEFA STEFANA

JOŽEF STEFAN
INTERNATIONAL
POSTGRADUATE SCHOOL

Determination of elements in river sediments at some selected Slovenian streams

Ana Kroflič, Mateja Germ, Vekoslava Stibilj
Study programme: Ecotechnology
Supervision: prof. dr. Vekoslava Stibilj
Institut Jožef Stefan, Jamova 39, 1000 Ljubljana
Jožef Stefan International postgraduate school, Jamova 39, 1000 Ljubljana

INTRODUCTION

Growing human population and related human activities have caused higher emission of various pollutants into the environment. Pollutants are released into aquatic system and they are eventually accumulated into sediments (atmospheric decomposition, industrial and agricultural activities).Research of element concentrations in sediments are good indicator for level of pollution. Because sediments are persistent material, digestion methods with different mineral acids is needed. The digestion of sediments is not easy task. In literature the mostly used method for digestion of sediment is acid digestion with various ratio and combination of acid such as HCl, HNO_3, HF, and $HClO_4$.

Aims of our study:

- **optimization of digestion procedure for elements (Cr, Cu, Zn, As, Se, Cd and Pb) in river sediments (microwave oven),**
- **determination of elements in river sediments at three selected Slovenian streams which flows through agricultural area.**

EXPERIMENTAL WORK

Sampling and sample preparation:

- Three streams in Notranjska and Central regions of Slovenia (Pšata, Lipsenjščica and Žerovniščica) (Fig. 1),
- Sampling performed in different months in 2009, 2010 and 2011,
- Samples were sieved and particles < agate bowls

Fig. 1: Sampling sites

Determination and detection:

- Around 0.25 g of milled sediments were digested,
- Digestion was made in two steps with digestion procedure 6 (Table 1),
- Digested samples were detected with ICP-MS (7500ce Agilent Technologies).

RESULTS AND DISCUSSION

Optimization of digestion:

- Digestion where 4 ml HNO_3, 2 ml HF and 1 ml HCl were used in a first step (30 min ramp to 210 °C, 60 min hold on 210 °C) and adding of 15 ml 4% H_3BO_3 in second step (15 min ramp to 220 °C, 30 min hold on 220 °C) (procedure 6, Table 1) showed a good agreement of certified (CRM 320R) and obtained values (Table 2).

Table 1: Temperature programmes for digestion optimization

Digestion procedure	First step of digestion		Second step of digestion	
	Chemicals	Temp. programme	Chemicals	Temp. programme
1	4 ml HNO_3 2 ml HF 1 ml HCl	30 min to 200 °C 45 min on 200 °C 1200 W	H_3BO_3	15 min to 200 °C 30 min on 200 °C 1200 W
2		30 min to 200 °C 60 min on 200 °C		
3		30 min to 220 °C 60 min on 220 °C	15 ml 4 % H_3BO_3	15 min to 220 °C 30 min on 220 °C
4		30 min to 230 °C 60 min on 230 °C		15 min to 230 °C 30 min on 230 °C
5		30 min to 200 °C 60 min on 200 °C		15 min to 220 °C 30 min on 220 °C
6		30 min to 210 °C 60 min on 210 °C		

Table 2: Comparison of obtained and certified values of digestion procedure 6 (mg kg^{-1})

	Cr	Cu	Zn	As	Se	Cd	Pb
Certified v.[a]	59.0 ± 4.0	46.3 ± 2.9	319 ± 20	21.7 ± 2.0	0.96 ± 0.18[b]	2.64 ± 0.18	85.0 ± 5.0
Obtained v.[c] (9)	55.1 ± 4.8	48.1 ± 6.5	317 ± 26	21.5 ± 1.9	0.97 ± 0.19	2.72 ± 0.26	88.1 ± 8.7

(9) - number of determination

[a] Results are given as certified values with uncertainty

[b] Result is given as indicative value with uncertainty

[c] Results are given as determined values with standard deviation or absolute error (n=2)

Elements in river sediments:

- Limits of detection for Cr, Cu, Zn, As, Se, Cd and Pb are 3.15, 4.81, 66.9, 0.19, 0.36, 0.25 and 1.01 mg kg^{-1}, respectively (Table 3),
- Concentrations of selected elements did not change much during consecutive years 2009 - 2011 (Table 3),
- At all three sediments, concentrations of elements are practically similar (exception is Zn in Lipsenjščica in 2011),
- Sequences of an average concentrations in sediments are; Zn>Cr>Pb>Cu>As>Cd>Se,
- Toxic elements Pb and Cd are in low concentrations,
- Lower concentrations of elements in sediments at selected Slovenia streams than in literature value (exception is Zn),
- Selected streams flows through agricultural area and values are lower then in Sava River (Milačič, et. al., 2010), which flows through industrial area.

Table 3: Determination of elements in river sediments (mg kg^{-1})

		#	Cr	Cu	Zn	As	Se	Cd	Pb
Detection limits			3,15	4,81	66,9	0,19	0,36	0,25	1,01
Stream	Year								
Pšata	2009	4	60.4 ± 11.9	11.8 ± 1.7	80.8 ± 10.7	4.00 ± 0.88	<LOD	0.29 ± 0.06	19.4 ± 3.9
	2010	2	775 ± 5.6	31.4 ± 11.1	<LOD	5.29 ± 0.34	<LOD	<LOD	14.4 ± 1,0
	2011	4	51.3 ± 17.3	10.5 ± 2.2	<LOD	4.57 ± 0.34	<LOD	<LOD	18.9 ± 7.7
Lipsenjščica	2009	2	64.4 ± 3.9	8.82 ± 1.32	<LOD	12.2 ± 0.4	<LOD	0.32 ± 0.08	23.4 ± 1.1
	2010	2	67.0 ± 3.0	13.9 ± 1,0	<LOD	12.6 ± 0.6	<LOD	0.39 ± 0.01	18.8 ± 1.1
	2011	2	65.4 ± 0.5	31.4 ± 0.2	1101 ± 58	11.0 ± 0.8	0.44 ± 0.17	1.18 ± 0.08	51.2 ± 0.9
Žerovniščica	2009	4	25.0 ± 13.8	12.3 ± 1.7	<LOD	2.37 ± 1.00	<LOD	0.27 ± 0.11	14.2 ± 5.6
	2010	4	31.3 ± 2.3	48.2 ± 9.8	72.2 ± 5.3	3.58 ± 0.82	<LOD	0.63 ± 0.49	16.6 ± 10.6
	2011	4	39.0 ± 28.2	4.5 ± 1.5	<LOD	4.07 ± 1.67	<LOD	0.37 ± 0.14	21.8 ± 20.7

#-number of determination

Results are given as average values with standard deviation or absolute error (n=2)

Table 4: Concentration ranges of selected elements (mg kg^{-1})

	Cr	Cu	Zn	As	Se	Cd	Pb
our study	25-77	6-48	<LOD-1102	2-13	<LOD-0.4	<LOD-1.2	14-23
Sava river (Milačič et. al., 2010)	23-381	11-50	55-361	3-25	/	0.2-1.4	12-122
Gallians river, USA (Martinez et. al., 2011)	/	16-50	72-683	2-9	/	0.3-6.7	17-63
Rivers in Turkey (Akcay et. al., 2013)	160-220	108-152	85-185	/	/	/	35-140
Xiangjiang, China (Sun et. al., 2012)	34-130	19-162	53-1099	1-47	/	1-56	40-431

FUTURE WORK

- Investigation of elements concentration in water and macrophytes on same sampling sides (bioaccumulation factor for selected elements in macrophytes).

REFERENCES

- R. Milačič, et. al.. A complex investigation of the extant pollution in sediments of the Sava River. Part 1: Selected elements. *Environ. Monit. Assess.*, 163:263-275, 2010 .
- W. Sun, et. al.. Trace metals in sediments and aquatic plants from the Xiangjiang River, China. *J. Soils Sediments*, 12:1649-1657, 2012.
- E. A. Martinez, et. al.. Determination of selected heavy metal concentrations and distribution in a southwestern stream using macrophytes. *Ecotox. Environ. Safe.,* 74:1504-1511, 2011.
- H. Akcay, et. al.. Study of heavy metal pollution and speciation in Buyak Menderes and Gediz river sediments. *Water Res.,* 37:813-822, 2003.

Geochemical investigation of molecular and isotopic composition and origin of coal seam gas in Velenje Basin

Jerneja Lazar[1,2]**, Tjaša Kanduč**[3]**, Sergej Jamnikar**[1, 2]**, Fausto Grassa**[4]
Simon Zavšek[1]
[1] Velenje Coal Mine, Velenje, Slovenia
[2] Jožef Stefan International Postgraduate School, Ljubljana, Slovenia
[3] Department of Environmental Sciences, Jožef Stefan Institute, Ljubljana, Slovenia
[4] Instituto Nazionale di Geofisica e Vulcanologia Sezione di Palermo, Italy
jerneja.lazar@rlv.si

The concentration of methane and carbon dioxide of coal seam gas, molecular and stable carbon isotope composition of methane and carbon dioxide, and stable hydrogen isotope composition of methane was investigated in the Velenje Basin. The aim was to obtain a better understanding of its origin and behaviour in advancement of the longwall face due to the high risk of CO_2 gas outbursts, and to obtain knowledge on the distributional behaviour of coal seam gases with advance of the longwall face. The average coal seam gas composition in the Velenje Basin is approximately CO_2:CH_4 $\geq$ 2:1. The study revealed that at a distance of around 100 m from the working face, the influence of face dynamics causes gas to migrate. Stable carbon isotope composition of methane and CO_2 indicates that methane was generated via acetate fermentation and reduction of CO_2. Secondary processes were induced by active mining causing the enrichment of residual methane with ^{13}C isotope.

GEOCHEMICAL INVESTIGATION OF MOLECULAR AND ISOTOPIC COMPOSITION AND ORIGIN OF COAL SEAM GAS IN VELENJE BASIN

Jerneja Lazar[1, 2], Tjaša Kanduč[3], Sergej Jamnikar[1, 2], Fausto Grassa[4], Simon Zavšek[1]
Study programme: Ecotechnology
Supervision: prof. dr. Sevket Durucan, dr. Simon Zavšek

[1] Velenje Coal Mine, Velenje, Slovenia
[2] Jožef Stefan International Postgraduate School, Ljubljana, Slovenia
[3] Department of Environmental Sciences, Jožef Stefan Institute, Ljubljana, Slovenia
[4] Instituto Nazionale di Geofisica e Vulcanologia Sezione di Palermo Italy

INTRODUCTION

Velenje Coal Basin is one of the basins with the thickest coal seam (up to 160 m) in the world and represents a large reservoir for coal seam gas with a mixture of carbon dioxide (CO_2) and methane (CH_4). Set of geochemical monitoring of coal seam gas was established in Velenje Coal Mine at different active mine areas with the aim to determine coal seam gas distribution in advancement of the working face, to determine the isotopic composition and origin of coal seam gas and to compare the results with other coal basins.

METHODS

- Coal seam gas sampling from boreholes (25 m long);
- Concentrations determination of CH_4, CO_2, N_2, O_2 and Ar was performed by using a custom-made NIER type mass spectrometer at Jožef Stefan Institute, Ljubljana;
- The isotopic composition of CH_4 ($\delta^{13}C_{CH4}$) and CO_2 ($\delta^{13}C_{CO2}$) was determined using an Europa 20-20 continuous flow isotope ratio mass spectrometer (CF-IRMS) with an ANCA-TG preparation module;
- Determinations of the $^2H/H$ ratio of CH_4 were performed on a Thermo Delta XP GC-TC/CF-IRMS coupled to a TRACEGC analyser at Istituto Nazionale di Geofisica e Vulcanologia Sezione di Palermo in Italy;
- Higher hydrocarbons were analysed with a Shimadzu 2010 gas chromatographic system with He as carrier gas and equipped with a Poraplot Qcolumn and FID detector;

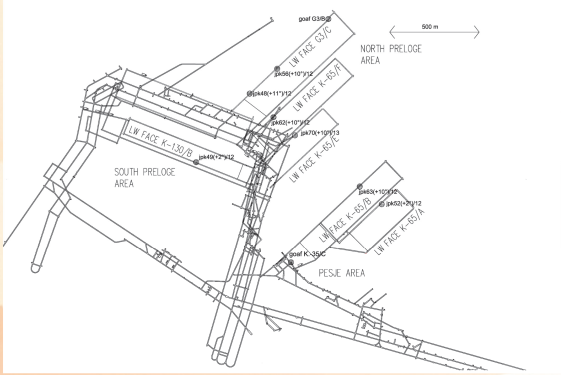

Figure 1: Gas sampling locations in Coal Mine Velenje.

RESULTS AND DISCUSSION

- Dynamic approach of the working longwall face influences on stress situation in front of the longwall face and consequently influences on coal seam gas migration in the excavated coal panel (around 70 m in front of the face) (Figure 2);
- High values of the CDMI (= $[CO_2/(CO_2+CH_4)]100$ (%)) index and $\delta^{13}C_{CO2}$ values between -7.0 to -1.8‰ indicate endogenic CO_2 and microbial CO_2 (Figure 3);
- Area of North Preloge Mine (face G3/C) lies on the carbonate floor strata and the $\delta^{13}C_{CO2}$ show CO_2 origin from thermal decomposition of dolomites;
- High CDMI index (up to 98.2%) and $\delta^{13}C_{CO2}$ values between -2.4 and -1.8‰ show that the origin of CO_2 at K.-65/B in Pesje area is endogenic mixed with microbial CO_2;
- $\delta^{13}C_{CH4}$ and δ^2H_{CH4} reveal that the coal seam gas in the Velenje Basin has mixed origin (microbial, thermogenic and mixed).

Figure 2: Distribution of gas concentration in advancement of the longwall face K.-65/F in Pesje Mine.

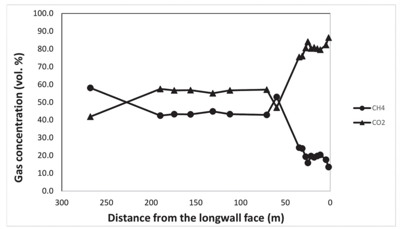

Figure 3: Interpretation of the origin of CO_2 at the longwall faces K.-65/F, G3/C, K.-65/B and K.-65/E.

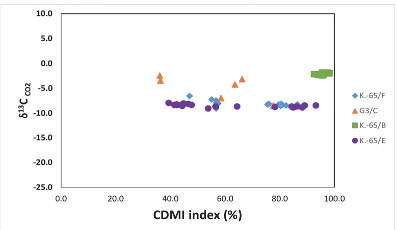

CONCLUSION

- Interpretation of the CH_4 origin in the Velenje Basin is much more complicated (secondary processes) due to excavation of coal and migration of gas, which could lead to additional isotopic fractionation, especially of CH_4;
- All aspects should be taken into account when interpreting the origin of coal seam gas (distance from the longwall, advancement rate of the longwall, location of the excavation fields with depth, pre-mining area and stress state) besides $\delta^{13}C_{CH4}$, $\delta^{13}C_{CO2}$, δ^2H_{CH4} and gas dryness values;
- Further research is required to determine the origin of coal seam gases and higher hydrocarbons in the Velenje Basin which should be correlated with the hydro-geochemical characteristics of the Basin.

Figure 4: Gas dryness (C1/(C2+C3)) versus $\delta^{13}C_{CH4}$ in coal seam gases in Velenje Basin. Gas origin in comparison with the Bowen Basin and the Powder River Basin.

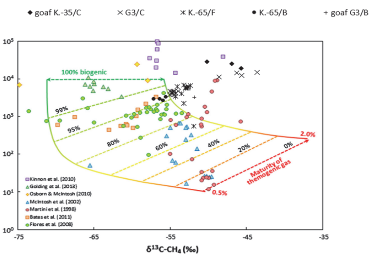

REFERENCES:
M.J. Kotarba. Composition and origin of coalbed gases in the upper Silesian and Lublin basins, Poland. *Organic geochemistry, 163-180,* 2001
D. Strapoć, M. Mastalerz, K. Dawson, J. Macalady, A.V. Callaghan, B. Wawrik, C. Turich, M. Ashby. Biogeochemistry of microbial coal-bed methane. *Ann. Rev. Earth Planet. Sci. 39, 617-656,* 2011
T. Kanduč, M. Markič, S. Zavšek, J. McIntosh. Carbon cycling in the Pliocene Velenje Coal Basin, Slovenia, inferred from stable carbon isotopes. *International Journal of Coal Geology 89, 70 – 83,* 2012

Determination of PBDEs in environmental water samples by GC-ICP-MS

Petra Novak[1,2], **Tea Zuliani**[1], **Radmila Milačič**[1,2], **Janez Ščančar**[1,2]
[1] Department of Environmental Sciences, Jožef Stefan Institute, Ljubljana, Slovenia
[2] Jožef Stefan International Postgraduate School, Ljubljana, Slovenia
petra.novak@ijs.si

Polybrominated diphenyl ethers (PBDEs) belong to the group of brominated flame retardants, which are added to different industrial products such as plastics, textiles, electronic equipment and building materials. Due to their widespread use PBDEs are frequently present as pollutants in all parts of the environment. They belong to lipophilic poorly degradable persistent organic pollutants (POPs) that are via food chain bioaccumulated or biomagnified in living organisms. In human, PBDEs may disrupt thyroid hormones and reproductive organs.
In the EU Water Framework Directive (WFD) six PBDE congeners (BDE 28, BDE 47, BDE 99, BDE 100, BDE 153 and BDE 154) are listed as priority substances. To prevent pollution of the aquatic environment, WFD recommends their regular monitoring. To meet the WFD requirements, highly sensitive analytical procedure for the determination of six PBDEs in environmental water samples by gas chromatography – inductively coupled plasma mass spectrometry (GC-ICP-MS) was developed. To demonstrate the applicability of the newly developed GC-ICP-MS procedure, PBDEs were determined in river and sea water samples.

MEDNARODNA
PODIPLOMSKA ŠOLA
JOŽEFA STEFANA

JOŽEF STEFAN
INTERNATIONAL
POSTGRADUATE SCHOOL

Determination of PBDEs in environmental water samples by GC-ICP-MS

Petra Novak*#, Tea Zuliani*, Radmila Milačič*#, Janez Ščančar*#

*Department of Environmenatal Sciences, Jožef Stefan Institut, Ljubljana, Slovenia
#Jožef Stefan International Postgraduate School, Ljubljana, Slovenia

ABSTRACT: Polybrominated diphenyl ethers (PBDEs) belong to the group of brominated flame retardants, which are added to different industrial products such as plastics, textiles, electronic equipment and building materials. Once such products are disposed of to landfills PBDEs can be easily released into the environment and enter via food chain in living organisms. Increasing concentrations of PBDEs in human tissues have caused worldwide health concerns due to their tendency to disrupt thyroid hormones. The aim of this study was to develop an analytical procedure that would meet the requirements set by the Water Frame Directive (WFD) for very sensible and reliable determination of the six PBDE congeners (28, 47, 99, 100, 153, 154) in the environmental water samples by GC-ICP-MS.

Methods

1. Extraction of PBDEs from water sample into iso-octane

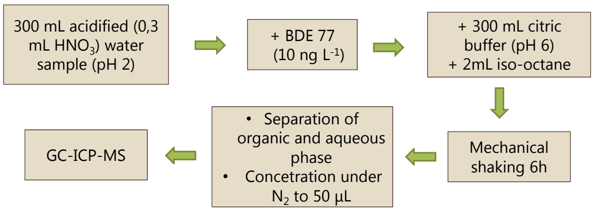

300 mL acidified (0,3 mL HNO_3) water sample (pH 2)

+ BDE 77 (10 ng L^{-1})

+ 300 mL citric buffer (pH 6) + 2mL iso-octane

Mechanical shaking 6h

- Separation of organic and aqueous phase
- Concetration under N_2 to 50 µL

GC-ICP-MS

2. Separation of PBDEs with gas chromatography (GC)

3. Detection of ^{79}Br with inductively coupled plasma mass spectrometry (ICP-MS)

GC operating parameters	
Column	HP-MS5 (15 m x 0,25 mm x 0,25 µm)
Injection mode	splitless
Injection volume	2 µL
Carrier gas (He)	1,5 mL min^{-1}
Inlet temperarure	280 °C
GC temperature program	120 °C to 300 °C (30 °C min^{-1}), 300 °C (5 min)
Transfer line temperature	280 °C
ICP-MS operating parameters	
RF power	1300 W
Carrier gas (Ar)	1,50 L min^{-1}
Optional gas (20 % $^v/_v$ O_2 in Ar)	10 %
Sample depth	6,8 mm
Isotopes measured Br (m/z)	79, 81
Integration time per isotope	0,1 s

Results

Chromatogram of six PBDEs congeners and internal standard BDE 77 (10 ng L^{-1})

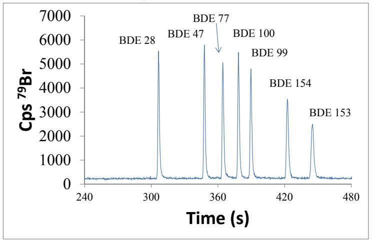

Influence of addition of citric buffer on extraction efficiency of PBDEs into iso-octane

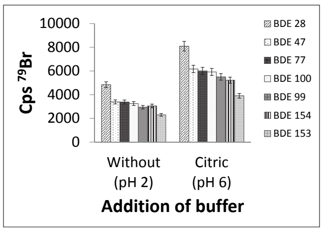

Stability of acidified (A) and non-acidified (B) river water samples

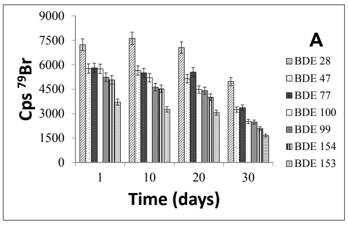

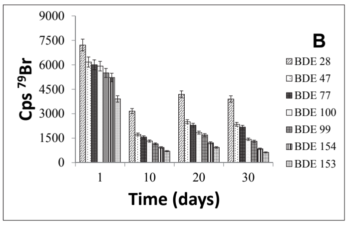

Determination of PBDEs in sea water samples

BDE (ng L^{-1})	Bele skale beach	Strunjan	Izola Dockyard	Port of Koper	Izola Marina
BDE 28	1,14±0,03	< 0,0052	< 0,0052	0,54±0,02	0,053±0,004
BDE 47	< 0,0054	<0,0054	< 0,0054	< 0,0054	< 0,0054
BDE 100	0,16±0,01	< 0,0047	0,19±0,01	0,18±0,01	0,009±0,003
BDE 99	< 0,0051	< 0,0051	0,12±0,004	0,13±0,004	0,074±0,002
BDE 154	< 0,0054	0,15±0,01	0,23±0,01	0,11±0,01	0,051±0,002
BDE 153	< 0,0051	0,21±0,01	0,34±0,02	< 0,0051	0,085±0,002

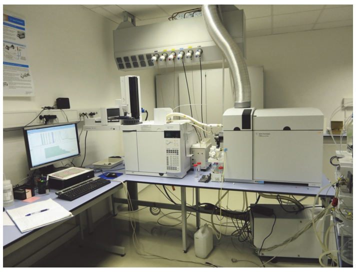

CONCLUSIONS:

A highly sensitive analytical procedure was developed for the determination of six PBDEs in environmental water samples by GC-ICP-MS. The acidification of water samples to pH 2 maintained the PBDEs stability for at least 20 days. The use of Tris-citrate buffer enabled efficient extraction of PBDEs from suspended particulate matter (SPM) and humic acids (HA). To demonstrate the applicability of newly developed procedure, PBDEs were determined in sea water samples.

Isotopically enriched tin tracers: a powerful tool to study the transformation of organotin compounds in landfill leachate

Kelly Peeters[1,2], **Tea Zuliani**[1], **Janez Ščančar**[1,2], **Radmila Milačič**[1,2]

[1] Department of Environmental Sciences, Jožef Stefan Institute, Jamova 39,
Ljubljana, Slovenia
[2] Jožef Stefan International Postgraduate School, Ljubljana, Slovenia
kelly.peeters@ijs.si

The present study is an evaluation of the process of biomethylation and degradation of OTC by microorganisms within leachates. Leachates were each spiked with another Sn-enriched isotopic tracer: ^{117}Sn-enriched tributyltin, ^{117}Sn-enriched $SnCl_2$ and ^{117}Sn-enriched $SnCl_4$. This allowed simultaneous observation of the transformation of OTC in the leachate itself and of the added spike. Based on the analysis of OTC by GC-ICP-MS, The transformation processes in the spiked leachates were followed for 6 months or 10 days. To discriminate between biotic and abiotic transformations, data from sterilized leachates was compared with non-sterilized samples. During the course of the experiment the biotic degradation of TBT to inorganic tin was clearly observed. Methyltin products were only formed when the leachate was spiked with concentrations of $SnCl_2$ or $SnCl_4$, close to that found for total tin in landfill leachates. Hydrolysis of Sn^{2+} and Sn^{4+} species was found to control the extent of methyltin formation.

MEDNARODNA
PODIPLOMSKA ŠOLA
JOŽEFA STEFANA

JOŽEF STEFAN
INTERNATIONAL
POSTGRADUATE SCHOOL

Isotopically enriched tin tracers: a powerful tool to study the transformation of organotin compounds in landfill leachates

Kelly Peeters, Tea Zuliani, Janez Ščančar, Radmila Milačič
Department of Environmental Sciences, Jožef Stefan Institute

Introduction

Organotin compounds (OTC) are chemicals that possess a tin atom, which is covalently bound to 1-4 alkyl or aryl groups [1]. They are highly toxic even at ng L^{-1} concentration levels with high bioacummulation potential [2]. Detectable levels of OTC can be found in several household products which are disposed on landfills. Due to the decomposition of the garbage and by rainfall, OTC are leached out. Hence, landfill leachates can be also considered as an important pool of OTC. Once the OTC entered in the landfill leachate, the present microorganisms significantly influence their transformation processes. Biomethylation result in toxic methyltin formation, while biodegradation of OTC leads to detoxification in the leachate [1]. To better understand the processes that OTC undergo, the emphasis in present work was to follow the degradation and biomethylation of these OTC in leachate by the use of Sn-enriched isotopic tracers.

Landfil leachate

Methods

- Experimental set-up: three duplicates of 3 L amber bottles, each filled with 2 L of landfill leachate sample.
- Spiking: ^{117}Sn-enriched tributyltin (^{117}TBT), $^{117}SnCl_2$ or $^{117}SnCl_4$.
- The transformations the spikes were followed over 10 days or 6 months.
- Derivatisation, extraction and analysis by gas chromatography inductively coupled plasma mass spectrometry (GC-ICP-MS).

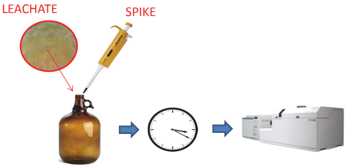

Experimental procedure

Results and discussion

Concentrations of $^{117}Sn^{2+}$ and $^{117}Sn^{4+}$ spikes (100 µg Sn L^{-1}) were close to the total Sn concentrations found in the landfill leachate investigated. The concentrations of methyltin species were determined 3 and 10 days after spiking (Fig. 1).
After 3 days, ^{117}Sn-enriched monomethyltin (^{117}MMeT) was formed from $^{117}Sn^{2+}$ and $^{117}Sn^{4+}$. The extent of ^{117}MMeT formation was higher from $^{117}Sn^{2+}$, presumably due to the higher extent of hydrolysis of Sn^{4+}. During longer incubation ^{117}Sn-enriched dimethyltin (^{117}DMeT) and ^{117}Sn-enriched trimethyltin (^{117}TMeT) were formed.

In the landfill leachate spiked with about 1000 ng L^{-1} ^{117}TBT (containing low amounts of ^{117}DBT), it can be seen that the concentration of ^{117}TBT and ^{117}DBT decreases with time, while ^{117}MBT is formed. This means that TBT degrades to DBT followed by degradation to monobutyltin (MBT) (Fig. 2A). MBT degrades further to ionic tin species. No ^{117}Sn-enriched methyltin species were formed (Fig. 2B).

$$Sn^{2+}\ or\ Sn^{4+} \rightarrow MeSn^{3+} \rightarrow Me_2Sn^{2+} \rightarrow Me_3Sn^{+}$$

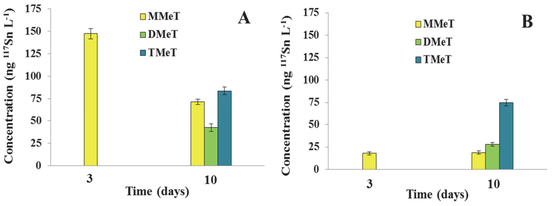

Fig. 1. Formation of methyltin compounds in landfill leachates. The leachate was spiked with (A) 100 µg Sn L^{-1} of ^{117}Sn-enriched $SnCl_2$ or (B) 100 µg Sn L^{-1} of ^{117}Sn-enriched $SnCl_4$. Concentrations were determined at m/z 117.

$$Bu_3Sn^{+} \rightarrow Bu_2Sn^{2+} \rightarrow BuSn^{+} \rightarrow Sn^{4+}$$

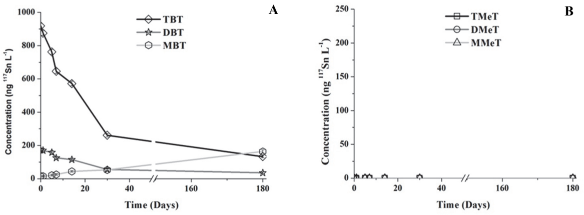

Fig. 2. Transformation of OTC in landfill leachates. The leachate was spiked with ^{117}Sn- enriched TBT (920 ng Sn L^{-1}). Concentrations were determined at m/z 117 for (A) butyltin compounds and (B) methyltin compounds.

Conclusions

- Sn-enriched isotopic tracers provide new insights into the mechanisms of methylation and degradation of OTC in landfill leachates by bacterial strains.
- Under landfill conditions methyltin formation occurred only from inorganic tin. Butyltin concentrations were far too low to produce by degradation sufficient concentration of inorganic tin, which could be further methylated by bacteria.
- Methylation processes were observed from Sn^{2+} and Sn^{4+} ionic tin species.
- Hydrolysis of Sn^{2+} and Sn^{4+} species is a limiting factor, which controls the extent of methyltin formation.

References

[1] Rosenberg, E., 2005. Speciation of Tin. In Handbook of Elemental Speciation II – Species in the Environment, Food, Medicine and Occupational Health. Eds. Cornelis, R., Caruso, J., Crews, H., Heumann, K., John Wiley & Sons, Ltd, Chichester, pp. 422-464.
[2] Fent, K., 2004. Ecotoxicological effects at contaminated sites. Toxicology 205, 223-240.

The influence of climate change on the quality of some Italian wine products: chemical characterization and environmental impacts

Fabio Paolo Polo[1], **Giulio Cozzi**[2], **Nives Ogrinc**[3,4]
[1] Department of Economics, Calle Larga Santa Marta, 2137, 30123 Venice, Italy;
[2] IDPA – CNR, Institute for the Dynamics of Environmental Processes, Calle Larga Santa Marta, 2137, I-30123 Venice, Italy;
[3] Department of Environmental Sciences Jožef Stefan Institute, Ljubljana, Slovenia.
[4] Jožef Stefan International Postgraduate School , Ljubljana, Slovenia.
fabio.polo@unive.it

This study wants to focus on the chemical, environmental and economic consequences of climate change on wine products. Some important vintages of varieties of wine from the North and from the South of Italy are being analyzed for a specific chemical description. The addition analyses of wine's parent musts, rain waters and soils from the grape fields during some specific vintages will give more information on the effects of climatic conditions. Stable isotopes of C and O are commonly used to understand the geographical origin of the wines or to detect illegal sugar additions, but they are also strictly related to temperature and climate change, which is the main target of this work. The stable isotope analysis (IRMS), the single elements analysis (ICP-MS) of metals and Rare Earth Elements in all the set matrices, together with the organoleptic analysis are going to give a complete description of the samples. This paper shows some preliminary results.

THE INFLUENCE OF CLIMATE CHANGE ON THE QUALITY OF ITALIAN WINE PRODUCTS: CHEMICAL CHARACTERIZATION AND ENVIRONMENTAL IMPACTS

Fabio Paolo Polo[1],*, Giulio Cozzi[2], Nives Ogrinc[3]
1 PhD Programme on Science and Management of Climate Change, XXVIII Cycle, Department of Economics,
University of Venice, Ca' Foscari, Dorsoduro 2137, 30123 Venice, Italy.
2 Institute for the Dynamics of Environmental Processes-CNR (IDPA-CNR), Dorsoduro 2137, 30123 Venice, Italy.
3 Department of Environmental Sciences Jožef Stefan Institute, Ljubljana, Slovenia

fabio.polo@unive.it

INTRODUCTION: Climate change and environmental changes are currently the subject of important scientific research, as well as broader political and economic interest, as they can significantly affect the quality of life and human activities, which adversely may affect the climate in general. Although there will be gains in some crops in some regions of the world, the overall impact of climate change on agriculture are expected to be negative, threatening global food security (Antle, 2009). Wine is one of the most valuable Italian products and depends on climatic conditions.

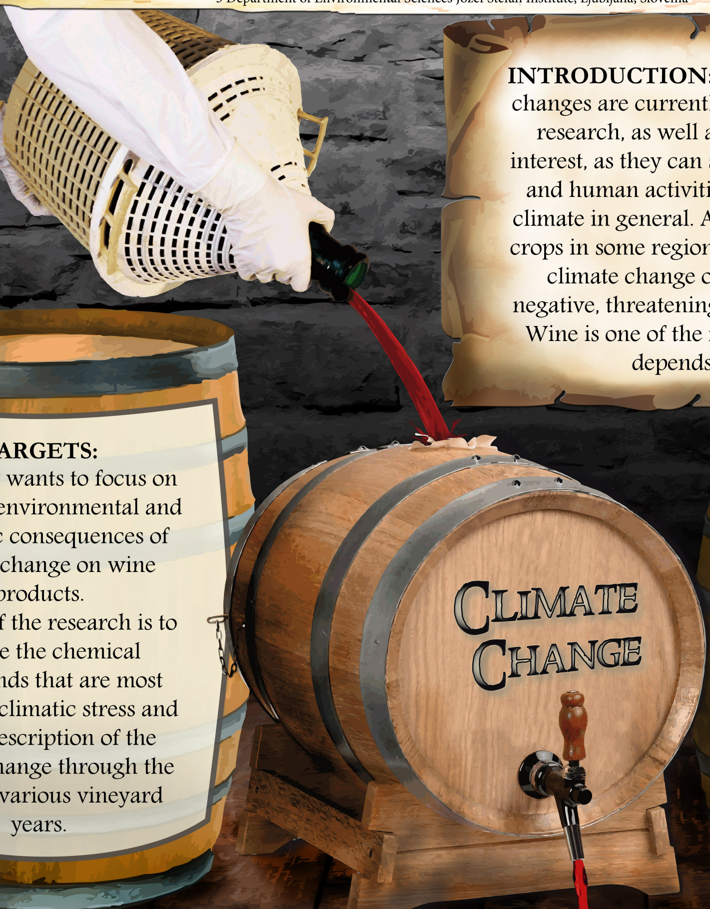

TARGETS:
This study wants to focus on chemical, environmental and economic consequences of climate change on wine products.
The aim of the research is to analyse the chemical compounds that are most related to climatic stress and give a description of the climate change through the study of various vineyard years.

MATERIAL AND METHODS:
In collaboration with the IDPA-CNR of Venice and the Jožef Stefan Institute, several wine and musts typologies from Italy are being analyzed. Past years' isotope ratio of some relevant elements (C, O, H) is being detected into wine products (GC-MS/IRMS, OIV methods). Organic compounds and trace elements analyses is based on analytical protocols developed in the laboratory (HRGC-LRMS, HRGC-HRMS, ICP-MS) through validated and new methods.

PRELIMINARY RESULTS AND COMMENTS:

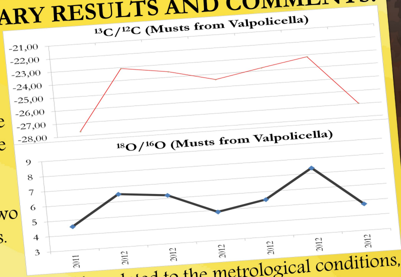

Results from musts (Figure) show that there should be some correlation between the trends of the two isotope ratios.

These differences could be related to the metrological conditions, which were different in 2011 comparing to 2012. The amount of precipitation was higher in 2011 and in addition there were more sunny days in 2012, which could lead to a higher $^{13}C/^{12}C$ values observed in 2012. However it should be mentioned that these are only preliminary results that has to be further evaluated in order to obtain more clear picture on the changes and distribution of stable isotopes in wine and must samples in relation to year and region of harvest.

References:

Antle M. John. Food System, adaptation to Climate Change. Resources for the future. 2009.
Intergovernmental Panel on Climate Change (2007). IPCC Fourth Assessment Report: Climate Change 2007, IPCC, Geneva.
Jones, G.V., White, M.A., Cooper, O.R., and Storchmann, K-H., Climate and Wine: Quality Issues in a Warmer World. Proceedings of the Vineyard Data Quantification Society's 10th Œonometrics Meeting. Dijon, France, May 2004.

OIV, International Organisation of Vine and Wine. www.oiv.int

Fatty acid composition as a tool for determination of adulteration of milk and dairy products

Doris Potočnik[1,2], **Nives Ogrinc**[1,2]
[1] Department of Environmental Sciences, Jožef Stefan Institute, Ljubljana, Slovenia
[2] Jožef Stefan International Postgraduate School, Ljubljana, Slovenia
doris.potocnik@ijs.si

Milk and dairy products are in considerable demand and relatively expensive, therefore, the authenticity and determination of geographical origin of these products are becoming important issues for providers and consumers. In this study fatty acid (FA) composition is used to obtain information about the provenience of milk and dairy products and to detect possible adulteration. Milk samples from different geographical regions (Mediterranean, Pannonia, Dinaric and Alpine) in Slovenia were collected and used to determine the content and isotopic composition of individual FA. FA composition was analyzed using the *in-situ* trans-esterification method and characterized by gas chromatography with FID detector (GC-FID), while isotopic composition was determined with compound specific isotope ratio mass spectrometry (CS-IRMS). In order to verify authenticity of cheese, 26 samples of high price cheeses in Slovenian market were analyzed. It was found that 20% of them do not correspond to the declaration. In addition the adulteration of raw milk with vegetable palm tallow could be detected at 1.1%.

Institut
"Jožef Stefan"
Ljubljana, Slovenija

MEDNARODNA
PODIPLOMSKA ŠOLA
JOŽEFA STEFANA

JOŽEF STEFAN
INTERNATIONAL
POSTGRADUATE SCHOOL

Fatty acid composition as a tool for determination of adulteration of milk and dairy products

Doris Potočnik[a,b], **Nives Ogrinc**[a,b]
[a] *Jožef Stefan Institute, Department of Environmental Sciences, Ljubljana, Slovenia*
[b] *Jožef Stefan International Postgraduate School, Ljubljana, Slovenia*

INTRODUCTION

Milk and dairy products are in considerable demand and relatively expensive, therefore, the authenticity and determination of geographical origin of these products are becoming important issues for providers and consumers. Fatty acid (FA) composition is used to obtain information about the provenience of milk and dairy products and to detect possible adulteration [1].

The aim of this work is to determine FA composition of milk that has been mixed with different amount of vegetable tallow and to verify the authenticity of cheese from cow, sheep and goat milk available on Slovenian market. Another important part of this research is to examine the effect of season and geographical location on proportional changes in milk fat content in relation to the diet composition.

EXPERIMENTAL WORK

Collection of samples

Adulteration:

- adulteration of cow's milk with vegetable palm fat: (1%, 2%, 4%, 7%, 9%, 11%, 13%, 16%, 18% and 20% of vegetable palm fat were added to pristine cow's milk),
- adulteration of cheese: 26 samples of higher price cheese (goat, sheep, cow) of different geographical origin from different European countries available on Slovenian market were collected.

Geographical origin:

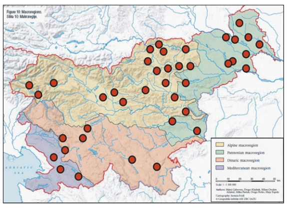

Figure 1: Sampling location

The sampling of cow's milk was performed four times per year covering different geographical regions (Mediterranean, Pannonia, Dinaric and Alpine) in Slovenia.

Study methods

FA composition was analyzed using the *in-situ* trans-esterification method and characterized by gas chromatography with FID detector (GC-FID), while isotopic composition was determined with compound specific isotope ratio mass spectrometry (CS-IRMS).

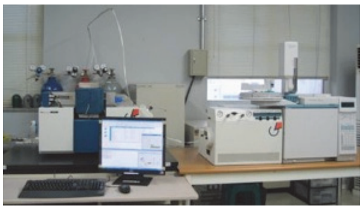

Figure 2: GC-C-IRMS

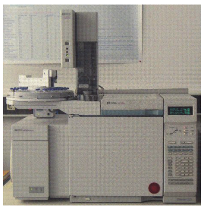

Figure 3: GC-FID

REFERENCES

[1] R. Karoui, J. De Daerdemaeker. A review of the analytical methods coupled with chemometric tools for determination of the quality and identity of dairy products. *Food Chemistry*, 102: 621 – 640, 2007.
[2] J. Dennis. Recent 1developments in food authentication. *Analyst*; 123: 151R – 156R, 1998.

RESULTS

Adulteration of milk with palm fat

Important adulteration of dairy products appearing on the market is admixture of vegetable fat with raw milk. It is possible to determine very low concentrations of added vegetable fat, down to 1.2% [2].

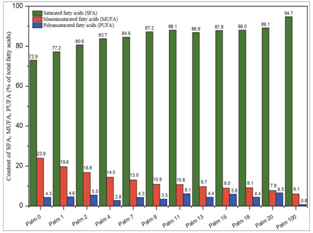

Palm 0 – unadulterated homogenized milk	Palm 11 – adulterated milk with 11% palm fat
Palm 1 – adulterated milk with 1% palm fat	Palm 13 – adulterated milk with 13% palm fat
Palm 2 – adulterated milk with 2% palm fat	Palm 16 – adulterated milk with 16% palm fat
Palm 4 – adulterated milk with 4% palm fat	Palm 18 – adulterated milk with 18% palm fat
Palm 7 – adulterated milk with 7% palm fat	Palm 20 – adulterated milk with 20% palm fat
Palm 9 – adulterated milk with 9% palm fat	Palm100 – 100% palm fat

Figure 4: Content of fatty acids in addition of different amount of palm fat. Adding different amounts of palm fat to pristine milk results in:

- increased content of SFAs,
- decreased content of MUFAs,
- decreased content of ω–3 and ω–6 PUFAs.

Adulteration of cheese available on Slovenian market

Samples [a]		Fatty acid (%)				
		C6:0	C8:0	C10:0	Σ (C6:0, C8:0, C10:0)	C16:0
Reference values from the literature	cow's milk	2.11	1.21	2.69	6.01	32.39
	cow's milk	2.50	1.50	3.20	7.20	27.90
	sheep milk	2.60	2.50	7.50	12.60	25.20
	sheep milk	2.80	2.70	9.00	14.50	25.40
	goat milk	2.90	2.70	8.40	14.00	24.60
	goat milk	3.17	3.50	10.78	17.45	25.90
	cow's milk	2.04	1.54	3.52	7.10	32.64
	cow's milk	3.16	2.00	3.93	9.09	29.58
	cow's milk	2.94	1.93	4.23	9.10	30.57
	cow's milk	2.64	1.68	3.56	7.88	32.72
	cow's milk	2.22	1.48	3.29	6.99	32.25
	cow's milk	1.50	1.17	2.95	5.61	32.48
	sheep milk	2.81	2.86	8.81	14.48	25.08
	sheep milk	2.98	2.78	7.70	13.47	25.46
	sheep milk	2.16	2.41	7.42	11.98	27.00
	sheep milk	2.13	2.53	8.11	12.78	25.63
	sheep milk	2.74	2.55	6.84	12.13	26.60
	sheep milk	2.52	3.19	9.44	15.15	24.87
	sheep milk	3.20	3.34	9.52	16.06	25.61
	sheep milk	3.93	4.65	14.58	23.17	21.45
	sheep milk	2.04	2.42	7.89	12.35	28.60
	sheep milk	2.16	1.31	2.36	5.82	34.07
	sheep milk	2.94	3.33	10.00	16.27	24.22
	sheep milk	1.69	2.20	7.68	11.56	28.08
	sheep milk	2.47	1.58	3.25	7.30	33.41
	sheep milk	2.15	2.99	10.64	15.79	27.14
	cow and sheep milk	2.41	1.73	4.10	8.23	33.33
	goat milk	2.30	3.50	12.88	18.68	26.42
	goat milk	2.85	3.32	10.45	16.62	26.93
	goat milk	2.12	3.12	10.71	15.95	25.52
	goat milk	3.20	3.64	11.56	18.41	25.61
	goat milk	2.31	2.72	8.42	13.45	25.10

- Approximately 20% of high-price cheese do not correspond to the declaration.
- We have sufficient reason to believe that at least 4 samples are adulterated (shaded in yellow).
- One of the samples declared as sheep cheese has FA composition comparable to cow cheese (shaded in orange).

Figure 5: Fatty acid composition (% of total fatty acid methyl esters) of goat, cow and sheep cheeses, which could be used to determine the correct labelling of cheese.

Geographical origin

The stable isotope composition in milk, reflects the isotopic composition of ingested food and drinking water and in turn can be used to determine geographical origin

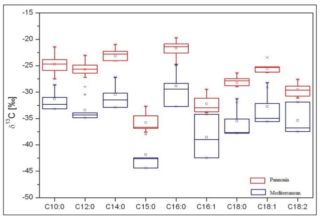

Figure 6: Stable carbon isotope composition for individual fatty acids for Mediterranean and Pannonia region. $\delta^{13}C$ values in FAs from Mediterranean were lower comparing to $\delta^{13}C$ values of Pannonia region, which indicated than corn was more often nutrient use for cow in Pannonia region.

CONCLUSION

The performed analyses of FA composition serve as a preliminary research, which could be used in the future to detect possible adulteration. The results indicated that FA composition is suitable for qualitative determination of cow's milk presence in goat's and sheep's milk or cheeses. In addition the presence of palm tallow in pristine milk and dairy products could be detected. Even though method showed that is suitable for qualitative and possible quantitative analyzes, further research is still needed to evaluate its real potential.

The work was performed within the project V4-1108 entitled "The use of specific methods for determination and prevention of adulteration of milk and dairy products" financially supported by Slovenian Research Agency and Ministry of Agriculture and the Environment. We thank Ljubljanske mlekarne, d.d., Pomurske mlekarne, d.d., Mlekarna Vipava d.d., Mlekarna Planika predelava mleka d.o.o. and Mlekarna Celeia for supplying cow samples.

Nitrate origin and distribution in the Sava River Basin

Janja Vrzel[1,3], **Nives Ogrinc**[2,3]
[1]Ecological engineering institute d.o.o., Maribor, Slovenia
[2] Department of Environmental Sciences, Jožef Stefan Institute, Ljubljana, Slovenia
[2] Jožef Stefan International Postgraduate School, Ljubljana, Slovenia
janja.vrzel@ijs.si

Environmental stressors such as climate change, change in land use and anthropogenic pollutants have a great impact on freshwater ecosystems. Nitrate (NO_3^-) is one of the special concerns since large amounts in the environment leads to several problems such as reduction of the water quality, eutrophication and creation of overall imbalance in the ecosystem. In this presentation we investigated the distribution and origin NO_3^- at selected locations in the Sava River Basin in Slovenia. Basic statistical analyses NO_3^- concentrations and $\delta^{15}N$ values according to the year, season, water temperature and discharge have shown that the Sava River is not polluted by anthropogenic NO_3^-. Its concentrations are yearly depended. Intra-annual changes of the concentrations and isotopic composition of NO_3^- was observed as well. These data extend our knowledge in understanding the hydrological cycle of the Sava River, which would be helpful to evaluate its future changes.

Nitrate origin and distribution in the Sava River Basin

Janja Vrzel[a,c*], Nives Ogrinc[b,c]

[a]*Ecological engineering institute d.o.o., Maribor, Slovenia*
[b]*Department of Environmental sciences, Jožef Stefan Institute, Ljubljana, Slovenia*
[c]*International Postgraduate School Jožef Stefan, Ljubljana, Slovenia*

JSI

IEI

Investing in your future
Operation part financed by the European Union
European Social Fund

**Correspondence: janja.vrzel@iei.si*

Environmental stressors such as climate change, change in land use and anthropogenic pollutants have a great impact on freshwater ecosystems. Nitrate (NO_3^-) is one of the special concerns since large amounts in the environment leads to several problems such as reduction of the water quality, eutrophication and creation of overall imbalance in the ecosystem. In this purpose we investigated the distribution and origin NO_3^- at selected locations in the Sava River Basin in Slovenia. Basic statistical analyses NO_3^- concentrations and $\delta^{15}N$ values according to the year, season, water temperature and discharge have shown that the Sava River is not polluted by anthropogenic NO_3^-. Its concentrations are yearly depended. Intra-annual changes of the concentrations and isotopic composition of NO_3^- was observed as well. These data extend our knowledge in understanding the hydrological cycle of the Sava River, which would be helpful to evaluate its future changes.

THE AIM OF THE WORK

To evaluate the changes of nitrate in the Sava River at selective locations in Slovenia (Fig. 1). The study is one of the steps to the better understand multiple stressors effects on freshwater ecosystem and thus to better predict their responses to future changes.

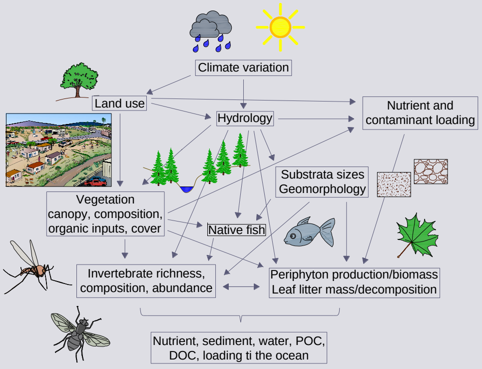

Climate variation

Land use

Hydrology

Nutrient and contaminant loading

Substrata sizes Geomorphology

Vegetation canopy, composition, organic inputs, cover

Native fish

Invertebrate richness, composition, abundance

Periphyton production/biomass Leaf litter mass/decomposition

Nutrient, sediment, water, POC, DOC, loading ti the ocean

Figure 2: Effect of multiple stressors in freshwater ecosystems under strong pressure for water resources in Slovenia (adapted from Cooper *et al.*, 2013).

MULTIPLE STRESSORS IMPACTS ON FRESHWATER

Environmental stressors may lead to complex, irreversible changes in ecological structure, functioning and the delivery of ecosystem services (UNESCO, 2009). At the top of all stressors is climate change that influences shifts in temperature, precipitation, run-off patterns, and in nitrogen deposition. Numerous other anthropogenic stressors impact on water quantity and quality, including acidification, pollution (e.g. by nitrates), land use and land cover change (Fig. 2).

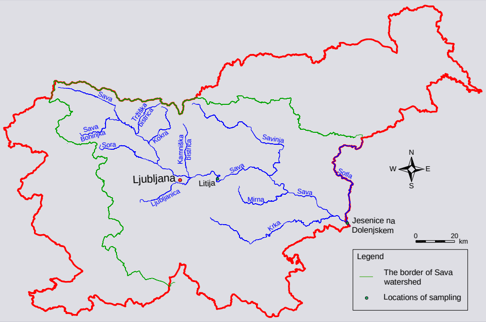

Figure 1: Map of sampling locations in SRB.

SAVA RIVER BASIN

The study area is Sava River Basin. Sava River is the largest river in Slovenia, including Sava Dolinka with headwater in Zelenci. It is a tributary of Danube River.

Sava River Basin is a very heterogeneous climate and exceptional diversity in terms of morphology, geology, pedology and vegetation.

Table 1: Results od statistical analyses.

	Litija	Jesenice na Dolenjskem
	NO_3^- [mg/l]	
Season	×	✓
Year	✓	✓
Water temp.	×	×
Discharge	×	×
	$\delta^{15}N_{NO3}$ [‰]	
Season	×	/
Water temp.	×	/
Discharge	×	/

DATA ANALYSES

Data were analysed by ANOVA to test for the differences in NO_3^- concentrations and $\delta^{15}N_{NO3}$ values according to the year, season, water temperature and discharge. The NO_3^- concentrations and $\delta^{15}N_{NO3}$ values were collected during the period 2006–2012 and from May 2010 to April 2011, respectively.

RESULTS

a) Significant difference was observed between the year and NO_3^- concentrations at Litija and between season, year and NO_3^- at Jesenice na Dolenjskem (Table 1). The results are shown up in the diagrams in Fig. 3

b) Dilution effect is present at both locations, but it is much more obvious at Litija (Fig. 4).

c) Main $\delta^{15}N_{NO3}$ value of 5.6‰ indicates that NO_3^- dynamics of the Sava's ecosystem is influenced mostly by natural inputs and only by negligible anthropogenic inputs → **Sava is not polluted with anthropogenic nitrogen.**

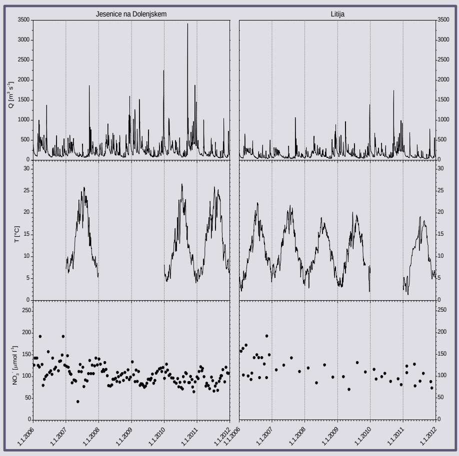

Figure 3: The annual mean discharge, temperature and nitrate concentrations since 2006 at Litija and Jesenice na Dolenjskem.

Figure 4: The relationship between discharge and NO_3^- at Litija and Jesenice na Dolenjskem.

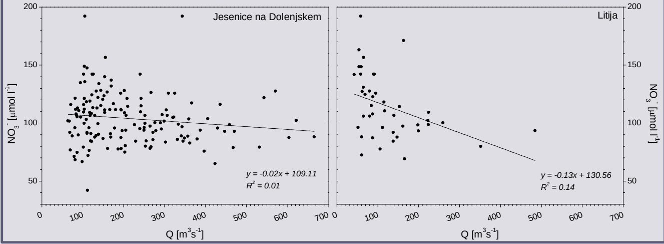

ACKNOWEMENTS

The research was financially supported by the international European project GLOBAQUA – Managing the effects of multiple stressors on aquatic ecosystem under water scarcity (EU Project 7 OP). Operation part financed by the European Union, European Social Fund.

REFERENCES

S. D. Cooper, P. S. Lake, S. Sabater, J. M. Melack, J. L. Sabo. The effects of land use changes in streams and rivers in Mediterranean climates. *Hydrobiologia*, 719: 383–425, 2013.

UNESCO. *World Water Assessment Programme (2009). Water in a Changing World.* The United Nations World Water Development Report 3, 2009.

Informacijske in komunikacijske tehnologije (Information and Communication Technologies)

Analysis of the open advertising data set

Martin Frešer[1,2], **Domen Košir**[3]
[1] Department of Intelligent Systems, Jožef Stefan Institute, Ljubljana, Slovenia
[2] Faculty of Mathematics and Physics, Faculty of Computer and Information science, Ljubljana, Slovenia
[3] Faculty of Computer and Information science, Ljubljana, Slovenia
martin.freser@gmail.com

A crucial task of world's biggest search engines, which want to make revenue out of advertising (ads), is to predict impressions of ads, clicks on ads and Click-Through-Rate(CTR) for ads, so that they could show ads to the interested users, according to their search queries. So it is not surprising, that companies like Google and Microsoft invest a lot of money in researches for this field. This paper analyses, how values of impressions, clicks and CTR vary over time. The analysis is done on the open advertisement data set, retrieved from the University College London (UCL). Those three values are also the main focus of this work. We will test, if markets of US and UK are correlated. At the end, we will try to predict CTR value of US-market learned from UK-market, using various machine learning techniques.

MEDNARODNA
PODIPLOMSKA ŠOLA
JOŽEFA STEFANA

JOŽEF STEFAN
INTERNATIONAL
POSTGRADUATE SCHOOL

Analysis of the open advertising data set

Martin Frešer, dipl. mat. (UN)
Študijski program: Interdisciplinarni študij računalništva in matematike,
Faculty of Mathematics and Physics, Faculty of Computer and Information science
MENTOR: Domen Košir
FMF, Jadranska cesta 32, 1000 Ljubljana

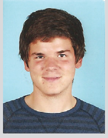

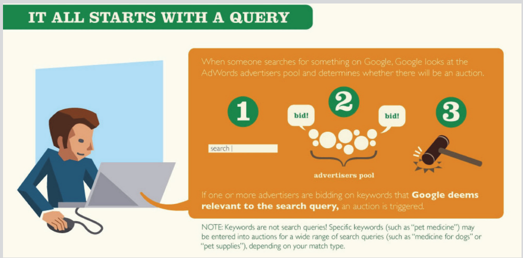

When someone searches for something on Google, Google looks at the AdWords advertisers pool and determines whether there will be an auction.

If one or more advertisers are bidding on keywords that **Google deems relevant to the search query,** an auction is triggered.

NOTE: Keywords are not search queries! Specific keywords (such as "pet medicine") may be entered into auctions for a wide range of search queries (such as "medicine for dogs" or "pet supplies"), depending on your match type.

Google‘s revenue in 2012:
- Out of advertising: 43.7 billion $
- Total revenue : 46 billion $

The best combined **CPC Bid x Quality Score** gets the best position:

Click-Through Rate (CTR) is one of the most important values for Quality Score.

- Data set contains ads from US and UK markets.
- We analyzed both markets for weekly average of impressions, clicks and CTR.
- We discovered correlation between much bigger US market and smaller UK market.
- We predicted weekly average CTR for US market, learned from UK market.

$$CTR = \frac{\#Clicks}{\#Impressions}$$

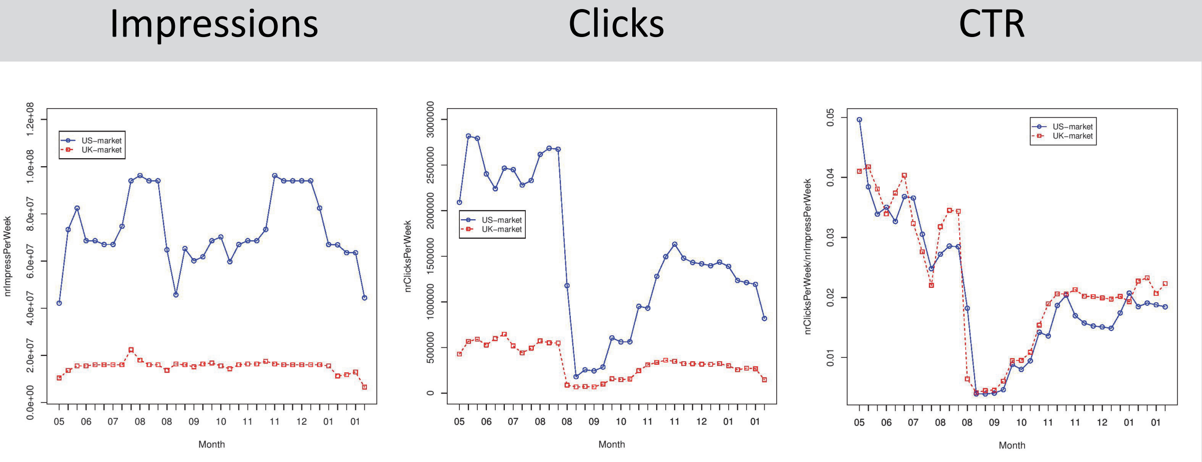
Impressions Clicks CTR

H_0: CTR between UK an US markets are independent

Test	p-value	correlation coefficient
Pearson's coefficient	2.2e-16	0.9371919
Spearman's ϱ	2.2e-16	0.929972
Kendall's τ	1.554e-15	0.8117647

We reject H_0 - CTR from both markets are dependant

Predicting CTR for US market, learned from UK market, Attributes: month, day

Algorithm	SE	MSE
Regression decision tree	52.5772	0.21637
Linear regression	298.6705	1.2291
Random Forest	53.8704	0.22169

Recognizing Human Activities and Detecting Falls in Real-time

Hristijan Gjoreski[1,2]**, Simon Kozina**[1,2]**, Mitja Luštrek**[1,2]**, Matjaž Gams**[1,2]
[1] Department of Intelligent Systems, Jožef Stefan Institute, Ljubljana, Slovenia
[2] Jožef Stefan International Postgraduate School, Ljubljana, Slovenia
`hristijan.gjoreski@ijs.si`

The paper presents a system that recognizes human activities and detects falls in real-time. It consists of two wearable accelerometers placed on the user's torso and thigh. The system is tuned for robustness and real-time performance by combining domain-specific rules and classifiers trained with machine learning. The offline evaluation of the system's performance was conducted on a dataset containing a wide range of activities and different types of falls. The F-measure of the activity recognition and fall detection were 96% and 78%, respectively. Additionally, the system was evaluated at the EvAAL- 2013 activity recognition competition and awarded the first place, achieving the score of 83.6%, which was for 14.2 percentage points better than the second-place system. The competition's evaluation was performed in a living lab using several criteria: recognition performance, user-acceptance, recognition delay, system installation complexity and interoperability with other systems.

MEDNARODNA
PODIPLOMSKA ŠOLA
JOŽEFA STEFANA

JOŽEF STEFAN
INTERNATIONAL
POSTGRADUATE SCHOOL

Recognizing Human Activities and Detecting Falls in Real-time

Hristijan Gjoreski, Simon Kozina, Mitja Luštrek, Matjaž Gams
Information and Communication Technologies,
Jožef Stefan International Postgraduate School
Jožef Stefan Institute

MOTIVATION

- The world's population is aging rapidly, threatening to overwhelm the society's capacity to take care of its elderly members
- Approximately half of the hospitalizations of the elderly are caused by falls
- Development of innovative ambient assisted living (AAL) technologies to help the elderly live independently for longer and with minimal support from the working-age population
- AAL systems must understand the user's situation, making activity recognition (**AR**) and fall detection (**FD**) essential components.

The RAReFall System
- **R**eal-time **A**ctivity **Re**cognition and **Fall** Detection-

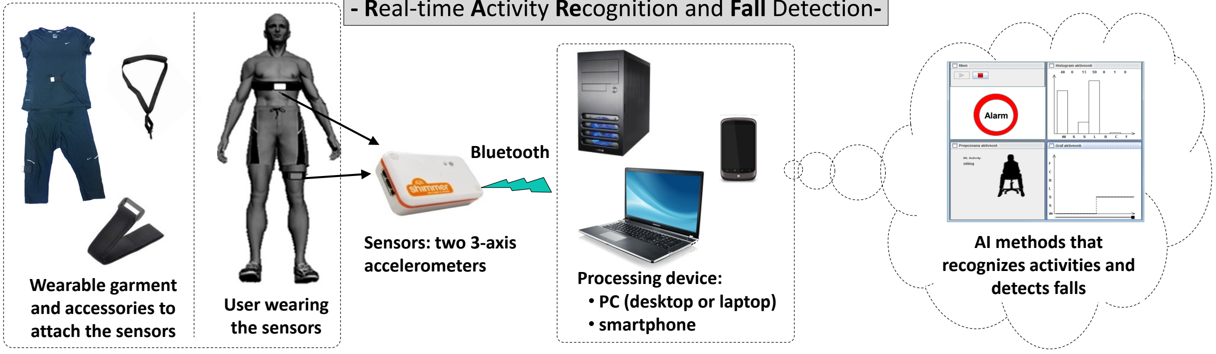

Wearable garment and accessories to attach the sensors

User wearing the sensors

Bluetooth

Sensors: two 3-axis accelerometers

Processing device:
- PC (desktop or laptop)
- smartphone

AI methods that recognizes activities and detects falls

Methodology

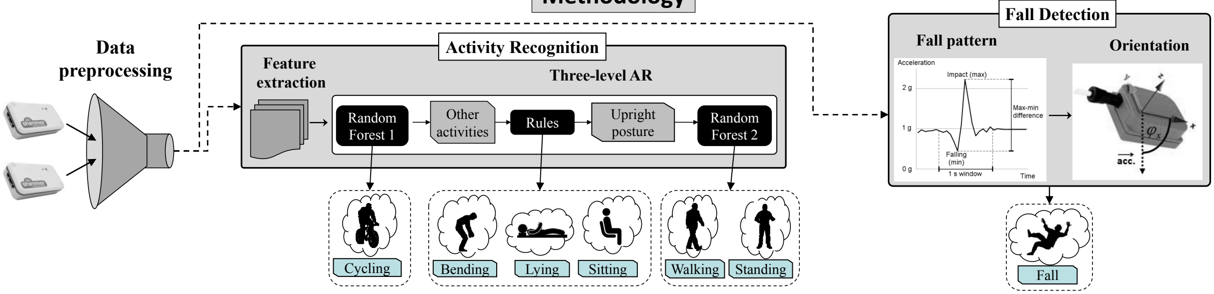

Data preprocessing

Activity Recognition

Feature extraction

Three-level AR

Random Forest 1 → Other activities → Rules → Upright posture → Random Forest 2

Cycling

Bending | Lying | Sitting

Walking | Standing

Fall Detection

Fall pattern

Orientation

Fall

Evaluation

Offline – Activity dataset*

Activity recognition & Fall detection performance

Performance	Activity Recognition	Fall Detection
Recall	96.19%	93.33%
Precision	96.53%	66.67%
F-measure	96.36%	77.78%

Fall detection detailed results

Events	Detected/All
Tripping	15/15
Fainting	13/15
Quickly lying	13/15
Quickly sitting	1/15
Other	0

* Publicly available at: http://dis.ijs.si/ami-repository/

International competition in activity recognition – EvAAL

	Team	Accuracy	Delay	Installation complexity	User Acceptance	Interoper-ability	Overall score '12	Overall score '13
EvAAL-AR '13	**RAReFall (Slovenia)**	**6.94**	**10**	**10**	**8.55**	**7.2**	**8.45**	**8.36**
	CNR (Italy)	4.04	10	10	7.04	6.15	7.19	6.94
	Seville'13 (Spain)	4.68	9	10	6.99	5.54	7.05	6.89
	Chiba'13 (Japan)	4.43	10	0	5.44	2.24	4.8	4.86
EvAAL-AR '12	Seville'12 (Spain)	4.33	9	10	7.47	7.63	7.39	7.07
	CMU&Utah (USA)	7.17	9	0	7.93	6.15	6.5	6.51
	Chiba'12 (Japan)	1.44	5	0	5.6	5.09	3.52	3.13
	Dublin (Ireland)	0	0	10	5.2	1.25	2.99	2.67

Conclusions

- The competition setting is closer to real life than most AR evaluations, so our result at the competition is evidence of RAReFall's practical applicability.
- Similar implementations of the RAReFall system are widely used in observational studies (evaluated by hundreds of people) of two European projects: Confidence and Chiron.
- A smartphone implementation is considered for future development.
- **Ultimate goal**: a system that has only one wearable device comprising several sensors, such as: accelerometer, ECG, body temperature, body humidity, etc. The system should not only recognize the activity of the user, but also should be able to reason about the user's behavior and health in general.

Network-Coding-Based Retransmission Scheme for Real Time Streaming Applications in Wireless Broadcast Networks

Melisa Junuzović[1,2], **Kemal Alič**[1], **Aleš Švigelj**[1,2]
[1] Department of Communication Systems,Jožef Stefan Institute, Ljubljana, Slovenia
[2] Jožef Stefan International Postgraduate School, Ljubljana, Slovenia
melisa.junuzovic@ijs.si

In this paper, the real-time streaming applications over wireless broadcast networks are considered. Deployment of real-time streaming applications into the wireless networks poses more challenges than deployment of non-real-time applications. Real-time streaming applications in wireless systems must cope with time-varying bandwidth, jitter, delay and must be resilient to packet loss. We propose a Network-Coding-Based Retransmission Scheme integrated into the application layer that maintains the required reliability and Quality of Service while posing lower bandwidth demands in comparison to the traditional approaches. In the proposed Retransmission Scheme, Network Coding is used to encode packets tended for retransmission.

MEDNARODNA
PODIPLOMSKA ŠOLA
JOŽEFA STEFANA

JOŽEF STEFAN
INTERNATIONAL
POSTGRADUATE SCHOOL

Network-Coding-Based Retransmission Scheme for Real-Time Streaming Applications in Wireless Broadcast Networks

Melisa Junuzović[1,2], Kemal Alič[2], Aleš Švigelj [1,2]
SUPERVISOR: dr. ALEŠ ŠVIGELJ, assist.prof.
[1]Jožef Stefan International Postgraduate School
Study program: Information and Communication Technologies
[2]Department of Communication Systems, Jožef Stefan Institute, Jamova cesta 39, 1000 Ljubljana

INTRODUCTION TO NETWORK CODING

Promising for Wireless Networks !

- New research area (Ahlswede et. al. 2000)
- Changes the way we think of transmitting information in a network
- Benefits many areas : networking, wireless communications, cryptography, computer science etc.
- Has a potential for improving : throughput, robustness, reliability and security of networking

- Real-time applications that use wireless broadcast
- Due to the channel erasure some packets would be lost

Retransmissions are required !

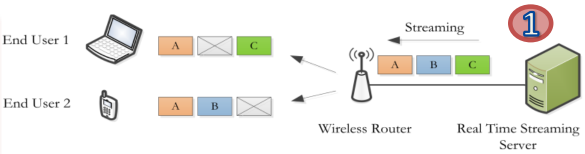

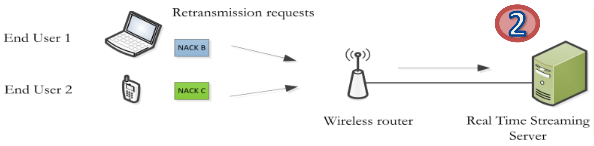

- NACK-based Retransmission Protocol

Diversity of lost packets across different users creates coding opportunities.

- Coding using simple XOR operation

1 retransmission instead of 2 :
- Increase throughput
- Saves bandwidth !

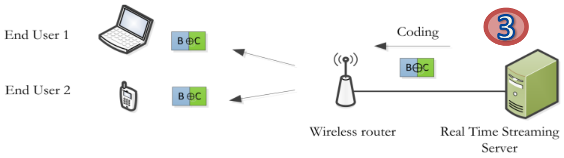

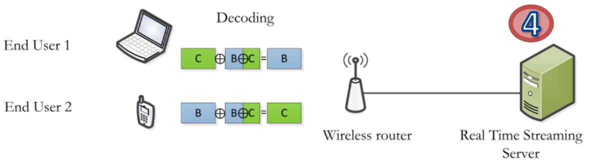

- Encoded packet should be decoded by as many users as possible
- Reducing decoding complexity using simple XOR operation

$C \oplus (B \oplus C) = B$

PRELIMINARY EVALUATION OF THE PROPOSED NETWORK MODEL

- Packet loss at the end users is highly variable i.e. **from** 20% **to** 50%
- **Wireless channel is lossy** –> suitable for Retransmission Scheme
- Packet loss is **asymmetric** at the end-users –> Network Coding

Lossy wireless channel promises high Network-Coding gains.

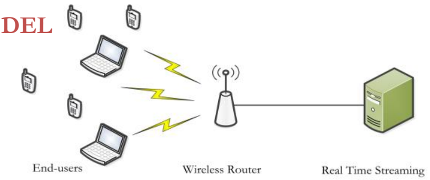

Wireless network is Network-Coding capable.

Performance evaluation of ITU-R P.1546 Propagation Model

Arsim Kelmendi[2], **Tomaž Javornik**[1,2], **Igor Ozimek**[1], **Andrej Vilhar**[1],
Andrej Hrovat[1, 2], **Gorazd Kandus**[1, 2]
[1] Department of Communication Systems, Jožef Stefan Institute, Ljubljana,Slovenia
[2] Jožef Stefan International Postgraduate School, Ljubljana, Slovenia
arsimkelmendi@gmail.com

This paper presents the performance evaluation of the ITU-R P.1546 propagation model implemented in an open source network planning tool GRASS RaPlaT. The ITU-R P.1546 propagation model is implemented as a separate path loss module r.ITUR1546. The path loss predictions obtained by the r.ITUR1546 module were compared with path loss predictions calculated by the WinProp propagation modelling tool and the r.hataDEM GRASS RaPlaT module. We noticed high agreement between the WinProp and r.ITUR1546 model results for distances up to 100 km and between the r.hataDEM and r.ITUR1546 model results for distances up to 10 km.

MEDNARODNA
PODIPLOMSKA ŠOLA
JOŽEFA STEFANA

JOŽEF STEFAN
INTERNATIONAL
POSTGRADUATE SCHOOL

Performance evaluation of ITU-R P.1546 Propagation Model

Arsim Kelmendi[1], Tomaž Javornik[1,2], Igor Ozimek[2], Andrej Vilhar[2], Andrej Hrovat[1, 2], Gorazd Kandus[1, 2]
MENTOR: prof. dr. GORAZD KANDUS
[1]Jožef Stefan International Postgraduate School
Study program: Information and Communication Technologies
[2]Department of Communication Systems, Jožef Stefan Institute, Jamova cesta 39, 1000 Ljubljana

ITU-R P.1546 PROPAGATION MODEL

- The ITU-R propagation model P.1546 is used for point-to-area radio propagation predictions for terrestrial services in the frequency range of 30 MHz to 3000 MHz.
- The model consists of several curves obtained by extensive measurement campaigns, describing electrical field dependency on the distance between a transmitter and a receiver and on other parameters such as carrier frequency, average terrain height, transmitter antenna height and time percentage of the service availability.

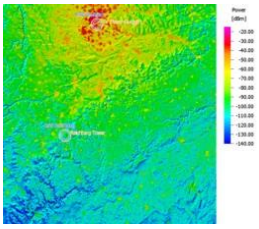

Radio propagation prediction
for DAB service in Stuttgart area

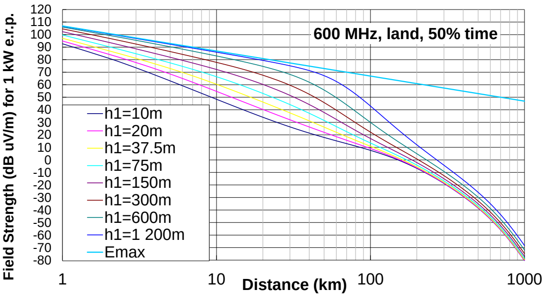

ITU-R P.1546 electrical field strength curves

GRASS-RAPLAT RADIO PLANNING TOOL

GRASS-RaPlaT is an open-source tool, based on the open-source Geographical Resources Analysis Support System (GRASS). Its structure is modular and characterized by a high level of flexibility and adaptability.

PATH LOSS PREDICTION MODULES :

- r.fspl (Free Space Path Loss model),
- r.hata (Okumura-Hata model),
- r.cost231 (COST 231 model),
- r.hataDEM (modified Hata model),
- r.waik (Walfish-Ikegami model),
- r.ITUR1546 (the ITU-R P.1546 model)

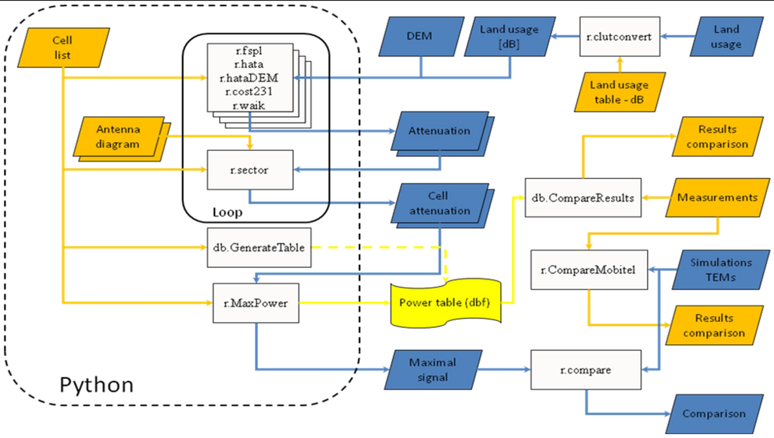
Cell list
r.fspl
r.hata
r.hataDEM
r.cost231
r.waik
Antenna diagram
r.sector
Loop
db.GenerateTable
r.MaxPower
Python
DEM
Land usage [dB]
r.clutconvert
Land usage
Land usage table - dB
Attenuation
Cell attenuation
Power table (dbf)
Maximal signal
Results comparison
db.CompareResults
Measurements
r.CompareMobitel
Simulations TEMs
Results comparison
r.compare
Comparison

PERFORMANCE EVALUATION AND COMPARISON OF R.ITUR1546 MODULE WITH WINPROP PROPAGATION TOOL

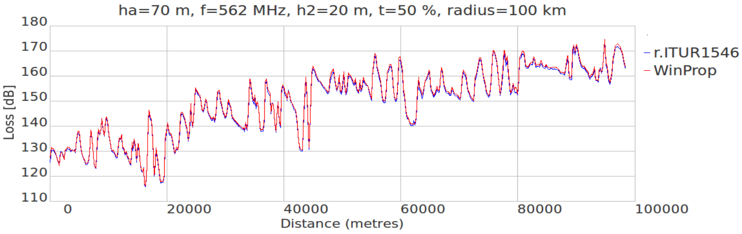

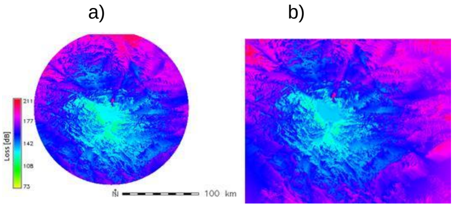

Path loss prediction by a) r.ITUR1546 module and b) WinProp tool for distances 0 to 100 km from the Krvavec transmitter

Model predictive control of bioreactor with Evolving Gaussian process model

Martin Stepančič[1,2], **Juš Kocijan**[2,3]
[1] Department of systems and control, Jožef Stefan Institute, Ljubljana, Slovenia
[2] Jožef Stefan International Postgraduate School, Ljubljana, Slovenia
[3] University of Nova Gorica, Nova Gorica, Slovenia
martin.stepancic@ijs.si

The paper presents a case study on adaptive nonlinear model predictive control (MPC) based on a Gaussian process (GP) model. MPC requires a model of the controlled system. We identify a NARX GP model using only 15 measurements of inputs and outputs. The model prediction itself is a normally distributed random variable. The information from a normally distributed prediction is used for implementation of probabilistic model predictive control. Our goal is to illustrate the effects on the controlled system performance. By examining the empirical results under the specified requirements, we can infer that the control performance is acceptable.

MEDNARODNA
PODIPLOMSKA ŠOLA
JOŽEFA STEFANA

JOŽEF STEFAN
INTERNATIONAL
POSTGRADUATE SCHOOL

Model predictive control of bioreactor with Evolving Gaussian process model

Introduction

We present an advanced, adaptive and stochastic control of a nonlinear bioreactor. Our task is to show how the bioreactor can be efficiently controlled without any prior knowledge of its dynamics. The goal is to perform the control task with the probabilistic on-line-trained model, based on low number of identification datapoints.

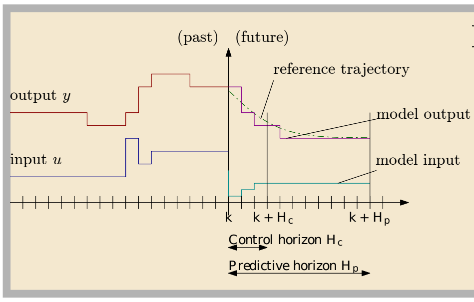

Model predictive control

- -Requires a model,
- -Requires a cost function,
- -Finds the optimal control input, for a finite future horizon
- -Handles control constraints by nature.

Gaussian process model

- -A probabilistic black-box model
- -Provides prediction confidence
- -Requires a set of datapoints
- -Parameter tuning is not necessary
- -Used model in an autoregressive form

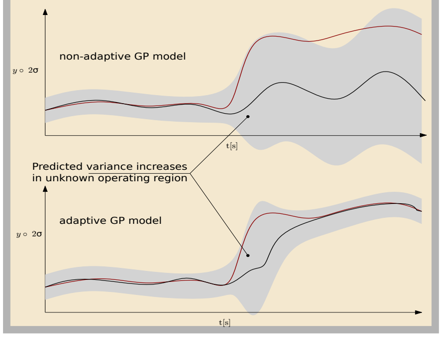

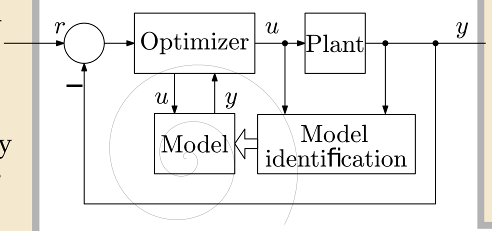

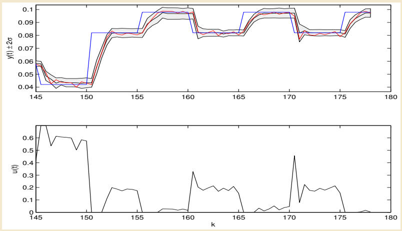

Bioreactor

- -Computer simulation
- -The core process in biotech industry
- -It is nonlinear and dynamic system
- -Control signal: output flow rate
- -Output signal: microorganism concentration
- -Additional noise

Evolving concept

- -A self-developing model
- -Adapts the model identification set and parameters on-line
- -Useful for highly nonlinear processes
- -Suitable for modeling streams from data
- -Allows real-time applications

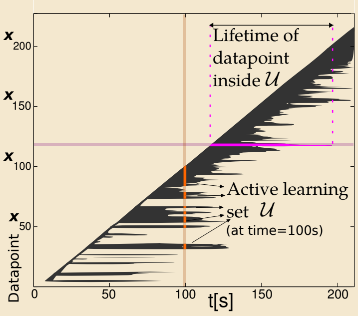

Conclusions

The adaptive model predictive control provides satisfactory closed-loop performance.
The quality of closed-loop control is based on cost function design and on-line model identification.
Evolving strategy yields efficient GP model identification.
The on-line modeling algorithm can be used for time-varying models of a highly nonlinear process.

Smart-Home Energy Management System: A Trade-off between Energy Consumption and Thermal Comfort Experience According to Occupant's Activity

Domen Zupančič[1,3] , **Božidara Cvetkovič**[2,3], **Matjaž Gams**[2,3]
[1] Robotina d.o.o., OIC-Hrpelje 38, SI-6240 Kozina, Slovenia
[2] Department of Inteligent Systems, Jožef Stefan Institute, Ljubljana, Slovenia
[3] Jožef Stefan International Postgraduate School, Ljubljana, Slovenia
domen.zupancic@ijs.si

Energy consumption and occupant's comfort are key factors when evaluating smart home environments. The focus of this paper is on thermal comfort, which is highly affected by environmental factors (temperature, humidity, radiation of elements and air movement), as well as by occupant-related factors (occupants' level of activity and clothing insulation). To satisfy a thermal comfort objective, energy is needed for heating and cooling. However, the energy saving aspect should not be omitted. This paper's contribution is two-fold: (i) a proof-of-concept analysis of smart home control based on occupants' activity level, which was estimated using an activity monitoring method and (ii) a trade off analysis between the energy consumption and thermal comfort when the activity level is served as an input into an intelligent home energy management system.

MEDNARODNA
PODIPLOMSKA ŠOLA
JOŽEFA STEFANA

JOŽEF STEFAN
INTERNATIONAL
POSTGRADUATE SCHOOL

Smart Home Energy Management System: A Trade-off between Energy Consumption and Thermal Comfort Experience According to Occupant`s Activity

Domen Zupančič BSc., Božidara Cvetkovič BSc
Study Program: Information and Communication Technologies
Jožef Stefan International Postgraduate School
SUPERVISOR: dr. Matjaž Gams
Robotina d.o.o., OIC-Hrpelje 38, SI-6240 Kozina, Slovenia
Jožef Stefan Institute, Jamova cesta 39, 1000 Ljubljana

How to find a satisfactory trade-off between energy consumption and thermal comfort experience in free-living situations at home?

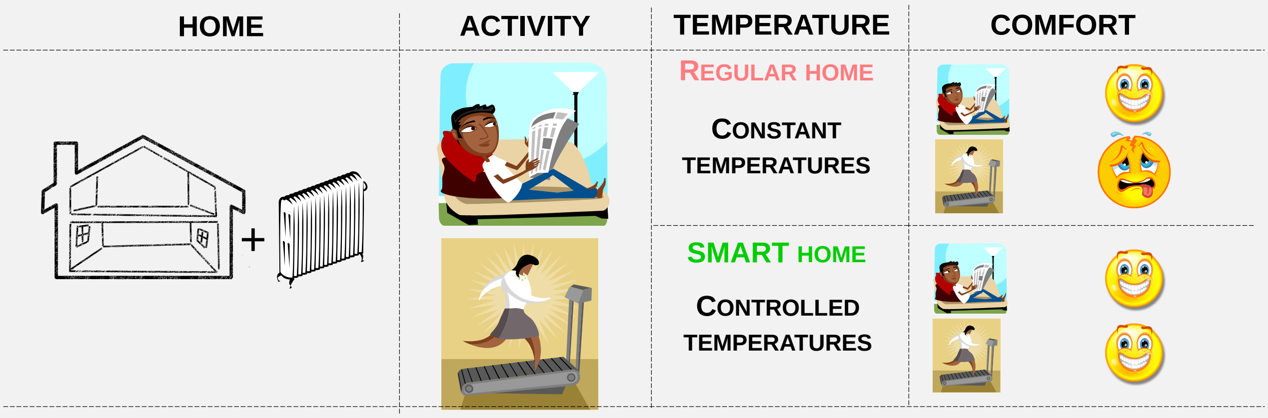

HOME | ACTIVITY | TEMPERATURE | COMFORT

REGULAR HOME

CONSTANT TEMPERATURES

SMART HOME

CONTROLLED TEMPERATURES

ACTIVITY MONITORING

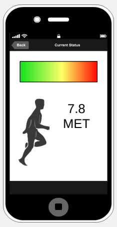

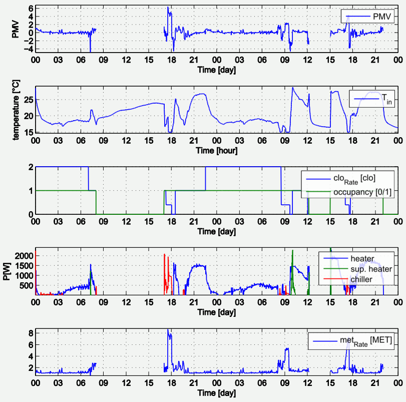

CONTROL SYSTEM

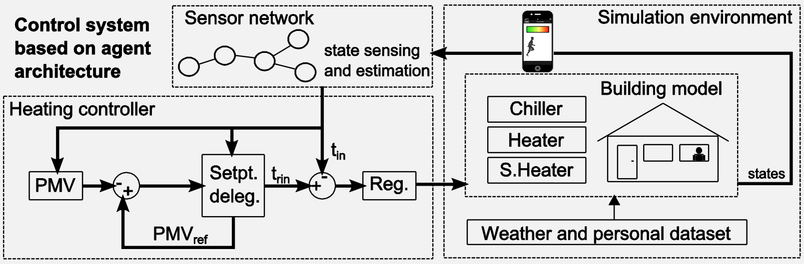

Control system based on agent architecture

Sensor network
state sensing and estimation

Simulation environment

Heating controller
PMV
Setpt. deleg.
t_{rin}
t_{in}
Reg.
PMV_{ref}

Building model
Chiller
Heater
S.Heater
states

Weather and personal dataset

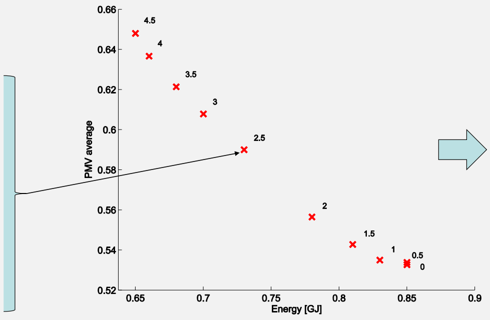

- PMV regulation
- Estimation of EE is equal to occupant`s activity level
- Trade-off between energy consumption and thermal comfort

Acknowledgements
Operation part financed by the European Union, European Social Fund. Operation implemented in the framework of the Operational Programme for Human Resources Development for the Period 2007- 2013, Priority axis 1: Promoting entrepreneurship and adaptability, Main type of activity 1.1.: Experts and researchers for competitive enterprises.

Nanoznanosti in nanotehnologije (Nanosciences and Nanotechnologies)

Transformations of alcohols with silanes under green reaction conditions

Njomza Ajvazi[1]**, Stojan Stavber**[2,3]
[1] Jožef Stefan International Postgraduate School, Ljubljana, Slovenia
[2] Department of Organic and Bioorganic Chemistry, Jožef Stefan Institute, Ljubljana, Slovenia
[3] Centre of excellence for integrated approaches in chemistry and biology of proteins
njomzaajvazi@hotmail.com

Different structure types of alcohols were proceeded with silanes, such as chlorotrimethylsilane (TMSCl), bromotrimethylsilane (TMSBr), azidotrimethylsilane (TMSN$_3$) and trimethylsilylcyanide (TMSCN) without the catalyst under solvent-free reaction conditions. Various primary, secondary and tertiary benzyl alcohols and tertiary alkyl alcohols were directly transformed to corresponding benzyl or alkyl halides using halogen atom bearing silanes (TMSCl and TMSBr) with quantitative conversion and high selectivity, while in the case with TMSN$_3$ and TMSCN under the same conditions we got silylation of hydroxyl substrates.

MEDNARODNA PODIPLOMSKA ŠOLA JOŽEFA STEFANA
JOŽEF STEFAN INTERNATIONAL POSTGRADUATE SCHOOL

Transformations of alcohols with silanes under solvent-free reaction conditions

Njomza Ajvazi[1] and Stojan Stavber[2,3]

Study program: Nanosciences and Nanotechnology
[1] Jožef Stefan International Postgraduate School, Ljubljana, Slovenia
[2] Jožef Stefan Intstitute, Ljubljana, Slovenia
[3] Centre of excellence for integrated approaches in chemistry and biology of proteins, Ljubljana, Slovenia

AIM OF THE WORK

Aim of this work: direct transformation of the hydroxyl group in alcohols using different substituted trimethylsilyl derivatives *(trimethylhalosilanes, trimethylsilyl* azide and *trimethylsilyl cyanide)* under **catalyst-free** and **solvent-free reaction conditions (SFRC).**

RESULTS

Scheme 1. Chlorination of secondary benzyl alcohol with trimethylchlorosilane **(TMSCl)** under SFRC

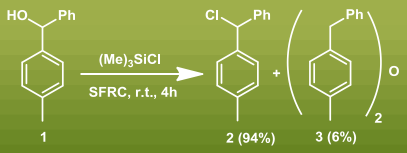

Scheme 2. Chlorination of naphtalen-1-yl(phenyl)methanol (4) with **TMSCl** under SFRC

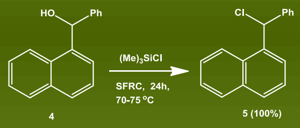

Table 1. Chlorination of various primary benzyl alcohols with **TMSCl** under SFRC

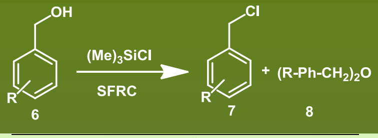

Entry	R	Conv.(%)^b of 6	Relative distribution(%)^b 7	8
1	H (6a)	78	68	10
2	4-Me (6b)	100	87	13
3^c	4-OMe (6c)	100	100	/
4	4-F (6d)	100	88	12
5	4-Cl (6e)	84	75	9
6	3-NO$_2$ (6f)	/	/	/

^{c} rt, time 2-24h at temp. 70-75^{0}C

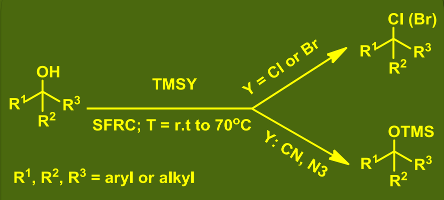

General concept and work-plan of the research

Scheme 6. Trimethylsilylation of phenyl(p-tolyl)methanol (1) with **TMSCN** or **TMSN$_3$** under SFRC

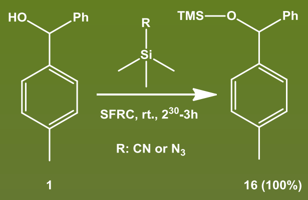

Scheme 3. Chlorination of 1-phenyl-1,2-ethanediol (9) with **TMSCl** under SFRC

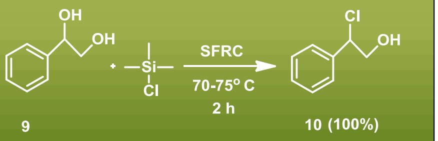

Scheme 4. Chlorination of tertiary alkyl alcohols with **TMSCl** under SFRC

11a : R^1 = R^2 = R^3 = Et 12a (100%)
11b : R^1 = R^2 = Me, R^3 = -(CH$_2$)$_2$Ph 12b (100%)

Scheme 5. Bromnation of benzyl and tertiary alkyl alcohols with **TMSBr** under SFRC

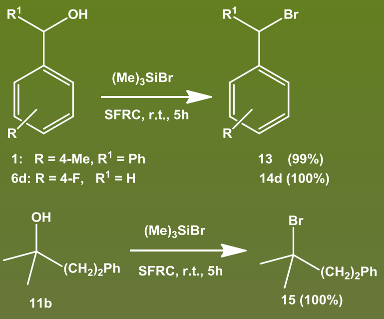

1: R = 4-Me, R^1 = Ph 13 (99%)
6d: R = 4-F, R^1 = H 14d (100%)

CONCLUSION

- We have demonstrated a novel and efficient method for direct conversion of benzylic and tertiary alkyl alcohols to corresponding chlorides or bromides by nucleophilic substitution of hydroxyl group using *trimethylhalosilanes* as sources of halogen moiety. Reactions performed under **solvent-free reaction conditions** gave high to quantitative yields of halogenated products, while under similar reaction conditions using *cyanotrimethylsilane* or *azidotrimethylsilane* resulted in the trimethylsilylation of the hydroxyl group in target molecules.
- From the green chemical point of view newly developed methods represent a significant improvement of related known methodology

Priprava porozne keramike svinčevega cirkonata titanata z uporabo polimetil metakrilata

Tina Bakarič[1,2], **Danjela Kuščer-Hrovatin**[1], **Barbara Malič**[1,2]
[1] Inštitut Jožef Stefan, Ljubljana, Slovenija
[2] Mednarodna podiplomska šola Jožefa Stefana, Ljubljana, Slovenia
`tina.bakaric@ijs.si`

V prispevku poročamo o pripravi porozne keramike s sestavo $Pb(Ti_{0,53}Zr_{0,47})O_3$ (PZT) s homogeno mikrostrukturo, ki bi bila uporabna kot podporni dušilec v ultrazvočnih pretvornikih. Keramiko smo pripravili iz mešanice PZT in polimetil metakrilata (PMMA), ki smo ga dodali kot tvorec por.

Delce PZT in PMMA smo razpršili v vodi pri pH 7, tako da so imeli na površini delci PZT pozitivni in delci PMMA negativni naboj. Po sušenju smo pridobili prah z enakomerno porazdelitvijo obeh faz. Prah smo stisnili v surovce, odstranili PMMA in vzorce sintrali pri temperaturi 1000 °C in 1050 °C. Mikrostrukturo keramike smo preučevali z vrstičnim elektronskim mikroskopom, količino poroznosti ter porazdelitev velikosti por pa smo določili z živosrebrovo porozimetrijo.

Keramika PZT je imela enakomerno razporejene pore okroglih oblik z velikostjo med 1 in 1,5 µm, kar je ustrezalo obliki in velikosti delcev PMMA. Poroznost je naraščala z večjo količino PMMA, zmanjševala se je z višjo temperaturo sintranja.

MEDNARODNA
PODIPLOMSKA ŠOLA
JOŽEFA STEFANA

JOŽEF STEFAN
INTERNATIONAL
POSTGRADUATE SCHOOL

Priprava porozne keramike svinčevega cirkonata titanata z uporabo polimetil metakrilata

Tina Bakarič[1,2], **Danjela Kuščer-Hrovatin**[1], **Barbara Malič**[1,2]
[1] Inštitut Jožef Stefan, Ljubljana, Slovenija
[2] Mednarodna podiplomska šola Jožefa Stefana, Ljubljana, Slovenija

Študijski program: Nanoznanosti in nanotehnologije

Mentor: doc. dr. Danjela Kuščer

UPORABA

Porozno keramiko lahko uporabljamo kot podporni dušilec v ultrazvočnih pretvornikih, ki delujejo pri frekvencah višjih od 20 MHz

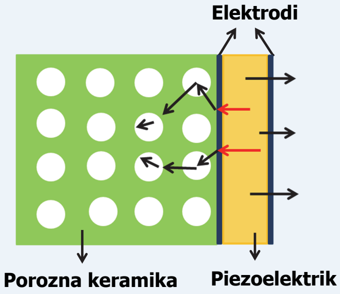

Shematski prikaz ultrazvočnega pretvornika

Preiskovani medij

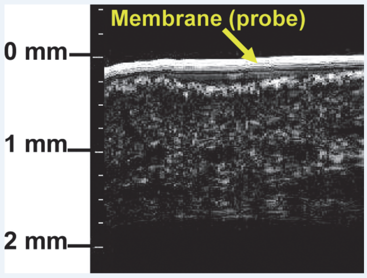

in vivo prikaz slike z visoko ločljivostjo kože na podlahti.

- **PORE – zadušijo** ultrazvočne valove, ki se širijo v **neželeno smer**.
- UČINKOVITO DUŠENJE – **pore** morajo biti **enakomerno razporejene** in enako velike.

PROCES HETERO-KOAGULACIJE H-K

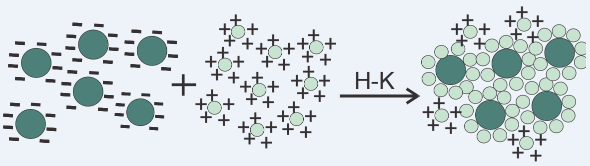

Negativno nabiti delci
Pozitivno nabiti delci
Enakomerna porazdelitev delcev

- Hetero-koagulacija je proces, pri katerem se **nasprotno nabita delca** v topilu **privlačita** zaradi elektrostatskega privlaka.
- V vodi proces hetero-koagulacije uravnavamo s pH.

S procesom hetero-koagulacije nadzorujemo porazdelitev kemijsko različnih delcev.

Rezultat enakomerne porazdelitve delcev PZT in PMMA je enakomerna poroznost v keramiki.

PRIPRAVA POROZNE KERAMIKE PZT

$Pb(Ti_{0,53}Zr_{0,47})O_3$ PZT
Polimetil metakrilat PMMA

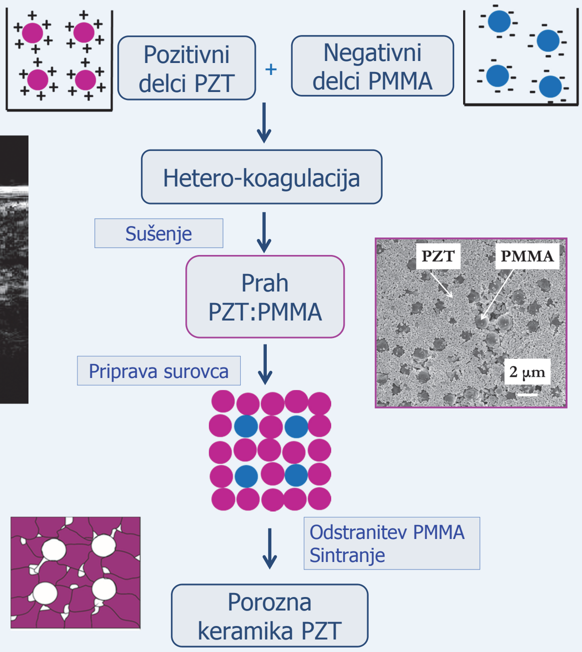

Pozitivni delci PZT + Negativni delci PMMA

Hetero-koagulacija

Sušenje

Prah PZT:PMMA

Priprava surovca

Odstranitev PMMA
Sintranje

Porozna keramika PZT

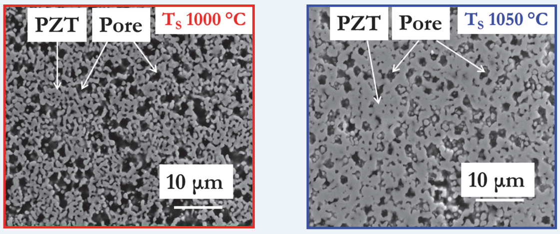

Mikrostrukturi keramike PZT, pripravljeni iz prahu PZT:PMMA z volumenskim razmerjem 70:30, sintrani pri 1000 °C in 1050 °C .

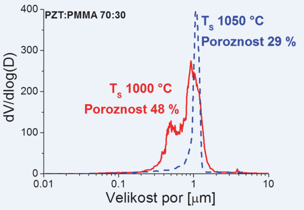

Porazdelitev velikosti por in količina poroznosti določena z živosrebrovo porozimetrijo za keramiko PZT sintrano pri 1000 °C in 1050 °C.

Količina poroznosti se zvišuje s količino PMMA in znižuje z višjo temperaturo sintranja.

Oblika in velikost por ustreza obliki in velikosti PMMA.

Synthesis of composite nanoparticles using coating of the core nanoparticles with cobalt ferrite layers

Blaž Belec[1,2], **Darko Makovec**[1,2]
[1] Department for Material Synthesis, Jožef Stefan Institute, Ljubljana, Slovenia
[2] Jožef Stefan International Postgraduate School, Ljubljana, Slovenia
blaz.belec@ijs.si

The synthesis of the composite nanoparticles, combining magnetic spinel cobalt ferrite ($CoFe_2O_4$) shell with different core nanoparticles was studied. In our research, the silica (SiO_2) nanoparticles were used as the cores to study the synthesis of cobalt-ferrite shell. The synthesis method was based on the known synthesis procedure for coating magnetic spinel iron oxide (maghemite - γ-Fe_2O_3) with heterogeneous nucleation at the core nanoparticles in an aqueous suspension. The problem of cobalt ferrite synthesis is in large difference of pH values where Fe^{3+}/ Co^{2+} ions precipitate. The cobalt-ferrite shell was formed with co-precipitation and heterogeneous nucleation of the solid product onto the core nanoparticles. The co-precipitation of the Fe^{3+}/Co^{2+} ions was provoked by addition of solid hydroxide; a mixture of $Mg(OH)_2$ and CaO pressed into a tablet. The stoichiometric and nonstoichiometric Co/Fe atomic ratio was used. Although the pH value for cobalt precipitation was reached, the stoichiometric composition of cobalt-ferrite shell was not obtained, even the excess amount of Co was introduced into the starting suspension.

MEDNARODNA
PODIPLOMSKA ŠOLA
JOŽEFA STEFANA

JOŽEF STEFAN
INTERNATIONAL
POSTGRADUATE SCHOOL

Synthesis of composite nanoparticles using coating of the core nanoparticles with spinel ferrite layer

Blaž Belec [1,2], Darko Makovec[1,2]

[1] Department for Material Synthesis – K8, Jožef Stefan Institute, Jamova cesta 39, 1000 Ljubljana, Slovenija
[2] Jožef Stefan International Postgraduate School, Jamova cesta 39, 1000 Ljubljana, Slovenija
blaz.belec@ijs.si; *supervisor prof.dr. Darko Makovec

INTRODUCTION

- Composite nanoparticles are particles consisting at least two different materials .
- They have large potential to exhibit the novel physical and chemical properties.
- Synthesis of composite nanoparticles is complex: one possibilitie is to synthesize core-shell nanoparticles (CSn).
- Alternative approach to synthesize CSn with magnetic spinel maghemite shell (Υ-Fe_2O_3) was proposed by Primc [1].

OUR RESEARCH

- Investigation of cobalt ferrite ($CoFe_2O_4$) shell synthesis onto the silica (SiO_2) core nanoparticles.
- Cobalt ferrite is among all spinel ferrites the only one hard magnetic and has the large magnetostriction from all oxide materials.

THE PROBLEM OF $CoFe_2O_4$ SYNTHESIS

- Large difference in pH values where $Fe^{3+}$and Co^{2+} ions precipitates, Fe^{3+} at pH = 2.8 and Co^{2+} at pH = 8.

EXPERIMENTAL

Core nanoparticles

- Suspension of core nanoparticles prepared with dispersing of the SiO_2 powder into water.

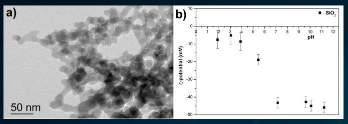

Silica (SiO_2) core nanoparticles (a) and ζ- potential measurments of silica core nanoparticles (b).

Synthesis of ferrite shell

- Stable aqueous suspension of the silica core nanoparticles (A = 5,45 x 10 ^{18} nm^2) is heated under argon flow at 60 °C.
- Addition of the Fe^{3+}-urea complex and Me^{2+} ions (M^{2+} = Fe^{2+} or Co^{2+}).
- After 10 minutes of thermal hydrolysis at elevated temperature, base is added.
- After 2 hours reaction is completed, product is collected and purified with distillated water.

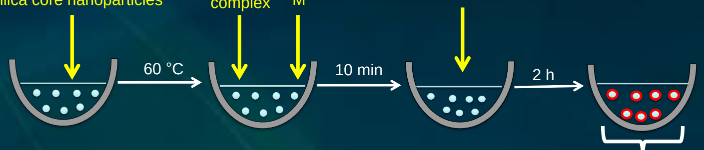

Silica core nanoparticles
60 °C
Fe^{3+} urea complex
M^{2+}
10 min
Base
2 h
Composite nanoparticles

RESULTS

Ratio of Fe^{3+}/M^{2+} = 0.5

Maghemite shell [1]

- $Mg(OH)_2$
- M^{2+} = Fe^{2+}

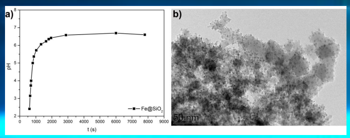

pH vs. time curve (a) and TEM image (b) of the Fe@SiO_2 composite nanoparticles.

Cobalt ferrite shell

- $Mg(OH)_2$
- M^{2+} = Co^{2+}

pH value not high enough for precipitation of Co^{2+} ions.

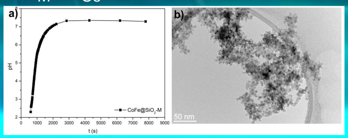

pH vs. time curve (a) and TEM image (b) of the CoFe@SiO_2-M composite nanoparticles.

Solution

- mixture of $Mg(OH)_2$ and CaO pressed into tablet

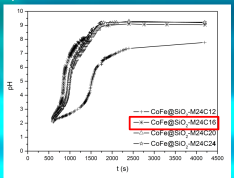

Influence of different $Mg(OH)_2$/CaO ratios on pH vs. time curve.

Cobalt ferrite shell

- Ratio of Fe^{3+}/Co^{2+} = 0.5
- $Mg(OH)_2$ + CaO

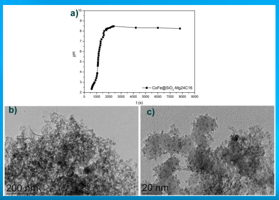

pH vs. time curve (a), representative TEM image (b) of the CoFe@SiO_2-M24C16 composite nanoparticles and TEM image of small heterogeneous nucleated crystalline nanoparticles on the core nanoparticles.

Ferrite shell contains only ≈ 4 at. %of cobalt instead of 14 at.% required for stoichometric $CoFe_2O_4$.

Increased Co^{2+} and CaO concentration

- Ratio of Fe^{3+}/Co^{2+} = 0.5
- $Mg(OH)_2$ + CaO

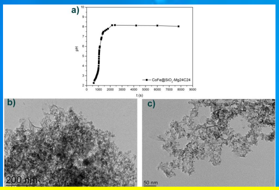

pH vs. time curve (a), representative TEM image (b) of the CoFe@SiO_2-M24C24 composite nanoparticles and TEM image of small heterogeneous nucleated crystalline nanoparticles on the core nanoparticles.

Ferrite shell contains only ≈ 4 at. % of cobalt instead of 14 at.% required for stoichometric $CoFe_2O_4$.

[1] Primc, D., *Heterogeneous nucleation of iron oxides (Υ-Fe_2O_3) in colloidal systems*. 2013, Jožef Stefan Postgraduate School: Ljubljana.

TNFα-induced apoptosis in U937 cell line is independent of cathepsin D and cysteine cathepsins

Katja Bidovec[1,2], **Veronika Stoka**[1,2], **Vito Turk**[1,2]

[1] Department of Biochemistry and Molecular Biology, Jožef Stefan Institute, Ljubljana, Slovenia

[2] Jožef Stefan International Postgraduate School, Ljubljana, Slovenia

katja.bidovec@ijs.si

The role of cysteine and aspartic cathepsins in Tumor Necrosis Factor-alpha (TNFα)-induced apoptosis was investigated using U937 cell line. Apoptosis was caspase-dependent and accompanied by lysosome membrane permeabilization and release of cathepsin D into the cytosol. However, cysteine cathepsin inhibitor E64d and aspartic protease inhibitor pepstatin A did not prevent the initiation or progression of apoptosis, suggesting that neither cysteine cathepsins nor cathepsin D are critically involved in triggering or progression of the TNFα-induced apoptosis in U937 cell line. Cathepsins may, however, be involved in the amplification of the death receptor-mediated apoptosis pathway in certain cell lines or under different stimulation conditions.

TNFα-induced apoptosis in U937 cell line is independent of cathepsin D and cysteine cathepsins

Katja Bidovec, B.Sc.
Study programme: Nanosciences and Nanotechnologies, Jozef Stefan International Postgraduate School
MENTOR: Prof. Dr. Vito Turk
CO-MENTOR: Prof. Dr. Veronika Stoka
Jožef Stefan Institute, Jamova cesta 39, 1000 Ljubljana

INTRODUCTION

Apoptosis is the major mechanism by which eukaryotic organisms eliminate potentially dangerous, superfluous and damaged cells. Many of the key apoptotic proteins in the apoptotic pathway have been identified to date, however, the molecular mechanisms of action or activation of these proteins are not fully understood and are thus the focus of continued research. The importance of understanding the mechanistic machinery of apoptosis is vital because apoptosis is a component of both health and disease. ***TNFα*** is one of the most important pro-inflammatory cytokines and has a crucial role in the pathogenesis of immune disorders and tumor development. Detailed understanding of TNFα triggered pathways will enable the development of a new generation of anti-TNFα therapies that will cause fewer side effects, whilst maintaining high efficacy in the treatment of cancer and immune disorders.

AIM

Determine the pathway(s) of programmed cell death and investigate the role of cysteine cathepsins and cathepsin D in TNFα mediated apoptosis in U937 cells that are known to express high levels of cathepsins and respond well to TNFα.

CONCLUSIONS

The induction of apoptosis by TNFα and cycloheximide in U937 cell line results in:

- **caspase -8 and -3 activation**
- **cleavage of protein Bid**
- **permeabilization of lysosomal membrane and release of cathepsin D to the cytosol**
- **unability of cysteine cathepsin inhibitor E64d and aspartic protease inhibitor Peptstatin A to rescue apoptosis, indicating that neither cysteine cathepsins nor cathepsin D are critically involved in the induction of apoptosis**

METHODS

Quantification of cell death*:* Annexin V-PE and PI were used to determine the phosphatidylserine exposure and the loss of membrane integrity; Acridine Orange was used to assess the integrity of the lysosomes. Analysis was made with FACSCalibur flow cytometer.
Caspase -3 activity measurement*:* Total cell extracts were tested for DEVDase activity by measuring the cleavage of the substrate Ac-DEVD-AFC.
Immunoblotting*:* Total and cytosolic cell extracts were loaded and resolved in SDS-PAGE gels and electrotransferred to the nitrocellulose membranes. Blots were probed with different primary antibodies and horseradish peroxidase-conjugated secondary antibodies were added followed by visualization with enhanced chemiluminescence.

ACKNOWLEDGEMENTS

The work was supported by Slovenian Research Agency. The authors would like to thank Boris Turk for his valuable comments and suggestions to improve the quality of the paper.

RESULTS

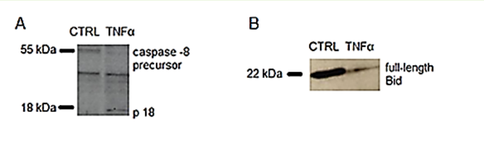

Figure 1: (A) Activation of caspase -8 and (B) Bid cleavage following treatment with 10 ng/ml TNFα and 1 μg/ml cycloheximide for 12 h.

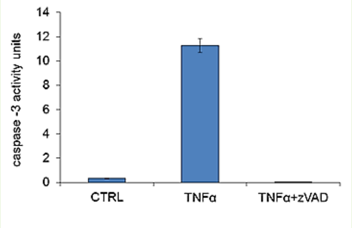

Figure 2: DEVDase activity after TNFα-induced apoptosis in U937 cell line. Cells were treated with 10 ng/ml TNFα and 1 μg/ml cycloheximide for 24 h. The inhibitor Z-VAD-FMK was added 2 h prior to TNFα treatment at a concentration of 20 μM. Caspase activity was determined using the fluorogenic substrate Ac-DEVD-AFC. The results are expressed as relative fluorescence.

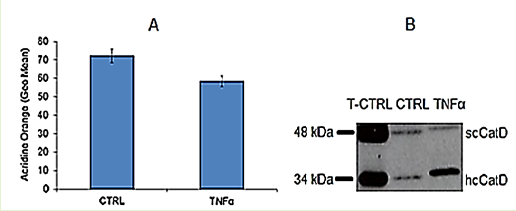

Figure 3: Lysosome integrity during TNFα-induced apoptosis in U937 cell line. (A) The cells were treated with TNFα (10 ng/ml) and cycloheximide (1 μg/ml) for 24 h. Acridine Orange uptake indicates the percentage of cells with decreased fluorescence. (B) Immunodetection of Cathepsin D in total cell extracts (T-CTRL) and cytosolic cell extracts without treatment (CTRL) and after treatment with TNFα (10 ng/ml) and cycloheximide (1 μg/ml) for 12 h. scCatD, single-chain mature cathepsin D; hcCatD, heavy chain of mature cathepsin D.

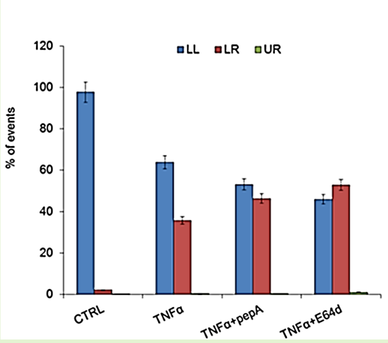

Figure 4: Cysteine and aspartic cathepsin inhibitors do not reduce the cytotoxic potential of TNFα. Cells were pretreated for 2 h with cysteine cathepsin inhibitor E64d (10 μM) and aspartic cathepsin inhibitor Pepstatin A, Penetratin (1 μM) and incubated with TNFα (10 ng/ml) and cycloheximide (1 μg/ml) for 12 h. Cells are distributed as follows: Ann-/PI- (living cells) (LL); Ann+/PI- (apoptotic cells) (LR); Ann+/PI+ (UR).

Tailoring relaxor dielectric response by blending P(VDF-TrFE-CFE) terpolymer with a ferroelectric P(VDF-TrFE) copolymer

Goran Casar[1,2], **Xinyu Li**[3], **Barbara Malič**[4], **Qiming Zhang**[3], **Vid Bobnar**[1,2],
[1] Condensed Matter Physics Dept., Jožef Stefan Institute, Ljubljana, Slovenia
[2] Jožef Stefan International Postgraduate School, Ljubljana, Slovenia
[3] Materials Research Institute, The Pennsylvania State University, USA
[4] Electronic Ceramics Dept., Jožef Stefan Institute, Ljubljana, Slovenia
goran.casar@ijs.si

We report dielectric properties of relaxor P(VDF-TrFE-CFE) terpolymer (a polymer system that exhibits fast response speeds and high electric energy density, giant electrostriction and large electrocaloric effect) blended with ferroelectric P(VDF-TrFE) copolymer. We show that blends exhibit a relaxor-like linear dielectric response at low copolymer content. In samples with 20-50 wt. % of P(VDF-TrFE) the ferroelectric and relaxor states coexist and nonlinear dielectric spectroscopy appears as a very appropriate tool for revealing such coexistence. Moreover, the temperature dependence of the third harmonic dielectric response reveals the onset of ferroelectric behavior also in blends with a low copolymer amount, due to a high VDF content in the P(VDF-TrFE-CFE) terpolymer, which increases the ferroelectric interactions. In addition, the coexistence of ferroelectric and relaxor states is confirmed by differential scanning calorimetry, DSC, which further reveals the influence of blending on the terpolymer crystallinity and melting point.

TAILORING RELAXOR DIELECTRIC RESPONSE BY BLENDING P(VDF-TrFE-CFE) TERPOLYMER WITH A FERROELECTRIC P(VDF-TrFE) COPOLYMER

Goran Casar[1,3], Xinyu Li[4], Barbara Malič[2,3], Qiming Zhang[4], Vid Bobnar[1,3]
[1] Condensed Matter Physics Dept., Jožef Stefan Institute, Ljubljana, Slovenia
[2]Electronic Ceramics Dept., Jožef Stefan Institute, Ljubljana, Slovenia
[3]Jožef Stefan International Postgraduate School, Ljubljana, Slovenia
[4]Materials Research Institute, The Pennsylvania State University, USA

Exciting properties of relaxors:

- Giant electromechanical response;
- Large electrocaloric effect;
- High electric energy density, fast response speeds.

Potential applications:

- Actuators, sonars, artificial muscles;
- Heating/cooling devices of new generation;
- Capacitors.

- **Ferroelectrics** ↔ Long-range dipolar order;
- **Inorganic relaxors** ↔ Compositionally disordered systems, short-range dipolar order;
- **Relaxor polymers** ↔ Disorder is introduced into a ferroelectric polymer by either high-energy electron irradiation or incorporation of additional monomers into the polymer chain.

Dielectric spectroscopy, particularly nonlinear dielectric investigations, and differential scanning calorimetry reveal the **coexistence of ferroelectric and relaxor states in polymer blends.**

Linear dielectric response

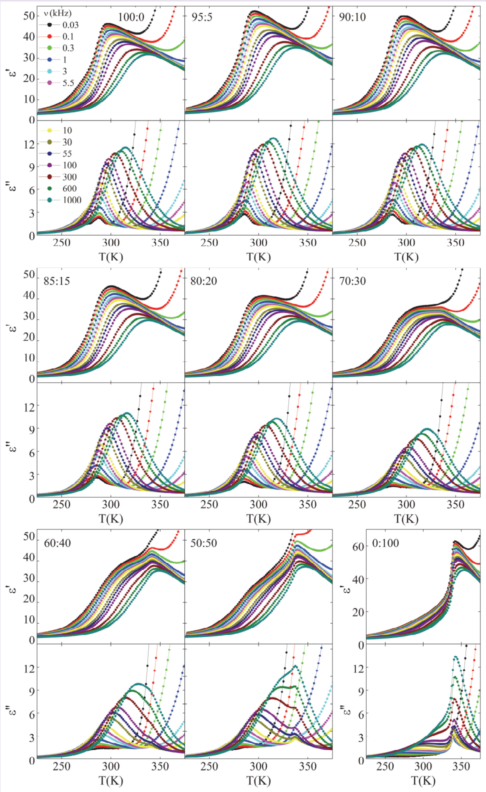

Figure 1: Temperature dependences of the real and imaginary parts of the complex linear dielectric constant in the pure P(VDF–TrFE–CFE) terpolymer (100:0), its blends with different wt.% (5–50) of P(VDF–TrFE) copolymer, and in the pure copolymer (0:100). In samples with copolymer amount ≥ 20 wt. %, a frequency independent peak due to the ferroelectric phase transition in the copolymer starts to form in addition to the broad terpolymer's relaxor maximum, which indicates that in these blends ferroelectric and relaxor states coexist. Complex linear dielectric constant was measured by HP4284A Precision LCR Meter during cooling runs with the rate of -0.5 K/min.

Nonlinear dielectric response

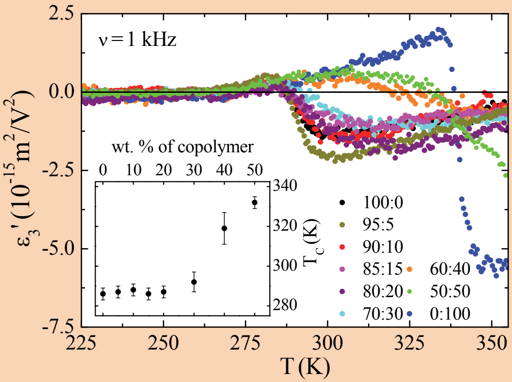

Figure 2: The nonlinear dielectric response, i.e. the third harmonic vs. temperature, which changes sign, reveals the ferroelectric behaviour of P(VDF–TrFE–CFE)/P(VDF–TrFE) blends. The inset shows the temperature where ε_3' changes sign vs. copolymer content. The nonlinear dielectric response was measured by using HP35665A Dynamic Signal Analyzer.

Thermal properties

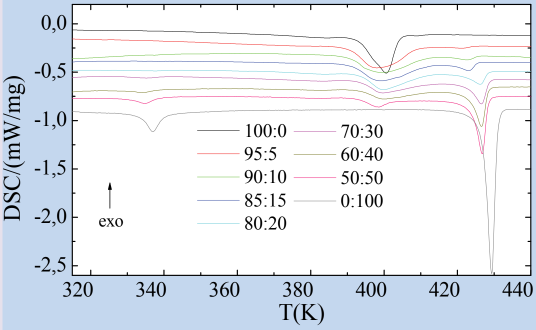

Figure 3: DSC traces confirm the coexistence of relaxor and ferroelectric phases. Peaks occur at around three different temperatures, 340 K, 400 K, and 430 K. The peak at ~340 K denotes the ferroelectric phase transition, while the other two peaks are due to the melting of the terpolymer (~400 K) and copolymer (~430 K) crystallites. The curves were recorded on a Netzsch DSC 204 F1 calorimeter. Temperatures at peaks maxima are phase transition temperatures and the area of peaks is proportional to the crystallinity of samples.

Blending a relaxor terpolymer with the ferroelectric copolymer resulted in the system with coexisting ferroelectric and relaxor states, showing similar properites to P(VDF–TrFE) copolymer, irradiated with low doses of high-energy electrons, where such a coexistence has been shown to strongly influence materials' properties (J. Mater. Sci. 48, 7920, 2013). This blend polymer system could thus be suggested as a model system for tailoring various materials' properties, not only the dielectric response, reported in this work (J. Appl. Phys. 115, 104101, 2014).

Bioactive Peptides Derived from Egg White Hydrolyzate

Ana Gluvić[1]

[1] Jožef Stefan International Postgraduate School, Ljubljana, Slovenia

anadgluvic@gmail.com

Hen egg white has exceptional potential as an inexhaustible source for a variety of peptide products with unique properties. These active peptides are valuable for human health and nutrition and can be used as raw material for diverse purposes in the cosmetic and pharmaceutical industries. The studies thus far have established that enzymatic hydrolysis of egg white water solution can release **active peptides**. Possible therapeutic effects of these peptides are antioxidant, antihypertensive, anti-inflammatory and antimicrobial, while functional properties of egg white hydrolyzate are better foaming, digestion, and solubility of food products. The aim of this work is to determine and describe which peptides have mentioned abilities and to propose some new abilities such as anti-aggregation and autophagy-stimulating effects and their possible application as drug or functional food.

MEDNARODNA
PODIPLOMSKA ŠOLA
JOŽEFA STEFANA

JOŽEF STEFAN
INTERNATIONAL
POSTGRADUATE SCHOOL

BIOACTIVE PEPTIDES DERIVED FROM EGG WHITE HYDROLYZATE

ANA GLUVIĆ, M. Eng. Tech-Biotech.
Study program: Nanosciences and nanotechnologies,
International Postgraduate School Jožef Stefan
mentor: prof. dr. EVA ŽEROVNIK,
J. Stefan Institute and J. Stefan Postgraduate School, Ljubljana

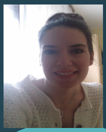

Bioactive peptide represents short amino acid sequence which is found encrypted in the proteins. Its activation demands hydrolysis of source protein.

It has been recognised that food, whitin its structure have different peptide sequences.

Hen egg white have exceptional potential as an inexhaustible source for a variety of bioactive products with unique properties.

Two-step enzyme hydrolysis:

- Pretreatment of egg white solution with ultra sound allows better enzyme approach
- Two types of enzymes provide approach to the egg white proteins backbone from many sides
- Mild reaction parameters
- Consequences: increased solubility, decreased viscosity, changes in foaming, gelling, and emulsifying properties of hydrolyzed egg white solution compared to those of native proteins

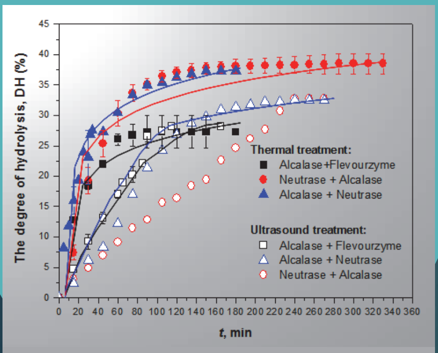

Schematic presentation of two-step hydrolysis of 10% egg white water solution with termic and ultrasound pretreatment

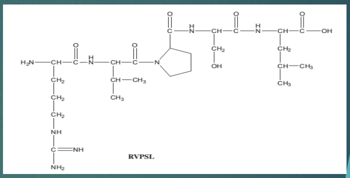
RVPSL

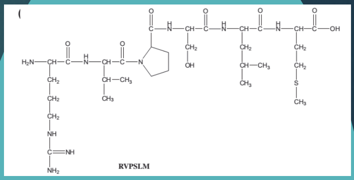
RVPSLM

- Chemical structures of peptides derived from egg white protein ovotransferrin with potential antidiabetic activity

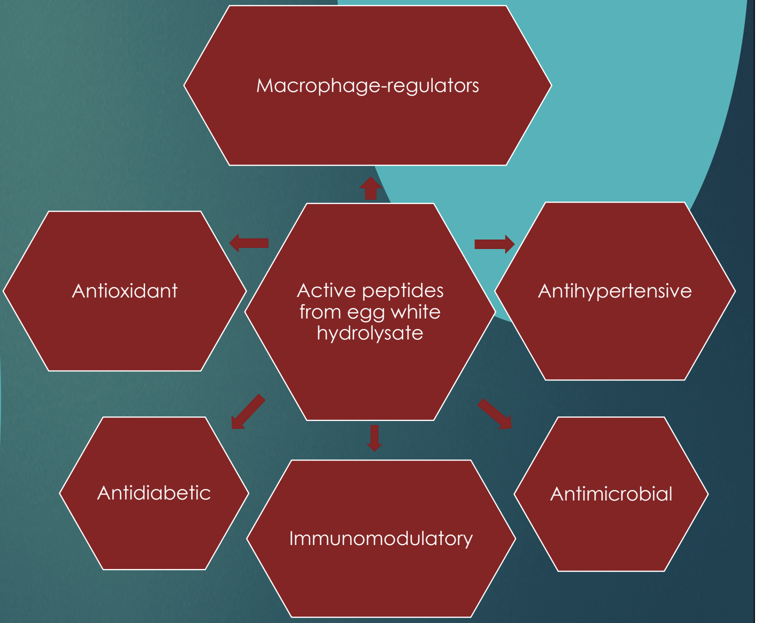

Macrophage-regulators

Antioxidant

Active peptides from egg white hydrolysate

Antihypertensive

Antidiabetic

Immunomodulatory

Antimicrobial

Potential commercial applications:

- **Antihypertensive products**
- **Cosmetic products**
- **Functional food**
- **Food packing**

The role of different niobium pentoxide precursors in the solid-state synthesis of potassium sodium niobate

Jitka Hreščak[1,2], **Andreja Benčan**[1,2], **Tadej Rojac**[1], **Barbara Malič**[1,2]
[1] Electronic Ceramics Department, Jožef Stefan Institute, Ljubljana, Slovenia
[2] Jožef Stefan International Postgraduate School, Ljubljana, Slovenia
jitka.hrescak@ijs.si

The lead-free ceramics based on the solid solution of potassium sodium niobate have been extensively studied in recent years. Different authors reported preparation of qualitatively extremely different ceramics, although they used comparable processing methods. The repeatability of the preparation of the potassium sodium niobate systems thus is an issue. In this study, two batches of $K_{0.5}Na_{0.5}NbO_3$ were prepared, using the orthorhombic and the monoclinic Nb_2O_5 polymorphs for the solid-state synthesis. Our results showed a clear influence of the Nb_2O_5 polymorhic form on the formation of a homogeneous potassium sodium niobate solid-solution and its further densification behaviour. To achieve a perfect reproducibility in the potassium sodium niobate ceramics processing this point is crucial and was not considered so far.

MEDNARODNA
PODIPLOMSKA ŠOLA
JOŽEFA STEFANA

JOŽEF STEFAN
INTERNATIONAL
POSTGRADUATE SCHOOL

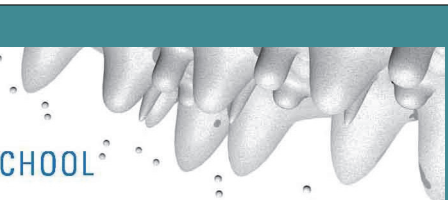

THE ROLE OF DIFFERENT NIOBIUM PENTOXIDE PRECURSORS IN THE SOLID-STATE SYNTHESIS OF POTASSIUM SODIUM NIOBATE

Jitka Hreščak[1,2], Andreja Benčan[1,2], Tadej Rojac[2], Barbara Malič[1,2]
[1]Jožef Stefan International Postgraduate School, Jamova cesta 39, 1000 Ljubljana
[2]Inštitut Jožef Stefan, Jamova cesta 39, 1000 Ljubljana

Study program: Nanoscience and Nanotechnologies III
Supervisor: doc. dr. Andreja Benčan Golob

INTRODUCTION

In the last decade, a lot of effort in the field of piezoelectric ceramics has been dedicated to finding lead-free materials which would substitute the currently mostly used lead zirconate titanate. Since the report of Saito et al. in Nature in 2004, one of the most studied lead-free systems are materials based on the potassium sodium niobate solid solution. However, difficult processing of potassium sodium niobate based materials hinders them from being used in larger scale. Nb_2O_5 is the most used source of Nb for the solid-state synthesis of these ceramics. We observed that when using the Nb_2O_5 from different producers, ceramics of extremely different quality was obtained.

Our study

Two batches of $K_{0.5}Na_{0.5}NbO_3$ (KNN) were prepared using the same procedure, but different Nb_2O_5; i.e. orthorhombic and monoclinic.

PREPARATION METHOD

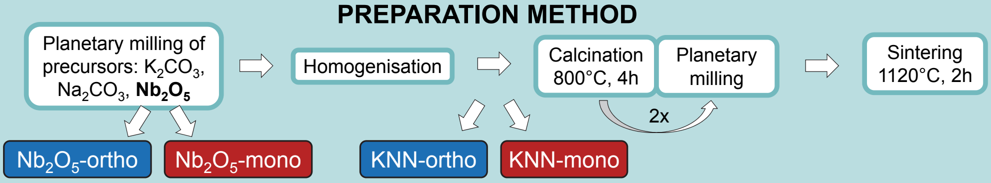

Planetary milling of precursors: K_2CO_3, Na_2CO_3, **Nb_2O_5**

Homogenisation

Calcination 800°C, 4h

Planetary milling

2x

Sintering 1120°C, 2h

Nb_2O_5-ortho

Nb_2O_5-mono

KNN-ortho

KNN-mono

RESULTS

Milling of the Nb_2O_5

Although, the as-received orthorhombic Nb_2O_5 remained unchanged by the milling step, the as-received monoclinic Nb_2O_5 after milling partially transformed to nanoparticles with orthorhombic syngony, which were attached to the surface of the remaining micron-sized monoclinic particles.

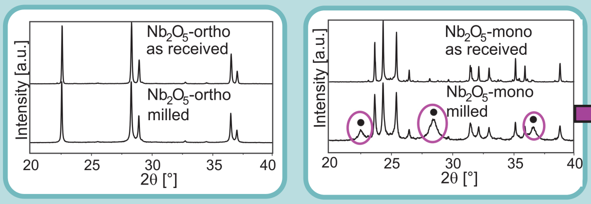

XRD patterns of Nb_2O_5 precursors: Peaks marked with • correspond to the newly introduced orthorhombic phase.

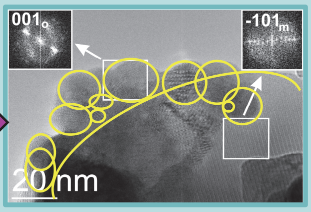

HR-TEM image of the milled Nb_2O_5-mono particles with insets showing FFTs of the selected areas.

Synthesis, densification and sintering of the KNN

The two-phase Nb_2O_5-mono reacted to form inhomogeneous potassium sodium solid solution after calcination, which resulted in the abnormal grain growth during the densification. The inhomogeneous powder was additionally homogenized by annealing at 950°C,4h and sintered (KNN-mono-950). Sintering of this powder resulted in the ceramics with very poor density (86.6% TD). The sintered KNN-ortho had uniform grains and density of 92.4% TD.

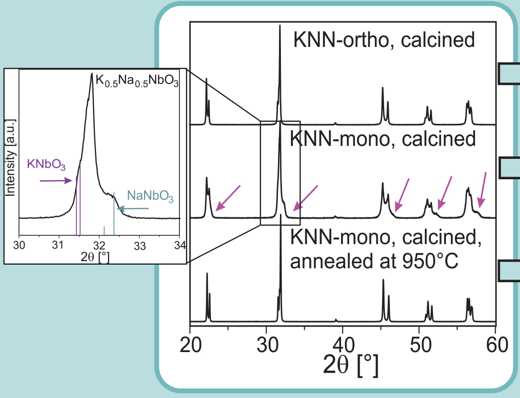

XRD patterns of powders after calcination. The shoulders are marked with arrows

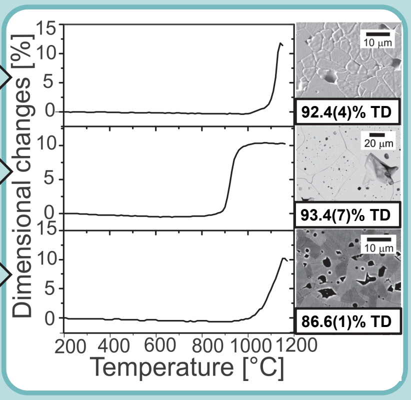

Dimensional changes with temperature of calcined powders and corresponding SEM images and densities of the sintered ceramics.

This study shows that the choice of the Nb_2O_5 precursor phase is of a key importance for the quality of the final KNN ceramics. Care should be taken with the phase composition and the particle size distribution of the starting powders as they are received from the producer.

Pump-probe reflectivity study of $HgBa_2CuO_{4+\delta}$ cuprate superconductor

Ivan Madan[1,2], **Janusz Karpinski**[3], **Tomaž Mertelj**[1], **Dragan Mihailović**[1]
[1] Department of Complex matter, Jožef Stefan Institute, Ljubljana, Slovenia
[2] Jožef Stefan International Postgraduate School, Ljubljana, Slovenia
[3] ETH Zuirch, Zurich, Switzerland
ivan.madan@ijs.si

$HgBa_2CuO_{4+\delta}$ (Hg-1201) cuprate compound is a single Cu-O layer member of mercury cuprate superconductor family. We present general characterization of the nonequilibrium relaxation dynamics: focusing on its temperature and polarization dependence. We also investigate photodestruction of superconducting condensate by ultrafast laser pulses and the ensuing recovery. We find that superconducting fluctuations make a significant contribution to the transient reflectivity in the temperature region >25 K above T_c.

MEDNARODNA
PODIPLOMSKA ŠOLA
JOŽEFA STEFANA

JOŽEF STEFAN
INTERNATIONAL
POSTGRADUATE SCHOOL

Pump-probe reflectivity study of Hg-1201 cuprate superconductor.

Ivan Madan.
Mednarodna podiplomska šola Jožefa Stefana
MENTOR: prof. dr. Dragan Mihailovic
Inštitut Jožef Stefan, Jamova cesta 39, 1000 Ljubljana

Temperature dependence

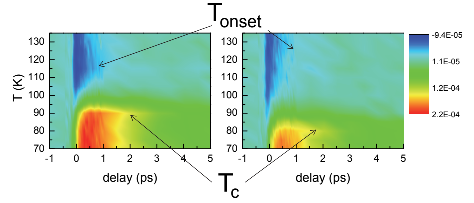

Temperature dependences for two samples is shown, consisting of negative pseudogap and positive superconducting components. Critical slowing down of quasiparticle relaxation occurs at Tc. Onset of superconducting response occurs at much higher temperature, suggesting presence of superconducting gap, without macroscopic phase coherence

Experiment description

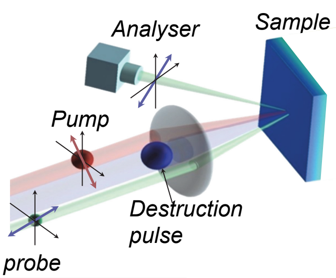

2 Pulse: "Pump" pulse excites non-equilibrium quasiparticle population which gives rise to a reflectivity change probed by "probe" beam after certain time delay

3 Pulse: Destruction pulse destroys the superconducting state. With recovery of the state after some time pump beam excites non-equilibrium superconducting state which further is "probed" by third pulse

Ultrafast characterization

Fluence dependence

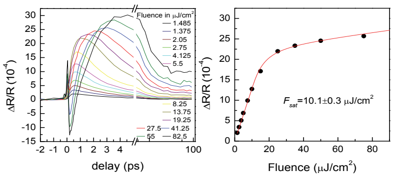

Superconducting response shows saturation behavior, with linear response in weak excitation regime, suggesting destruction of superconducting condensate by femtosecond laser pulse above F_{sat}=10μJ/cm².
Negative pseudogap response is hidden at low fluences but becomes dominant at high.

Polarization dependence

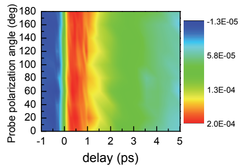

Absence of polarization dependence is a signature of preserved D4h symmetry which is often violated in other cuprates

Recovery after photodestruction

3 Pulse experiment

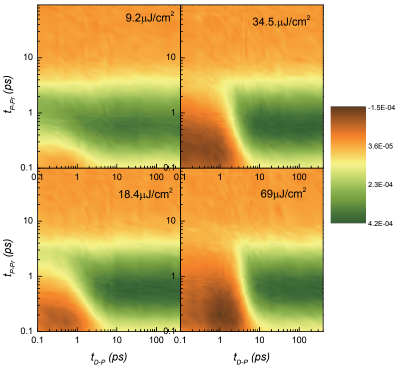

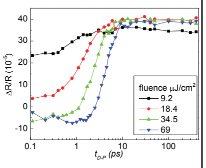

Read-out of the signal at 0.7 ps after pump pulse

Superconducting signal is progressively suppressed with increasing D pulse fluence. Signal is completely recovered within first 10 ps. For the highest fluence also the suppression and recovery of the pseudogap component is observed. Recovery is delayed and faster than exponential in contrast to the exponential quasiparticle relaxation.

Possible applications - Ultrafast electrical and optical switches

Computations and data storage

Communications

Metamaterials

Synthesis and functionalization of α-$NaYF_4$ nanoparticles

Olivija Plohl[1,2], **Darja Lisjak**[1,2], **Maja Ponikvar-Svet**[4], **Slavko Kralj**[1], **Darko Makovec**[1,2,3]
[1] Department of K8, Jožef Stefan Institute, Ljubljana, Slovenia
[2] Jožef Stefan International Postgraduate School, Ljubljana, Slovenia
[3] CENN Nanocenter, Ljubljana, Slovenia
[4] Department of K1, Jožef Stefan Institute, Ljubljana, Slovenia
olivija.plohl@ijs.si

In this paper the synthesis of α-$NaYF_4$ nanoparticles with coprecipitation under reflux using ethylene glycol as a solvent and polyvinylpyrrolidone as stabilizing agent is described. The polyvinylpyrrolidone stabilized nanoparticles in ethanol were coated with silica using modified Stöber procedure. The silica coated nanoparticles were further functionalized with aminopropyltriethoxysilane and dispersed in water. The efficiency of the two processes was confirmed with electrokinetic measurements (from zeta potential and isoelectric point). Morphology and chemical composition of the synthesized nanoparticles was characterized with transmission electron microscopy combined with energy-dispersive X-ray spectroscopy while their crystal structure was analysed with X-ray powder diffraction. The chemical instability of the as-synthesized nanoparticles was observed in aqueous media and the released fluoride ion in aqueous media was measured with fluoride ion selective electrode. The efficiency of the silica coating against the dissolution of fluoride was examined.

SYNTHESIS AND FUNCTIONALIZATION OF α-NAYF$_4$ NANOPARTICLES

Olivija Plohl, univ.dipl.inž.kem.tehn.[a,b,*], Darja Lisjak[a,b,§], Maja Ponikvar-Svet[c], Slavko Kralj[a], Darko Makovec[a,b,d]
[a] „Jožef Stefan“ Institute, Department for materials synthesis, K8, Jamova cesta 39, 1000 Ljubljana
[b] „Jožef Stefan“ International postgraduate school, Jamova cesta 39, 1000 Ljubljana
*Programe: Nanosciences and nanotechnologies
§Supervisor: doc.dr. Darja Lisjak
[c] „Jožef Stefan“ Institute, Department for inorganic chemistry and technology, K1, Jamova cesta 39, 1000 Ljubljana
[d] CENN Nanocenter, Jamova ulica 39, 1000 Ljubljana

INTRODUCTION

- Lanthanide-doped nanoparticles, which show upconversion, were proposed as alternative biomarkers for fluorescence imaging.
- Upconversion is a process, where sensitizer ion (i.e, Yb^{3+}) absorbs the excitation radiation with specific wavelenght and transfer it as a non-radiative energy to activator ion (i.e., Er^{3+}, Tm^{3+}, Ho^{3+}), which emits at shorter wavelenght.
- Most extensively studied host matrices are fluorides due to their ability to incorporate lanthanide ions, have low phonon energies and high chemical stability.
- One of suitable upconversion fluorescent host matrix is cubic phase of sodium yttrium fluoride (α-NaYF$_4$).
- The purpose of this work was to examine the chemical stability of α-NaYF$_4$ nanoparticles in aqueous media and check permeability of silica coatings for fluoride ion.

APPLICATIONS

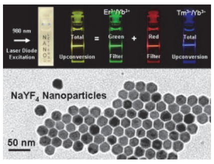

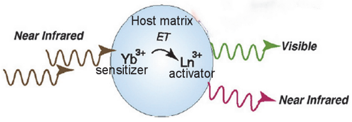

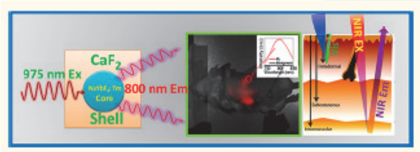

EXPERIMENTAL

α-NaYF$_4$

Nanoparticles were synthesized in ethylene glycol (EG) with coprecipitation under reflux at 160 °C for 2 h. Y(NO$_3$)$_3$x6H$_2$O, polyvinylpyrrolidone (PVP) and NaCl were added to EG and solution was heated to 80 °C. Second solution contained NH$_4$F and EG and was added to first solution at 80 °C.

α-NaYF$_4$@SiO$_2$

All synthesized α-NaYF$_4$/PVP nanoparticles were dispersed in ethanol and mixed with water and ammonia. Tetraethoxysilane (TEOS) dissolved in ethanol was then added slowly to the solution with continious stirring.

α-NaYF$_4$@SiO$_2$-APS

The obtained α-NaYF$_4$@SiO$_2$ nanoparticles were redispersed in 30 mL of ethanol and then 3 mL of aminopropyltriethoxysilane (APS) was added and react under refluxing at 80 °C for 3 h.

RESULTS

MEASUREMENTS OF RELEASED FLUORIDE ION

A high concentration of the dissolved fluoride ion **20.0 mg/l of α-NaYF$_4$** suggested that such nanoparticles would degraded severely in aqueous suspensions.

silica coatings

α-NaYF$_4$@SiO$_2$ aqueous suspensions confirmed **22.4 mg/l** of the dissolved fluoride ion for 8 nm thick silica layer similar to that of the uncoated samples.

XRD ANALYSIS

The XRD patterns of the α-NaYF$_4$ and α-NaYF$_4$@SiO$_2$ nanoparticles agree well with the data for the pure cubic NaYF$_4$ nanoparticles (JCPDS card No. 77-2042).

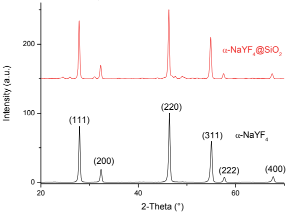

TEM ANALYSIS

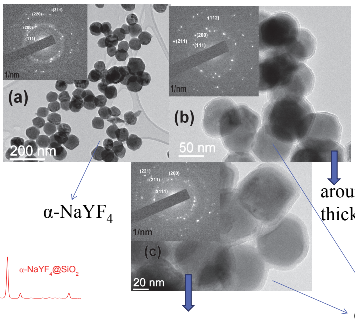

α-NaYF$_4$

around 8 nm thick silica layer

around 3 nm thick silica layer

α-NaYF$_4$@SiO$_2$

EDXS ANALYSIS

EDXS analysis of the α-NaYF$_4$ nanoparticles confirmed that the main present elements are Na, Y, F. EDXS analysis in the case of α-NaYF$_4$@SiO$_2$ confirmed that the main elements are Na, Y, F, O and Si.

ELECTROKINETIC MEASUREMENTS

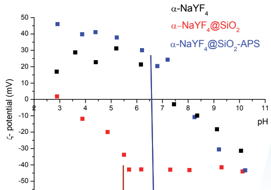

zeta potential is negative in all pH range due to silanol groups from the silica coatings

Zeta potential is pozitive due to protonated amino groups from APS

CONCLUSION

- We have successfully synthesized α-NaYF$_4$ nanoparticles by coprecipitation under reflux and stabilize them with PVP,
- the as-synthesized α-NaYF$_4$ nanoparticles were not chemically stable in aqueous suspensions and the dissolution of fluoride was detected,
- the nanoparticles were coated with 3 nm or 8 nm thick silica layer and further functionalized with APS,
- the concentration of the released fluoride ion did not differ between uncoated and coated nanoparticles.
- functionalization of the silica with APS is going to be used as a basis for further protective coatings of the nanoparticles.

ACKNOWLEDGEMENT: This work was financially supported by ARRS. The autors acknowledge for the use of equipment in the CENN Nanocenter.

LITERATURE: http://nanoscience.concordia.ca/people/johncapobianco/
Chen, G. *et al. American Chemical Society* **6**, 8280-8287 (2012).

Analyzing non-metallic inclusions in spring steel using Auger electron spectroscopy

Besnik Poniku[2], **Igor Belič**[1], **Monika Jenko**[1]

[1] Institute of Metals and Technology, Ljubljana, Slovenia

[2] Jožef Stefan International Postgraduate School, Ljubljana, Slovenia

besnik.poniku@gmail.com

Auger Electron Spectroscopy (AES) is a suitable technique for surface characterization. It is very surface sensitive, with the characteristic information coming from the top 0.4 -5 nm. Since also the electron beam can be focused down to about 10 nm in diameter, AES provides a powerful technique for performing analysis on the nano - scale. In the scope of this work AES was used to characterize non-metallic inclusions in spring steel. During this investigation a total of 52 analyses were performed on the first sample, and 41 on the second. Elements such as S, O, Ca, Mg, Mn, V, Cu, Al, Ti, Mo and C were found to be present. Having in mind the composition of spring steels, it is concluded that most of the inclusions which have a detrimental effect on their mechanical properties originated from the interaction of steel components with impurities during various stages of steel production.

MEDNARODNA
PODIPLOMSKA ŠOLA
JOŽEFA STEFANA

JOŽEF STEFAN
INTERNATIONAL
POSTGRADUATE SCHOOL

ANALYZING NON-METALLIC INCLUSIONS IN SPRING STEEL USING AUGER ELECTRON SPECTROSCOPY

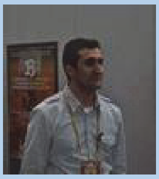

BESNIK PONIKU, mag. NiN
Study programme: Nanosciences and nanotechnologies,
Jozef Stefan International Postgraduate School
MENTOR: prof. dr. Monika Jenko
CO-MENTOR: doc. dr. Igor Belič
Institute of Metals and Technology, Lepi pot 11, 1000 Ljubljana

Auger Electron Spectroscopy (AES) is a suitable technique for surface characterization. It is very surface sensitive, with the characteristic information coming from the top 0.4 -5 nm. Since also the electron beam can be focused down to about 10 nm in diameter, AES provides a powerful technique for performing analysis on the nano – scale.
In the scope of this work AES was used to characterize non-metallic inclusions in spring steel. During this investigation a total of 52 analyses were performed on the first sample, and 41 on the second. Elements such as S, O, Ca, Mg, Mn, V, Cu, Al, Ti, Mo and C were found to be present. Having in mind the composition of spring steels, it is concluded that most of the inclusions which have a detrimental effect on their mechanical properties originated from the interaction of steel components with impurities during various stages of steel production.

Auger electron spectroscopy is a powerful technique for studying the surfaces of materials.

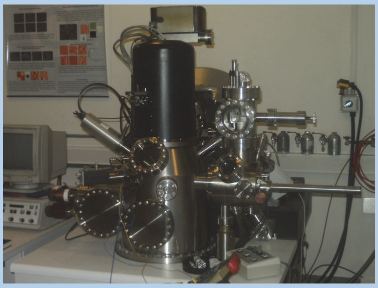

It is a very surface sensitive technique, where the characteristic signal comes from the top 0.4 – 5 nm of the sample surface.

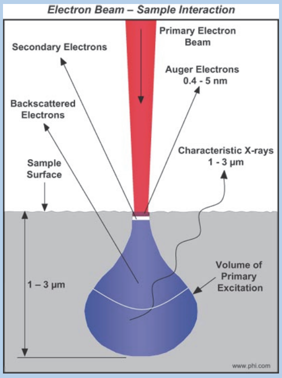

Apart from this fact, also the electron beam can be focused down to approximately 10 nm, making Auger electron spectroscopy very suitable for nano – scale surface analysis.

As part of this work non-metallic inclusions present in two spring – steel samples were analyzed using Auger electron spectroscopy, where 52 spectra were taken on the first sample whereas 41 spectra were taken on the second sample. The primary electron beam used was of 10 keV energy, 10 nA intensity, 10nm spot size.

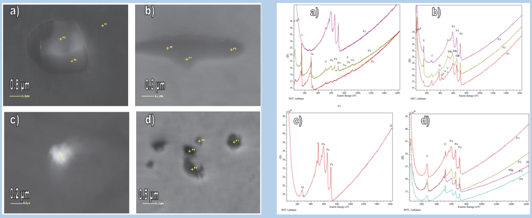

Auger maps showing the distribution of selected elements over a certain area of analysis were also performed.

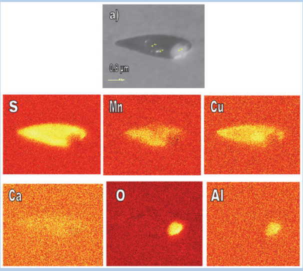

From the analysis it resulted that elements such as S, O, Ca, Mg, Mn, V, Cu, Al, Ti, Mo and C are present in the non-metallic inclusions. By observing the chemical composition of spring steels…

C%	Si% max	Mn%	P% max	S% max	Cr%	V%
0,47-0,55	0,40	0,70-1,10	0,025	0,025	0,90-1,20	0,10-0,25
± 0.02	± 0.03	± 0.05	+ 0.005	+ 0.005	± 0.05	± 0.02

…we come to the conclusion that most of the non-metallic inclusions are formed as a result of the interaction of the steel components with impurities during various stages of steel production.

Molecular dynamics study of incipient plasticity of the (1,1,19) nickel surface

Nuša Pukšič[1,2], **Monika Jenko**[1], **Matjaž Godec**[1]

[1] Institute of Metals and Technology, Ljubljana, Slovenia

[2] Jožef Stefan International Postgraduate School, Ljubljana, Slovenia

nusa.puksic@imt.si

Molecular dynamics simulations are used to study defect nucleation in nickel in response to uniaxial strain. The incipient plasticity of two nickel mono-crystalline substrates is investigated and compared, one with the nominal (0,0,1) surface and the other with the vicinal (1,1,19) surface. Surface relaxation at 0 K is performed by minimization, and then the substrates are equilibrated to 10 K and subjected to uniaxial tensile and compressive strain in accordance with the "strain-and-equilibrate" method, with a cumulative strain rate of 2.5% ps^{-1}. The surface condition influences the mechanical properties and the nucleation of defects. The defects form at smaller strain in the case of the Ni(1,1,19) surface and the defects mirror the regularity of the surface absent in the case of the nominal surface.

Molecular dynamics study of incipient plasticity of the (1,1,19) nickel surface

Author: Nuša Pukšič
Supervisor: Prof. Dr. Monika Jenko
Co-supervisor: Dr. Matjaž Godec
Institute of Metals and Technology, Ljubljana, Slovenia
Jožef Stefan International Postgraduate School, Ljubljana, Slovenia

Introduction

Research of mechanical properties of metallic materials has been extended in the last decades into the studies on the atomic level. Recently the atomistic simulations reached beyond the most basic simulations of single crystal samples and into a range of more realistic configurations, e.g. multi-layered thin films and polycrystalline samples. Vicinal surfaces are also of interest, as the sequence of steps on the surface leads to an elastic field that extends well into the bulk and causes a relaxation of near-surface atoms. This affects the dynamics of the surface, leading to a changed response to strain, as demonstrated by this example.

Results

Ni(0,0,1)
Compressive strain.

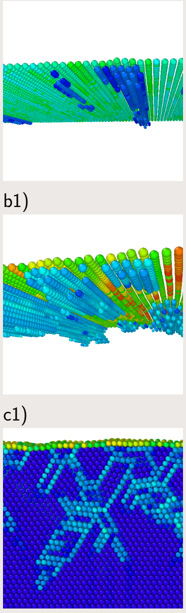

Snapshots
at the strains of:
a1) -0.078,
b1) -0.080, and
c1) -0.085.

Ni(0,0,1)
Tensile strain.

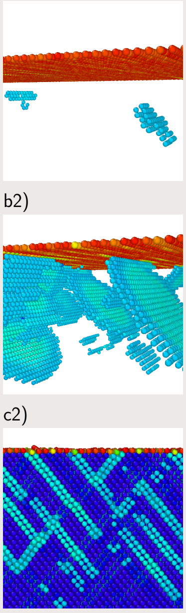

Snapshots
at the strains of
a2) 0.090,
b2) 0.091, and
c2) 0.093.

Ni(1,1,19)
Compressive strain.

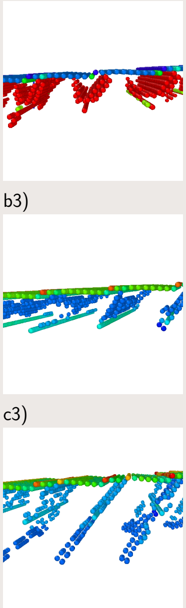

Snapshots
at the strains of
a3) -0.063,
b3) -0.078, and
c3) -0.080.

Ni(1,1,19)
Tensile strain.

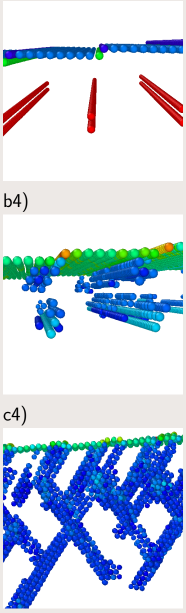

Snapshots
at the strains of
a4) 0.060,
b4) 0.065, and
c4) 0.068.

Applicative aspects of atomistic studies

Vicinal surfaces are of interest as periodic templates and as favorable sites for chemical reactions and nucleation. Their potential is not yet fully realized and their properties not fully cataloged.

Ever more advanced atomistic studies will bring a better understanding of how the results of nano-indentation studies depend on the local configuration of the sample (the presence of a grain boundary, an inclusion or a void). And also, how the mechanical properties of the sample depend on the type of grain boundaries prevalent in the sample and their volume fraction or the surface condition.

Studies of the influence of strain on mechanical properties are also important in the field of thin films, as lattice mismatch often induces stress when thin films are grown on various substrates.

Simulation basics

Substrate

A nickel single crystal was used in all simulations. The simulations were performed on a substrate with a (0,0,1) surface and a substrate with the vicinal (1,1,19) surface, consisting of a sequence of terraces and steps.

Surface relaxation

Damped dynamics method [1] was used to calculate surface relaxation at 0 K.

Uniaxial tension and compression

The samples were equilibrated to 10 K, then compressive and tensile strain were applied with the strain rate of 2.5% ps^{-1}. The axis of the compressive and tensile strains in the simulations is perpendicular to the steps on the vicinal surface along the $(1,\bar{1},0)$ direction.

Software

LAMMPS Molecular Dynamics Simulator was used and the EAM potential file for nickel provided by H. W. Sheng, included with the LAMMPS distribution. [2,3]
Post-processing was done using OVITO. [4]

Conclusions

In all the cases, the near-surface layers plastically deform at lower strain than the deeper bulk layers.

Compared to the Ni(0,0,1) case, the defects begin to form at lower strain in the case of the Ni(1,1,19) surface. Additionally, the regularity of the nucleated defects mirrors the regularity of the steps, absent in the case of the Ni(0,0,1) surface.

The condition of a free nickel surface influences its mechanical response to external uniaxial strain: the stability of the surface, the position and type of defects and the strain at which the defects nucleate are all subject to the state of the surface before deformation.

References:

[1] D. Sheppard, R. Terrell, and G. Henkelman. Optimization methods for finding minimum energy paths. *The Journal of chemical physics*, 128(13):134106, 2008
[2] S. Plimpton. Fast Parallel Algorithms for Short-Range Molecular Dynamics. *Journal of Computational Physics*, 117:1–19, 1995
[3] Sandia National Laboratories. LAMMPS Molecular Dynamics Simulator. http://lammps.sandia.gov/, 2014
[4] A. Stukowski. Visualization and analysis of atomistic simulation data with OVITO–the Open Visualization Tool. *Modelling and Simulation in Materials Science and Engineering*, 18(1):015012, 2010

Superhydrophilic surface of selectively plasma etched polyphenol composite

Harinarayanan Puliyalil[1,2], **Gregor Filipič**[1,2], **Uroš Cvelbar**[1,2]
[1] Department of Surface Engineering and Optoelectronics-F4, Jožef Stefan Institute, Ljubljana, Slovenia
[2] Jožef Stefan International Postgraduate School, Ljubljana, Slovenia
hari.puliyalil@ijs.si

Surface hydrophilicity is an important property of polymer materials for applications, where we bond or attach other materials to its surface. For tuning the hydrophilicity, plasma treatment has greater advantage over the commonly used chemical treatments, due to its efficiency and localized functionalization with polar or non-polar groups. In this work, we created a superhydrophilic surface of glass filled polyphenol composite by plasma selective etching of the composite matrix. The weakly ionized highly dissociated plasma was generated in oxygen gas at 35 Pa. Due to high concentrations of oxygen atoms in plasma, we achieved high selectivity of etching the polymer, leaving fillers unattached. The systematic studies of surface morphology and composition were performed using X-ray Photoelectron Spectroscopy (XPS) and Scanning Electron Microscopy (SEM) after different exposure times. The surface energy was measured with Water Contact Angle measurements. Whereas plasma etching process was controlled by optical emission spectroscopy. The superhydrophilic surface was achieved after polymer was selectively removed and surface was populated with polar oxygen functional groups after 9 s treatment.

OXYGEN PLASMA SELECTIVE ETCHING FOR THE IMPROVED SURFACE TRACKING PROPERTIES OF POLYPHENOL COMPOSITES

HARINARAYANAN PULIYALIL
Study program: Nanoscience and nanotechnology
Jožef Stefan International Postgraduate School
MENTOR: Dr. UROŠ CVELBAR

Inštitut Jožef Stefan, Jamova cesta 39, 1000 Ljubljana

Oxygen plasma selective etching of polymer composites is an efficient procedure to:

► Selectively remove the polymer matrix keeping the fillers intact.

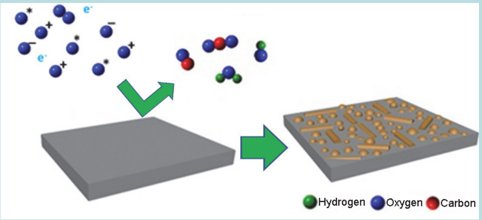

► Removal of the polymer from the surface decreases the carbonization on the surface and increases the comparative tracking index (CTI).

►Attain a super hydrophilic surface by introducing polar functional groups without using hazardous chemicals

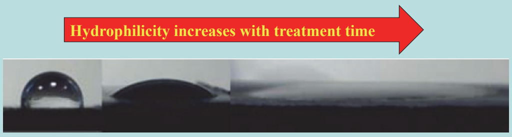

► Surface morphology (SEM)

Non-treated composite

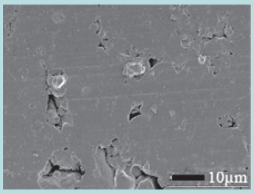

After 60 s treatment

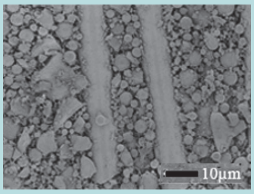

CONCLUSIONS

- Plasma species, interaction with the matrix and the surface changes on the material after treatment have been characterized.
- Plasma selective etching is simple, fast and green.
- It improves the CTI performances of composites without affecting the bulk up to a value of 350V.
- This is because the removal of polymer reduces the carbonization on the surface
- This method prevent the immediate chance of fire during short circuit.
- Promising for reducing the amount of flame retardant fillers
- Could be easily implemented in industries

Highly dissociated plasma contains mostly radicals along with other reactive species (ions, electrons, photons, etc.) which induce carbon oxidation even at room temperature.

► Variation of CTI

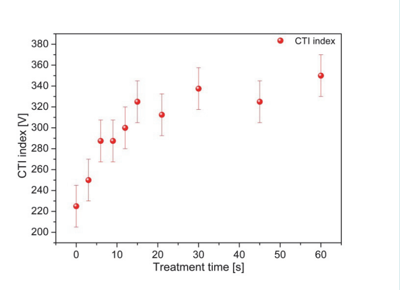

► Elemental composition on the surface A) XPS B) EDXS

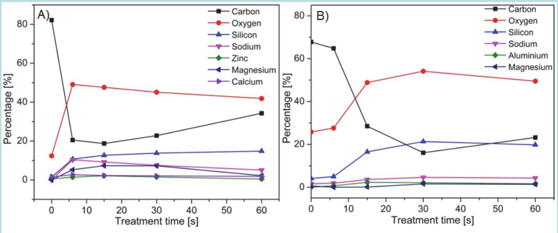

► Optical emission spectra for A) For the pulse at 6s. B) For the pulse at 60s

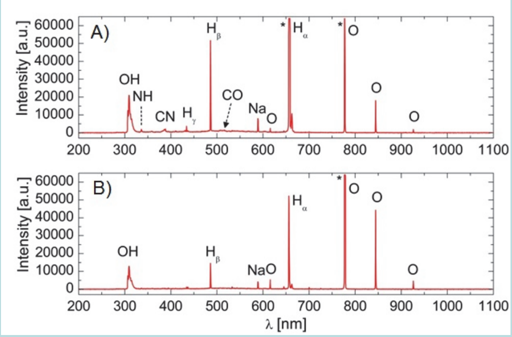

References

1. Electrical Insulation and Dielectric Phenomena, 1999 Annual Report Conference on, 1999. p. 154-157 vol.151.
2. Polymer Degradation and Stability. 2012;97(4):566-572.
3. Appl Surf Sci. 2003;210(3–4):255-261.
4. Nanotechnology. 2009;20(33):335501.
5. Polymer Degradation and Stability 2013;(98): 2653-2662.

The effect of silica and alumina co-doping on the properties of dental zirconia ceramic

Anastasia Samodurova[1,2], **Andraž Kocjan**[2], **Tomaž Kosmač**[2]

[1] Department of Engineering Ceramics, Jožef Stefan Institute, Ljubljana, Slovenia

[2] Jožef Stefan International Postgraduate School, Ljubljana, Slovenia

anastasia.samodurova@ijs.si

We report on the addition of alumina and silica as dopants to an 3-mol%-yttria-doped tetragonal zirconia (3Y-TZP) ceramic as an effective strategy to significantly decelerate the low temperature degradation (LTD), without any loss of fracture toughness of as-sintered materials. The results of transmission electron microscopy (TEM) and energy dispersive X-ray spectroscopy (EDS) analyses revealed that silica was mainly present as an amorphous phase concentrated at triple grain junctions. Focused ion beam scanning electron microscopy (FIB-SEM) studies of sub-surface region of aged for 24 h samples show substantially smaller transformed layer with lower amount of microcracks in alumina or silica doped 3Y-TZP. At the same time crack-free sub-surface with only 2-3 grains transformed was observed for alumina/silica-doped 3Y-TZP. Results indicate that alumina and silica has different mechanism behind the suppression of LTD and when combined they add-up resistance.

MEDNARODNA
PODIPLOMSKA ŠOLA
JOŽEFA STEFANA

JOŽEF STEFAN
INTERNATIONAL
POSTGRADUATE SCHOOL

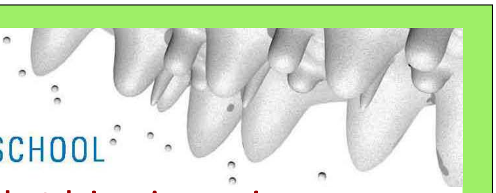

The effect of alumina and silica co-doping on the properties of dental zirconia ceramic

Anastasia Samodurova
Study programme: Nanosciences and Nanotechnologies,
Jožef Stefan International Postgraduate School
Supervisor: prof. dr. Tomaž Kosmač
Jožef Stefan Institute, Jamova 39, 1000 Ljubljana

Tetragonal zirconia

Early 1990s

- Orthodontic brackets (overlaid with veneering porcelain)
- Root posts for anterior teeth

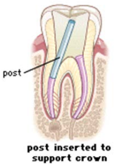

Nowadays

- Fixed partial dentures
- Implants

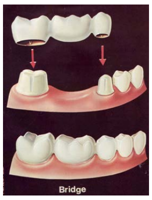

Why zirconia?

- High strength and fracture toughness
- Aesthetics
- Biocompatibility

Problems:

- Porcelain chipping (was bypassed with the emergence of chip-resistant monolithic full-contour Y-TZP)
- Low temperature degradation (LTD), i.e. ageing

Aim

To enhance the ageing resistance of 3Y-TZP by silica and alumina co-doping

Materials and methods

Powders (Tosoh, Japan)	Chemical characteristics	Abbreviations
TZ-3YB	Alumina free	TZ-3Y
TZ-PX-242A	0.05 wt% alumina	0.05A-TZ-3Y
TZ-3YSB-E	0.25 wt% alumina	0.25A-TZ-3Y

1. dry pressing
2. CIP (200 MPa)
3. Pre-sintering 900°C/1000°C

Infiltration with silica sol, synthesized *in situ* by the sol–gel method through hydrolysis of dynasylan.

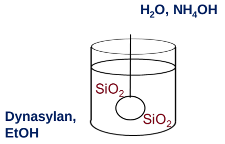

Final sintering, 1450°C, 4h

Autoclaving in water: 134°C, up to 48h

Characterization XRD, TEM, FIB-SEM

Results

Microstructural studies, densities and indentation toughness

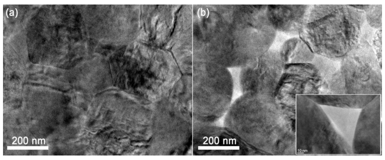

Fig. 1. TEM micrographs of 0.05A-TZ-3Y (a) and 0.05A-TZ-3Y/SiO_2 (b) specimens sintered at 1450 °C for 4 h.

Amorphous silica phase is positioned in multiple grain junctions, making grains more roundly shaped.

Table 1. Relative densities, grain sizes and fracture toughness of sintered for 4 h at 1450°C pure and silica-doped TZ-3Y, 0.05A-TZ-3Y and 0.25A-TZ-3Y materials.

Sample	Relative densities (%)	Grain sizes (mm)	Indentation toughness, K_{IC} ($MPa \cdot m^{1/2}$)
TZ-3Y	99.7	0.31 ± 0.12	4.4 ± 0.3
TZ-3Y/SiO_2	99.4	0.29 ± 0.13	4.3 ± 0.1
0.05A-TZ-3Y	99.8	0.31 ± 0.13	4.5 ± 0.7
0.05A-TZ-3Y/SiO_2	99.5	0.28 ± 0.12	4.2 ± 0.3
0.25A-TZ-3Y	99.8	0.35 ± 0.13	6.4 ± 1.0
0.25A-TZ-3Y/SiO_2	99.1	0.4 ± 0.15	6.3 ± 0.7

No significant differences in densities, grain sizes and indentation toughness were observed between alumina- or/and silica-doped specimens.

In-vitro ageing behavior

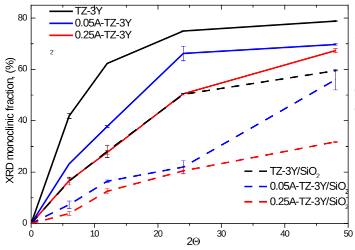

Fig. 2. Calculated monoclinic fraction versus *in-vitro* ageing time for pure and silica doped TZ-3Y, 0.05A-TZ-3Y and 0.25A-TZ-3Y materials.

The presence of alumina in 3Y-TZP greatly increases the resistance to ageing.
The addition of silica to alumina-doped 3Y-TZP further improves ageing properties.

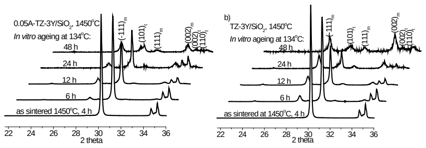

Fig. 3. XRD patterns obtained from a) 0.05A-TZ-3Y/SiO_2 and b) TZ-3Y/SiO_2 ceramic surfaces, sintered for 4 h at 1450 ˚C and aged in water at 134 ˚C for 6, 12, 24 and 48 h.

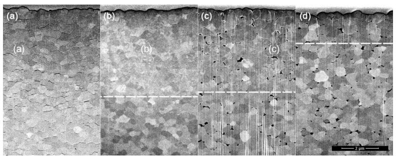

Fig. 4. FIB-SEM sub-surface microstructures of the TZ-3Y (a), 0.25A-TZ-3Y (b), TZ-3Y/SiO_2 (c) and 0.25A-TZ-3Y/SiO_2 (d) materials aged for 24 h.

The monoclinic layer of alumina- or silica-doped 3Y-TZP substantially thinner, compared to the TZ-3Y material aged under the same conditions. 0.25A-TZ-3Y/SiO_2 material aged for 24 h has a crack-free sub-surface microstructure with only 3-4 surface grains transformed.

Conclusions

The results of TEM revealed that silica was mainly presented as an amorphous phase concentrated at triple grain junctions. The presence of silica in alumina-free 3Y-TZP greatly increases the resistance to LTD. The addition of small amounts of silica to alumina-containig 3Y-TZP futher improves the ageing properties of 3Y-TZP without affecting indentation toughness of as-sintered material. Results indicate that alumina and silica has different mechanism behind the suppression of LTD and when combined they add-up resistance.

Kazalo Avtorjev (List of Authors)


ECO
samples
compounds
tea
mercury
high
products
bread
activity
temperature
separation
provide
care
release
environment
materials
milk
gas
MoS2
fate
results
PPCPs
applied
exist
organic
chromatographic
fractionation
confirm
spite
work
information
stable
different
enables
Monolithic
presence
experiments
data
human
ketoprofen
catalytic
years
low
columns
structure
follow
study
monolithic
chromatography
coal
small
solid
useful
effects
50Cr

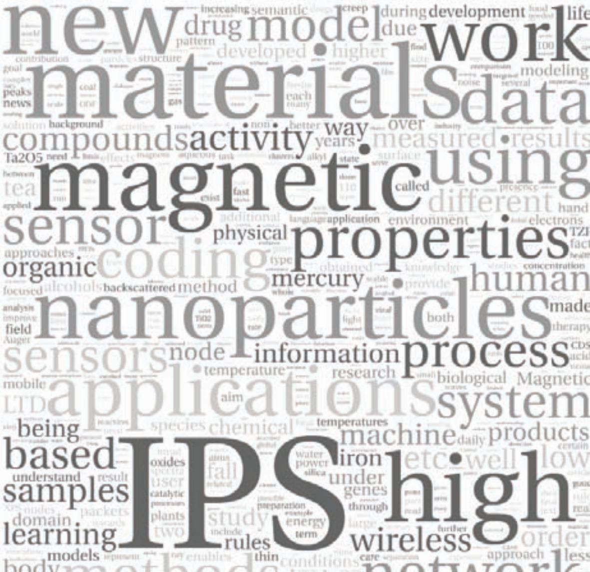
IPS
materials
magnetic
nanoparticles
applications
new
model
work
data
using
properties
process
system
high
network
methods
human
sensor
coding
compounds
activity
sensors
based
samples
learning
wireless
machine
products
drug
development
node
information
mercury
measured
results
different
organic
physical
body
devices
rules

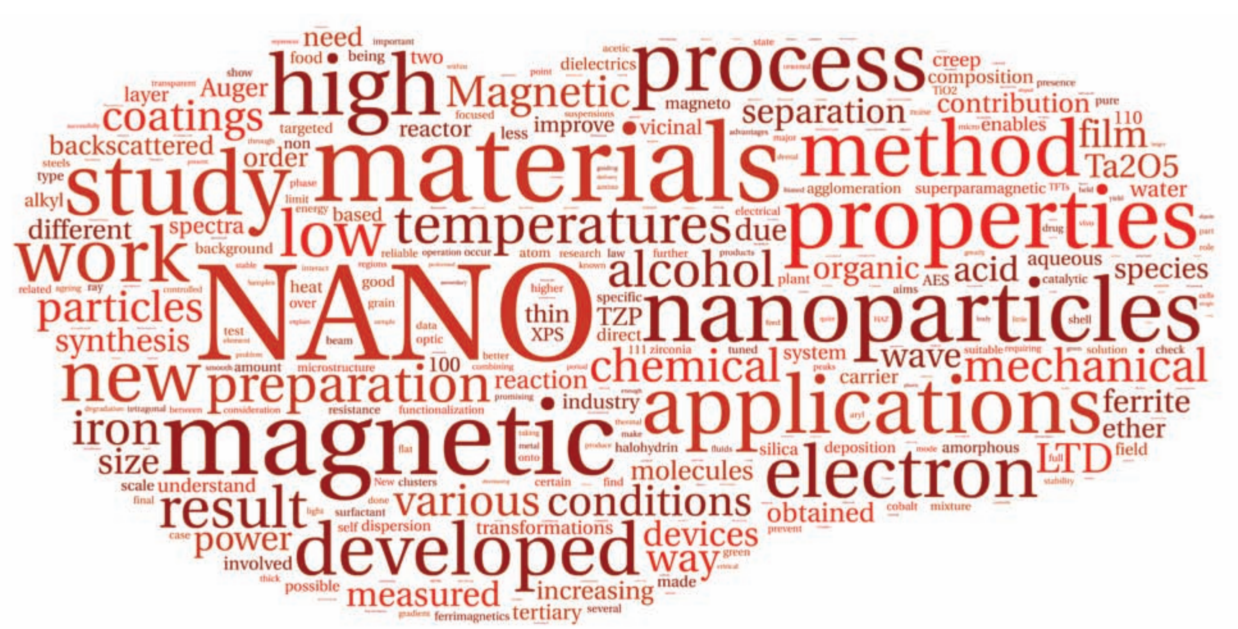
NANO
materials
magnetic
nanoparticles
properties
applications
process
high
method
study
electron
developed
work
new
preparation
temperatures
low
alcohol
chemical
mechanical
conditions
various
result
Magnetic
coatings
particles
synthesis
iron
film
Ta2O5
separation
reaction
ferrite
species
organic
acid
power
measured
devices
way
spectra
backscattered
Auger
wave
thin
XPS
TZP
LTD
size
molecules
increasing
obtained
tertiary
transformations

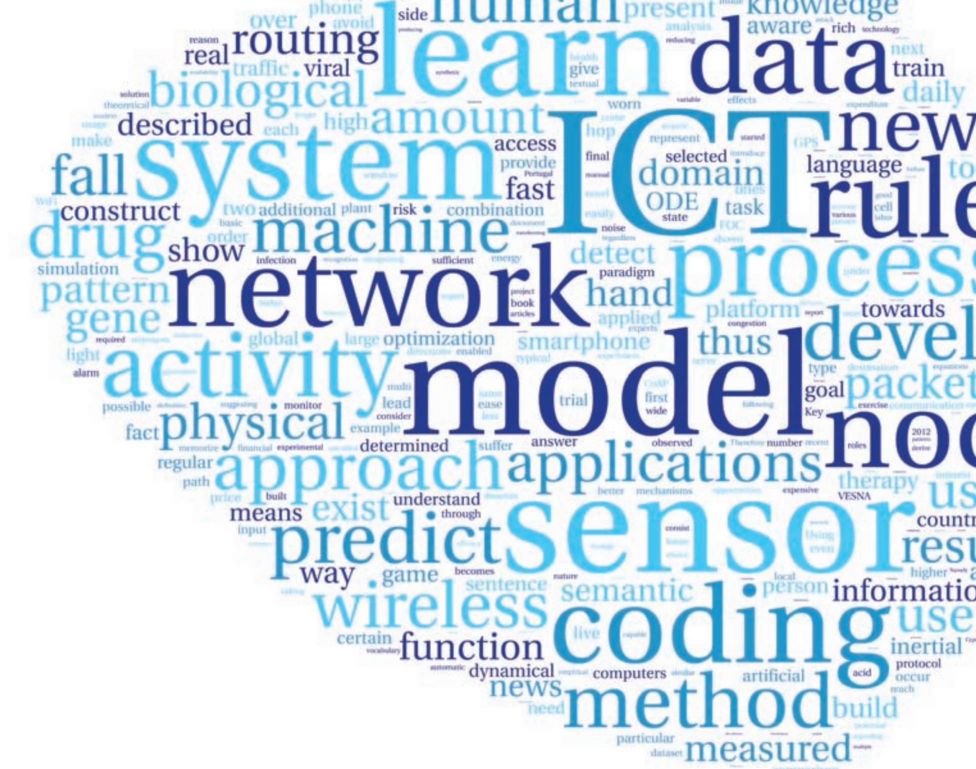
ICT
model
network
system
learn
data
sensor
coding
process
rule
node
activity
method
approach
develop
applications
new
human
predict
wireless
machine
drug
fall
routing
biological
amount
packet
physical
gene
pattern
using
result
user
function
semantic
information
domain
knowledge
measured
build
news
exist
detect
platform
smartphone
therapy
inertial
construct
described

MEDNARODNA
PODIPLOMSKA ŠOLA
JOŽEFA STEFANA

JOŽEF STEFAN
INTERNATIONAL POSTGRADUATE SCHOOL

Jamova 39, SI-1000 Ljubljana

T +386 (0)1 477 31 00
F +386 (0)1 477 31 10

E info@mps.si
www.mps.si

ISBN 978-961-92871-7-0